Universitat Politècnica de Catalunya
Departament de Llenguatges i Sistemes Informàtics
Master in Computing

MASTER THESIS

Ant Colony Optimization for Multicasting/Broadcasting in Wireless Ad-hoc Networks

Author: Hugo HERNÁNDEZ PIBERNAT
Director: Christian BLUM

Academic year 2007-2008

To my mother, Eva.

In the memory of
Lucía Hernández,
Giorgio Hernández (*Pipo*)
and
Fernando Hernández (*el Tío*),
you will live forever in my heart,
in my mind and in my smile.

Acknowledgements

This work could have never existed without the contributions of many different persons. In the following paragraphs I will briefly summarize them. Please, note that some persons who are not mentioned here has also helped me in this work. To those who have also helped me solving particular problems, to all of them, thank you very much.

Fist of all I want to thank the LSI department for letting me use their computing cluster. As mentioned in the *Scientific contributions* section, without it, I would have not been able to do most of the expermients in this work. I also want to acknowledge the ALBCOM research group for supporting the articles that this work has given origin to.

The edition of this document has been done with LaTeX. I want to thank Donald E. Knuth for the design and creation of TeX, a complete and precise typesetting and formatting language, and also for making it freely and fully available to everyone in the world. I also want to thank Leslie Lamport for developing the incredible macro package LaTeX, that makes working with TeX an easy task, and for making it freely available. I also thank the authors of *The not so short introduction to LaTeX 2ε* for writing such an exhaustive and comprehensive manual and, again, for making it freely available. I want to thank all collaborators of the TeX and LaTeX projects as well.

The implementation, organization and evaluation of the algorithms studied in this work and the writing of this thesis have been made on a computer running a Linux kernel obtained from an Ubuntu distribution. I want to thank Linus Torvalds for designing and developing Linux and all other open source developers that have worked and/or are working in projects related to Linux. I also thank Mark Shuttleworth for founding the Ubuntu project.

The next paragraphs are not in english but in the mother language of each acknowledged person, respectively.

Me gustaría agradecer la ayuda y el apoyo que he recibido por parte de algunos de mis familiares, no tanto para la realización de este trabajo como a lo largo de mis años de estudio. Cada cual creo que ya sabe cuanto agradezco lo que ha hecho por mí.

També m'agradaria donar les gràcies als meus companys de la FIB, que durant els últims cinc anys han aguantat les meves tonteries i mals humors. Sense cap mena de dubte, i encara que potser no els hi faci saber normalment, la seva companyia sempre m'ha ajudat amb la meva vida acadèmica. Gràcies també als meus amics de la FME, molt especialment, a la Georgina. La seva existència va suposar i suposa un gran motiu d'alegria per mi. Gràcies a

tots.

Vull donar infinites gràcies al Carles per fer-me tants i tants cops costat. Clarament ell es, tot sovint, l'*essència conceptual del moment*. Igualment, agrair a bona part de la seva família haver-me acollit com ho ha fet des de fa ja tants i tants anys. L'ajuda i el suport que m'han donat, la seva generositat, el seu tracte cap a mi i el coneixement que m'han aportat des de que en Carles i jo ens vem conèixer són un dels meus més grans motius d'orgull. Així mateix, vull dedicar un grandíssim pensament en record d'en Carlos Vancells Fina (1927-2008).

Ich würde gern mein Dissertationsleiter danken, Christian Blum. Ohne seine Hilfe, Ideen, Räte und mehrmalige Überprüfungen, wäre diese Dissertation nicht möglich gewesen. Außerdem, bin ich ihm für das Vertrauen und die Ermutigung dankbar, daß er bereits am Anfang geäuërt hat. Mit Christian Blum zu arbeiten ist eine der größten Ehren meiner akademischen Erfahrung gewesen, nicht nur wegen seinen Vorzüglichkeit, sowohl als Akademiker als auch als Forscher, sondern auch für seinen Respekt und gute Laune.

Durante los últimos seis meses he trabajado día y noche en esta tesis. Durante este tiempo, mi dedicación al completo (casi), mis pensamientos, esfuerzos y sueños se han centrado en esta tarea. Esto nunca hubiese sido posible si al levantarme las 8550 veces que lo he hecho no hubiese encontrado por la mañana cereales en el armario, al mediodía comida en la nevera y por la noche cena en la mesa (comida y cena diferentes cada día). Igual de importantes han sido las 8550 veces (o algunas más) que me he despertado sin necesidad de despertador o las que me leyeron un cuento para que me durmiera. Tampoco habría sido posible sin la ropa, los cepillos de dientes, los ordenadores, los juegos y los juguetes, las vacaciones, los lápices, las tarjetas de autobús, la beca de investigación más grande que me han concedido y que recibo desde que nací y los millones de cosas más de que dispongo y he dispuesto en mi vida sin dar nada a cambio. Pero todo eso, queda en nada al lado de la ayuda el cariño, los abrazos, la educación, las ideas, el conocimeinto, el amor, el respeto, el soporte, la comprensión, la confianza, la ternura, el perdón, la seguridad, la ilusión y mil intangibles, incomprables e insustituibles más que he tenido sin tampoco dar nada a cambio. Quien me ha dado todo lo anterior es alguien que apostó muchos de sus años de juventud por mí y es mi madre. A ella, a mi madre en exlusiva, le dedico este trabajo y mis veinticuatro años de estudio. Gracias, Mami, por todo lo que sé que nunca te podré devolver y por todo lo que sí te devolveré.

Scientific contributions

As it will be explained in the following pages, multicasting/broadcasting in static wireless networks is a problem well studied in the literature. Nevertheless, the algorithms introduced in this work for both scenarios, multicasting and broadcasting, are currently the best ones available. These algorithms outperform in best and average solutions other algorithms for the same problems appearing in the scientific literature. In addition, they also outperform other heuristic algorithms in computation time requirements.

The results of this work have been published in two conference articles (one accepted and the other submitted). We list them here:

- Hugo Hernández, Christian Blum and Guillem Francès. Ant Colony Optimization for Energy-Efficient Broadcasting in Ad-Hoc Networks. In *Proceedings of ANTS 2008, 6th International Conference on Ant Colony Optimization and Swarm Intelligence (ANTS 2008)*. Lecture Notes in Computer Science, Springer-Verlag, Berlin, Germany 2008. Full-length article accepted. Also, chosen for oral presentation.
- Hugo Hernández and Christian Blum. Energy-Efficient Multicasting in Wireless Ad-Hoc Networks: An Ant Colony Optimization Approach. *5th International Symposium on Wireless Communication Systems (IEEE ISWCS 2008)*. Submitted.

In addition, a longer article is in preparation to be sent to an international journal.

Note that a very exhaustive evaluation of the algorithms has been done and that results of this evaluation are mostly presented in tables. Therefore, many tables appear in the work, and many more in the appendices. These tables should not annoy the reader, summaries and important facts of all experiments appear in the text and graphics of the thesis. The tables are presented, simply, for completeness.

This exhaustive evaluation required, on a single processor, more than 564 days of computation to obtain the results presented in this work (excluding all prior experiments). All these calculations would have not been possible without the computation cluster of the *LSI department at the Universitat Politècnica de Catalunya*.

Another important aspect was the support of the projects FORMALISM (TIN2007-66523) funded by the Spanish government and FRONTS (FP7-ICT-2007-1) funded by the European Commission.

Contents

List of Algorithms

List of Figures

List of Tables

Chapter 1

Introduction

Wireless networks are becoming a very useful tool in various fields, like scientific research or civil applications. Their main advantages are a low infrastructure cost and a big scalability and flexibility. Two particular kinds of wireless networks, sensor networks and ad-hoc networks, have been applied in different ways and to different areas. Sensor networks are used, for example, in weather forecasting and in healthcare applications, while ad-hoc networks are commonly used in PDA or laptop networks. In contrast to wired or cellular networks no backbone infrastructure is needed in ad-hoc networks. All these applications justify why so many researchers from all over the world are focusing on wireless networks, with lots of papers published and conferences held every year.

In ad-hoc networks nodes are enabled to receive and transfer information packets. For this purpose they are equipped with radio antennas, that may be directional or omnidirectional. The network structure allows them to act both as hosts or routers. Using this fact, communication can be achieved not only by single-hop transmissions but also using other nodes as relay nodes, making multi-hop transmissions. One of the problems inherent to ad-hoc networks is that usually the devices acting as nodes depend on batteries. Hence, the network usability and lifetime is limited by battery power in wireless devices. Unfortunately, the capacity of batteries does not grow very fast.

Energy saving in ad-hoc networks can be approached from a transmission power control point of view, by adjusting adequately transmission ranges and searching the good transmission scheme for every communication. Mainly, deciding whether to use a single-hop or a multi-hop scheme and, in this case, deciding which subset of the nodes must act as relay nodes. To accomplish this objective the nodes distribution (their positions) and their mobility capabilities must be considered.

In this framework common transmissions are not only unicasts (sending information from a source to a host) or broadcasts (sending information from a source to all the hosts in the network). A generalization of both unicasting and broadcasting is considered. Multicasting is a service for distributing data to any group of nodes and it is a critical service in applications where a close collaboration between nodes is required to carry out a given task. The node that generates the multicast packet is called the *source node* and the set of target nodes, *multicast set*. The usage of multicast packets instead of several unicast packets (one for each node in

the multicast set) or one broadcast packet (that can be omitted by the nodes not included in the multicast set) is a good source for energy conservation when the multicast set has more than one node but does not include all possible nodes in the network. In the first case, some resources could be overused as the same information is sent several times; in the second one, several resources may be used unnecessarily as information reaches hosts which are not in the multicast set. It is also important to notice that if a unicast or broadcast transmission is needed in a network only equipped with a multicasting protocol, proper multicast sets can be used for emulating both of them. Furthermore, the behaviour of these multicast transmissions is indistinguishable both in energy conservation and in network efficiency from real unicast or broadcast signals, respectively.

In addition, many network protocols for wireless ad-hoc networks require broadcasting or multicasting communication primitives to update their states and maintain the routes between nodes. Multicasting is also widely used in sensor networks to disseminate information about environmental changes to other nodes in the network. These usages justify the importance of developing efficient broadcasting and multicasting protocols optimized for energy consumption.

In Figure 1.1 two different patterns for a broadcast transmission from node 1 are shown. Consumed power diminishes when a good communication pattern is chosen. Note that the light gray node (yellow node in the online version) is the source node.

(a) Basic transmission schema (b) Energy-aware transmission schema

Figure 1.1: Energy benefits of usage of relay nodes. (a) shows a configuration one-to-all, and (b) shows an energy-aware configuration using intermediate nodes.

Although minimizing energy consumption has been addressed only in few studies in the context of mobile ad-hoc networks ([19]), the equivalent optimization problem in the context of static ad-hoc networks (*static WANETS*) has been studied more extensively in the last years. The scope of this thesis will also cover this second case in which the node positions are known *a priori*, or equivalently, we consider that the network structure is given and static. This guarantees that the required power for a given transmission in some instant of time will remain invariable until the depletion of the battery of any node in the transmission's route.

If energy limitations are considered, then ad-hoc networks require an energy-aware metric in their routing algorithms. Typically, there are two main energy-aware metrics and their corresponding problem formulations for multicasting in WANETs are:

1. Minimizing the total transmission power consumption of all nodes involved in the multicast session.

2. Maximizing the operation time of the network until the battery depletion of any node in the multicast session.

In addition to the advances in energy-aware optimization obtained from the consideration of the above problems, which do not require modifications in the infrastructure used, the recent use of directional antennas in wireless communication has further enabled new approaches for energy saving in WANETs. Directional antennas can concentrate their beam to a particular target, saving the energy that would be usually used by sending in unwanted directions. Therefore, the study of the two software based solutions over this different kind of infrastructure (nodes equipped with directional antennas) suggests a new study of the energy saving capabilities of a network.

In Figure 1.2 a two transmission schemas for a network when omnidirectional (Figure 1.2(a)) or directional(Figure 1.2(b)) antennas ares used, respectively.

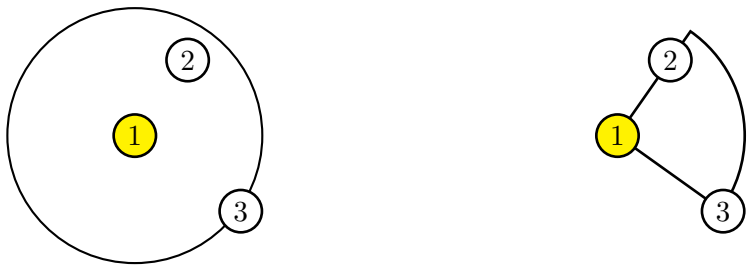

(a) Solution with omnidirectional antennas (b) Solution with directional antennas

Figure 1.2: Energy benefits of using of directional antennas. (a) shows a configuration with omnidirectional antennas, and (b) shows a configuration with directional antennas.

The recent beam-forming technology permits saving energy by concentrating RF transmission power where it is needed. In addition, as the beam is generated in one direction, it creates less interferences to other nodes outside the beam covered area allowing a higher level of information flow in the network and makes the system more secure since nodes outside the beam coverage do not receive the signal. These reasons generate big expectation about the implications (benefits) of directional antennas in energy-aware wireless networks.

With these technologies installed in the network infrastructure some new considerations should be taken into account. For example, and of maximum interest for energy-aware ad-hoc networks, the beam covered area can be extended in some different ways. If a given node is transmitting to a particular set of nodes and wants to reach a new one it can now consider several options, unlike when working with omnidirectional antennas where the only way to reach new nodes is by increasing the distance of the emission. Now, the antenna beam, and thus the antenna covering area, depends not only on the distance of emission but also on two

more variables: the direction of the emission or beam orientation (φ) and the beam width (θ). In Figure 1.3 four configurations for a directional antenna of a transmitting node are shown. Figure 1.3(a) shows a configuration in which the source node is only reaching one node, and in Figure 1.3(b), Figure 1.3(c) and Figure 1.3(d) new nodes are added and different variables are modified in order to reach all the new nodes.

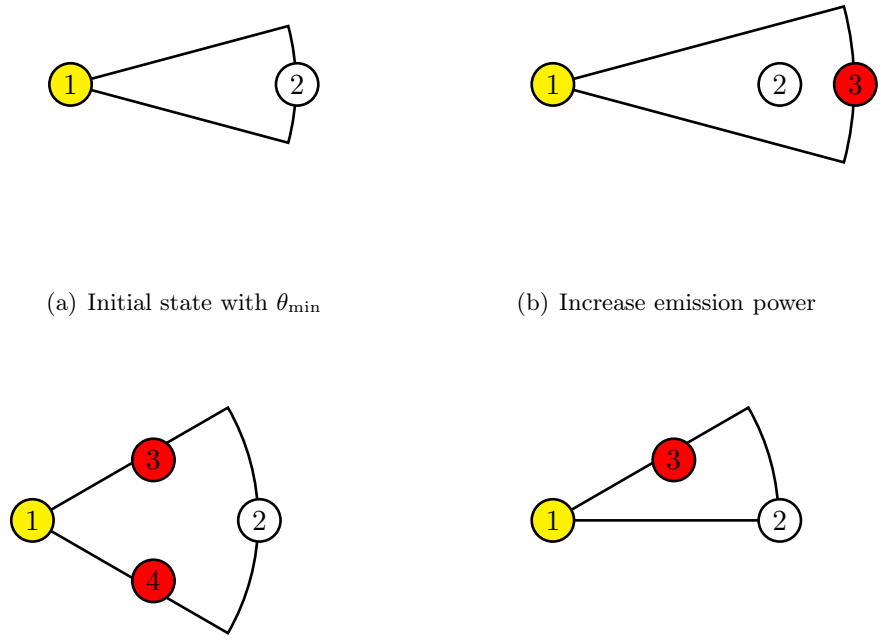

(a) Initial state with $\theta_{\min}$

(b) Increase emission power

(c) Increase beam width

(d) Change beam orientation

Figure 1.3: Methods for reaching new nodes from a transmitting node with a directional antenna. In this example the antenna has a minimum beam width of 30°. (a) shows the initial configuration, (b) beam distance extension, (c) beam width increase, and (d) orientation change. Note that the gray nodes (red nodes in the online version) are the new nodes added in each different configuration.

These methods for extending the area of reception of the signal play a key role when trying to improve the energy saving capabilities of the network.

The above explanation (see also [26]) suggests the consideration of the following two different problems in energy-aware wireless networks:

1. The minimum energy broadcast/multicast (MEM/MEB) problem in WANETs with *omnidirectional* antennas.

2. The MEM/MEB problem in WANETs with *directional* antennas.

We will give a technical description of these problems in Section 1.3.

As the MEM problem is NP-hard for both directional and omnidirectional antennas, even when restricting the information flow to broadcast packets (MEB problem). The exact algorithms known for solving them are not interesting for practical purposes. Instead, approximate, but faster, algorithms should be considered. Although the literature offers some polynomial time heuristic algorithms designed to solve it, in this work a metaheuristic will be developed. More specifically, the Ant Colony Optimization metaheuristic will be used. The Ant Colony Optimization metaheuristic was first introduced by Marco Dorigo and colleagues in the early 90s [13, 15, 16]. It is a nature inspired algorithm which is mainly based on the collective behaviour of ants and their behaviour of searching for good food sources.

The rest of this introduction is organized as follows. First, a description of the antenna model considered is given. Then, the *Wireless Multicast Advantage* is introduced. Finally, a formal definition of the *Minimum Energy Multicast/Broadcast* problem is given and previous work for this problem is shortly presented.

1.1 Antenna model

As most other works in this area the following wireless communication model will be considered (see [46]). Given a set of network nodes V, each node $v \in V$ can choose an emission power p_v such that $0 \leq p_v \leq p_{\max}$, where $p_{\max}$ is the maximum emission power possible. By setting $p_{\max}$ to ∞ it is assured that broadcasting is always possible. Signal power diminishes at a rate proportional to $r^{-\alpha}$, where r is the distance to the signal source, and α is a parameter that, depending on the environment, takes typically values between 2 and 4. In this work we choose (as in most other works) $\alpha = 2$[1]. A sender node v is able to successfully transmit a signal to a receiver node u if $p_v \geq k \cdot d(v,u)^\alpha$, where p_v is the emission power, $d(v,u)$ is the Euclidean distance between v and u, and k is the receiving node's power threshold for signal detection which is usually normalized to 1. The minimum emission power such that the transmission from node v reaches node u is:

$$p_{vu} := d(v,u)^\alpha \tag{1.1}$$

In the case of directional antennas we use an idealized model (as used, for example, in [52]) in which we assume that the transmitted energy is concentrated uniformly in a beam of width θ, that is, we neglect fading effects at the borders of the beam. We assume that the beam width θ can be chosen for each antenna so that $\theta_{\min} \leq \theta \leq 360$. As in [52], we choose $\theta_{\min} \in \{30°, 60°, 90°\}$. Furthermore, we assume that each antenna beam can be pointed in any desired direction in order to provide connectivity to a set of the nodes that are within communication range and within the sector covered by the beam. The energy spent by a node v transmitting to a node u with a beam width of θ_v is:

$$p_{vu}^{\theta_v} := \frac{\max\{\theta_v, \theta_{\min}\}}{360} \cdot d(v,u)^\alpha \tag{1.2}$$

This shows that a node v equipped with a directional antenna only uses $\frac{\theta_{\min}}{360}$ of the energy used by an omnidirectional antenna to transmit information to just one other node u.

[1] Note, however, that the algorithms presented in this thesis do not depend on α.

1.2 Wireless Multicast Advantage

WANETs must support typical communication patterns in classical networks. As mentioned before, this category includes broadcasting and multicasting. One of the big differences with traditional wired networks, is the key role played by energy. In wirless ad-hoc networks energy is the critical constraint. For example, in explorers or hikers ad-hoc networks, to recharge or replace the individual user's battery is impossible. In this situation when battery depletions begin to appear the network consistency will be thretened, dramatically decreasing network performance and partitioning the network in smaller independent networks not connected between them. As stated in [56], in the last eleven years battery capacity has only increased by a factor of 2.7. This *datum* suggests that energy saving procedures should be deployed in order to extend wireless ad-hoc networks lifetime and networks consistency and performance during their lifetimes.

The main energy consumer in WANETs is communication. Therefore, the selection of relay nodes, RF transmission power and correct beam width and beam direction are some of the major considerations in broadcast and multicast routing algorithm design.

For the next explanation the case of all nodes equipped with omnidirectional antennas will be considered, although the ideas are easily extensible to the case of directional antenna networks. When a source node emits an information packet it must decide its transmission power. Recievers of this signal must act as relay nodes in order for the packet to reach all its destination nodes. This is, to establish communication through the network each node must be assigned a transmission power. As stated before, with the antenna model used, if v is a transmitter, u is another node, p_v is the transmission power of node v and $d(v,u)$ is the Euclidean distance from v to u, the signal emitted by v reaches u if $p_v \geq d(v,u)^\alpha$. When the above inequality holds for an emitting node v and any other node u, we say that v is connected to u through a direct link. The other way of establishing a communication path is by means of intermediate nodes that will act as relay nodes. In this schema, a chain of pairs of nodes directly linked (i.e. holding the above inequality) must exist in order to guarantee the existence of a communication path from v to u.

But, as it would had been noticed, if v and u are such that $p_v \geq d(v,u)^\alpha$ then for all nodes w with $d(v,w) \leq d(v,u)$, $p_v \geq d(v,w)^\alpha$ holds trivially. This means that creating a direct link from v to u will also assure that v will establish a direct link to all nodes that are closer (or at exactly the same distance) to v than u. A transmission can be thought as an area of coverage and all nodes in the area will receive the signal with one single emission. Hence, a node v can transmit the same message to nodes $u_1, u_2, \ldots, u_k$, in only one transmission using the maximum of the powers required for reaching each host:

$$p_v^{wireless} = \max\{p_{vu_i} | 1 \leq i \leq k\} \tag{1.3}$$

By contrast, wired networks, require v making one different transmission for every node, and hence, the power required for transmitting from node v to nodes $u_1, u_2, \ldots, u_k$ will be the sum of the transmission power required for the connection from v to every host:

$$p_v^{wired} = \Sigma_{i=1}^{k} p_{vu_i} \tag{1.4}$$

Figure 1.4 shows the different communication schemas and infrastructure needed for two networks with the same nodes, one being a wireless network (Figure 1.4(a)) and the other a wired network (Figure 1.4(b)).

When talking about wireless networks, the benefit in power consumption of this different behaviour from wired networks on the consequences of establishing a connection between two nodes, which converts any wireless unicast transmission in a multicast transmission, is called *Wireless Multicast Advantage* [51] (or *WMA*). It must be noticed that the *Wireless Multicast Advantage* is inherent to the wireless network model because the communication channel of wireless networks is the air and, thus, any node in the area covered by the emission can receive the signal. Even for security reasons, wireless networks cannot establish real one to one connections like wired networks do. The *Wireless Multicast Advantage* offers benefits in power consumption for both broadcast and multicast sessions over mobile or static ad-hoc networks. However it is also the source of the higher level of complexity that presents the MEB problem, which recently has been classified as NP-hard [5, 43], while the analogous problem for wired networks can be easily solved creating a minimum spanning tree (MST), what situates the problem in P.

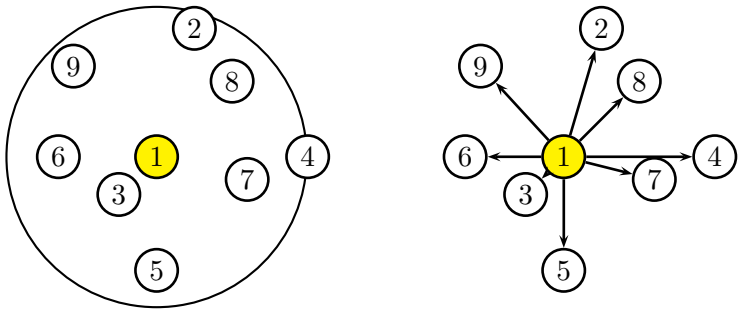

(a) Wireless Network (b) Wired network

Figure 1.4: *Wireless Multicast Advantage* in omnidirectional antennas.

It is also interesting to see that when working with directional antennas the *Wireless Multicast Advantage* also generates benefits in energy consumption although now the covered area is not only defined by the length of the emission but also by the beam width and beam orientation variables. In Figure 1.5 an example of the benefits of the *Wireless Multicast Advantage* over a wireless network with directional antennas is shown.

1.3 The Minimum Energy Multicast/Broadcast problem

The *Minimum Energy Multicast* (or MEM) problem is an NP-hard optimization problem [5] both in the case of omnidirectional and directional antennas. It can be stated as follows. Given is a set V of nodes with fixed positions in a 2-dimensional area. Introducing a directed link (v, u) between all (ordered) pairs $v \neq u$ of nodes such that $d(v, u)^\alpha \leq p_{\max}$, where $d(v, u)$

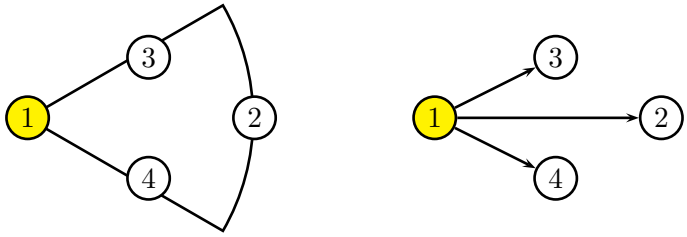

(a) Wireless Network (b) Wired network

Figure 1.5: *Wireless Multicast Advantage* in directional antennas.

is the Euclidean distance between v and u, induces a directed network $G = (V, E)$. In the following we first deal with the case of omnidirectional antennas. Given a source node $s \in V$ and a multicast set $M \subseteq V$, one must find emission powers for all nodes such that a multicast packet from s to all nodes in M is possible, and such that the sum of all emission powers is minimal. This corresponds to finding a directed tree $T = (V_T, E_T)$ in G with root node s and $M \subseteq V_T$ such that function $P_o()$ is minimized:

$$P_o(T) := \sum_{v \in V_T} \max_{(v,u) \in E_T} d(v,u)^\alpha \tag{1.5}$$

where $\max_{(v,u)\in E_T} d(v,u)^\alpha$ is the emission power chosen for node v. In the case of directional antennas, in addition to an emission power, a beam width θ_v and a beam direction must be chosen for each node $v \in V$. Again, this corresponds to finding a directed tree $T = (V_T, E_T)$ with root node s in G such that function $P_d()$ is minimized:

$$P_d(T) := \sum_{v \in V_T} \frac{\max\{\theta_v, \theta_{\min}\}}{360} \cdot \max_{(v,u) \in E_T} d(v,u)^\alpha \ , \tag{1.6}$$

where θ_v is set to the minimum beam width possible such that all children of v in T are reached. The beam direction follows automatically from the known locations of all the children of v in T. It must also be noticed that the reason because solutions to this problem are trees is because connectivity is a requirement as there is only one source for each session and that no cycles can appear in the solution. Note that, in what to energy efficiency refers, solutions containing one or more cycles can always be improved removing a certain edge of one of the cycles (the edge that is transferring data to a node which can be reached by a shorter path from the source). With this procedure a directed spanning tree can always be reached for any given network configuration.

Furthermore, the *Minimum Energy Broadcast* (MEB) problem is a particular case of the MEM problem in which all network nodes must be reached. That is, $M = V$.

Several approaches for solving this problem, in its different versions, have appeared in the literature. The Mixed Integer Linear Programming (MILP) formulation from [25] for the

MEM problem with directional antennas can be solved to optimality, but *unfortunately* this requires exponential time. This point makes it unusable for practical applications as solving instances of 50 nodes takes longer than 24 hours. This implies the need for faster algorithms offering good results (although without a global optimality guarantee). It must be noticed that as the above mentioned formulation solves the most general case of the problem it will also solve the special cases. For example, the omnidirectional antenna case can be considered a directional antenna case with $\theta_{\min} = 360°$. In Figure 1.6 this MILP formulation is shown (and in Table 1.1 additional details are given).

Table 1.1: Definition of constants A_{vu}, B_{vu} and C_{vu} of the MILP formulation in Figure 1.6. Note that $\forall v, u \in N\ \alpha_{vu} \in [0, 2\pi)$.

	$0 \leq \alpha_{vu} \leq \pi$	$\pi \leq \alpha_{vu} \leq 2\pi$
A_{vu}	-2	2
B_{vu}	$4\pi + 2\alpha_{vu}$	$8\pi - 2\alpha_{vu}$
C_{vu}	0	4π

In the heuristic field, there are also several solutions proposed. It is not the purpose of this work to analize them, but a broad classification in three different families is given in the extensive and comprehensive survey [26] and, for the MEB problem with omnidirectional antennas it is reproduced in Figure 1.7. Figure 1.8 shows a similar calssification for the MEM problem with omnidirectional antennas case. As stated by Guo and Yang ([26]) the categories are:

- Spanning tree algorithms: A class of greedy heuristics that obtains feasible solutions by constructing a rooted spanning tree.
- Topology control algorithms: Based on transmission power adjustment, topology control algorithms assign transmission powers to the nodes such that the resulting topology (not necessarily being a tree) achieves certain connectivity properties, and such that certain objective functions of the tranmission powers are optimized.
- Local search algorithms: This class of heuristics iteratively improves an initial feasible solution using local search technology.

In the following, the state of the art for the MEB problem will be described. The MEB problem in the case of omnidirectional antennas has been tackled with centralized heuristics as, for example, [51, 49, 44]. The most popular constructive technique is the *broadcast incremental power* (BIP) algorithm by Wieselthier et al. [51]. Moreover, local search methods including tree-based methods such as [37, 22] and power-based methods such as [11] have been developed. More recently the MEB problem was also tackled by metaheuristics [10, 33, 1, 55].

The best results known for the MEB problem when omnidirectional antennas are considered are those given in [55] which, on average, can solve 50 nodes random instances with an average excess of 2.50% over the optimal (or best known) solution in 5.5 seconds and finding optimal solutions on 7.53 out of 30 trials per problem instance. Or, if more time is given, same size instances can be solved with an average excess of 0.61% in 46 seconds and finding

Objetive Function: Minimize $\sum_{v \in N} Pv$
Subject to:

I) Rooted Tree Property

$$\sum_{v \in N} (Z_{vs1} + Z_{vs2}) = 0$$

$$\sum_{v \in N} (Z_{vu1} + Z_{vu2}) = 1; \forall u \in M \backslash \{S\}$$

$$\sum_{v \in N} (Z_{vu1} + Z_{vu2}) \leq 1; \forall u \in N \backslash M$$

$$\sum_{v \in N} (Z_{uv1} + Z_{uv2}) \leq (n-1) \sum_{v \in N} (Z_{vu1} + Z_{vu2}); \forall u \in N \backslash M$$

$$\sum_{v \in N} F_{vu} - \sum_{v \in N} F_{uv} = \sum_{v \in N} (Z_{vu1} + Z_{vu2}); \forall u \in N \backslash \{S\}$$

$$(Z_{vu1} + Z_{vu2}) \leq (n-1)(Z_{vu1} + Z_{vu2}); \forall u \in N \backslash \{S\}, v \in N$$

II) Wireless Multicast Advantage Property

$$p_{\max} \geq P_v \geq \frac{r_{uv}^{\alpha}}{2\pi} Y_{vu}; \forall v, u \in N$$

$$0 \leq Y_{vu} \leq 2\pi (Z_{vu1} + Z_{vu2}); \forall v, u \in N$$

$$Y_{vu} \leq \theta_v; \forall v, u \in N$$

$$\theta_v - Y_{vu} + 2\pi (Z_{vu1} + Z_{vu2}) \leq 2\pi; \forall v, u \in N$$

III) Antenna Coverage Property

$$A_{vu} \varphi_v - \theta_v + B_{vu} Z_{vu1} \leq c_{vu}; \forall v, u \in N$$

$$2\varphi_v - \theta_v + (4\pi - 2\alpha_{vu}) Z_{vu2} \leq 4\pi; \forall v, u \in N$$

$$2\varphi_v - \theta_v - 2\alpha_{vu} Z_{vu2} \geq 0; \forall v, u \in N$$

$$0 \leq \varphi_v < 2\pi; \forall v \in N$$

$$\theta_{\min} \leq \theta_v \leq \theta_{\max}; \forall v \in N$$

IV) Integrality Property

$$Z_{vu1} \in \{0,1\}, Z_{vu2} \in \{0,1\}; \forall v, u \in N$$

Figure 1.6: MILP formulation for the MEM problem for ad-hoc networks with directional antennas. Note that the set of nodes N, the multicast set M, the source node $s \in N$ and values $\theta_{\min}$, $\theta_{\max} \in [0, 2\pi)$ and $p_{\max} \in [0, \infty)$ are parameters. Additionally, $\forall v$, $u \in N$, α_{vu} $(0 \leq \alpha_{vu} < 2\pi)$ is the angle measured counter-clockwise from the horizontal positive axis to the vector $\vec{vu}$ and A_{vu}, B_{vu} and C_{vu} are constants defined in Table 1.1. Finally, $\forall v$, $u \in N$, Z_{vu1} and Z_{vu2} are binary variables and P_v, F_{vu}, Y_{vu}, θ_v and φ_v are continuous variables. Note that the number of variables is $\mathcal{O}(n^2)$. The number of constraints is, also, $\mathcal{O}(n^2)$.

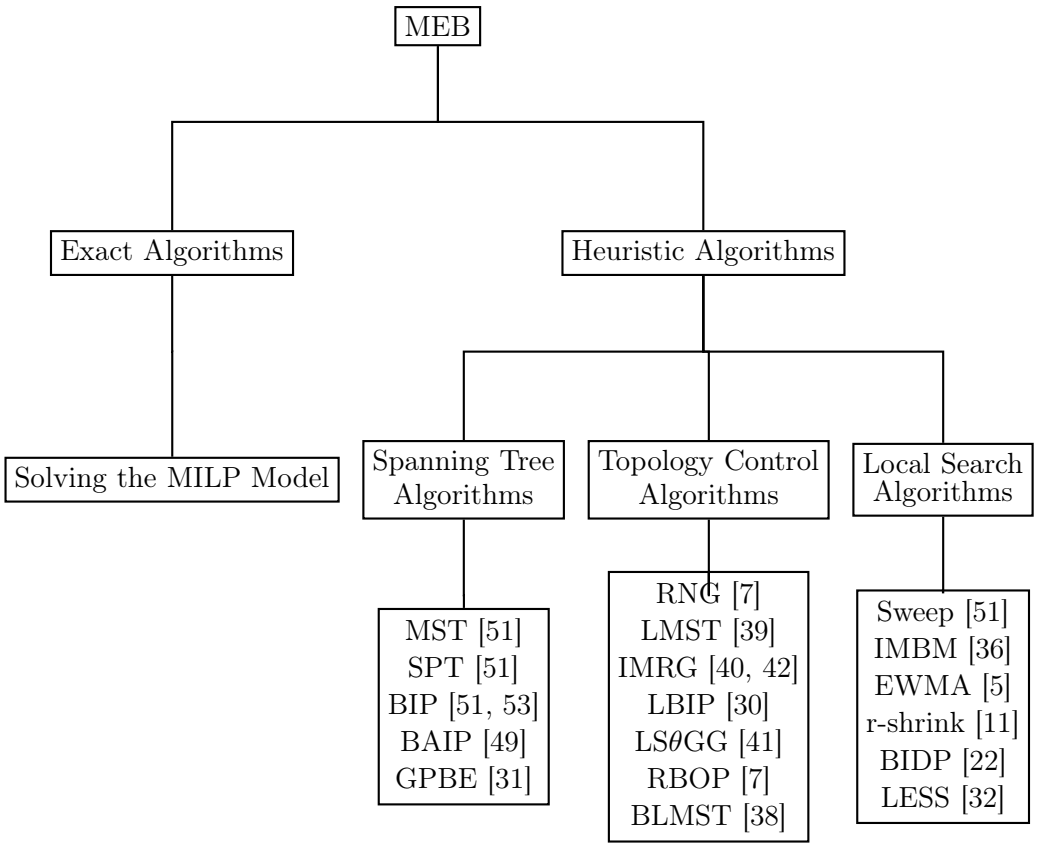

Figure 1.7: Taxonomy of MEB problem solutions in static ad-hoc networks with omnidirectional antennas

optimal solutions in 17.3 out of 30 trials.

The case of directional antennas is less studied. Constructive algorithms include, for example, the version of BIP for directional antennas: D-BIP [52]. Other approaches can be found, for example, in [8, 24].

Note that no exhaustive evaluation of any algorithm in comparison to optimal solutions for the MEM problem has been found in the literature and, thus, no reference values can be provided. Well performing algorithms for the MEM problem are, for example, the MIP (from [51]) and D-MIP (from [52]) algorithms or the distributed algorithm S-REMiT (from [50]).

A summary of the complexity of the problems described in the last two sections is shown in Table 1.2.

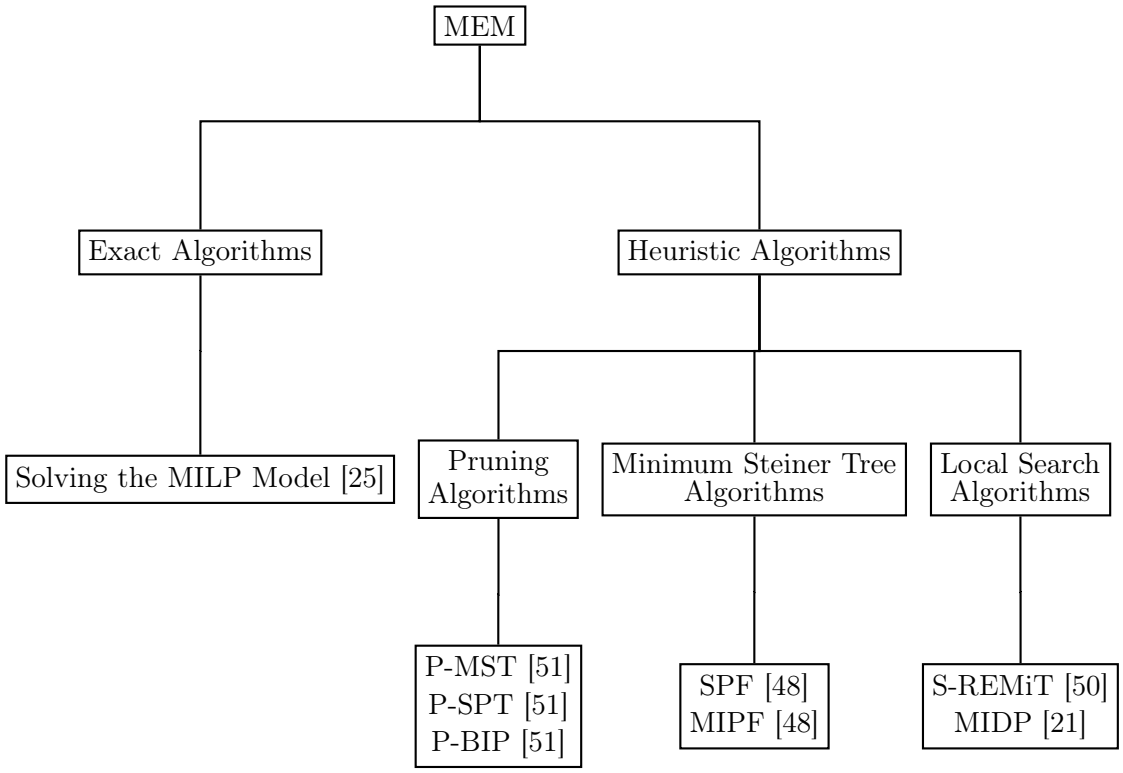

Figure 1.8: Taxonomy of MEM problem solutions in static ad-hoc networks with omnidirectional antennas

Table 1.2: Classification of energy-aware multicasting/broadcasting optimization problems.

	Minimum energy	
	MEB	**MEM**
Omnidirectional antenna	NP-hard	NP-hard
Directional antenna	NP-hard	NP-hard

Chapter 2

Ant Colony Optimization

As mentioned before, in this work we propose an *Ant Colony Optimization* (ACO) [17] algorithm for the MEM/MEB problem. ACO is a nature-inspired metaheuristic for the solution of combinatorial optimization problems introduced by Marco Dorigo [17] in the early 1990.

Metaheuristics are algorithm families which share a common skeleton. The idea of metaheuristics is to create abstract algorithms which only require to be defined in the behaviour of some functions which are dependant on each particular problem, for example, a neighbourhood space navigator or a best solution checker. Sharing this common structure, enables a faster and easier conception of the new heuristics. The field of metaheuristics design for solving combinatorial optimization problems has received high attention in the last years [3]. Their applications and interest through the scientific community has grown considerably, until it has become a huge and independant area of research. There are well known metaheuristics in the literature, a good example is the *Simulated Annealing* metaheuristic [35, 9].

The ACO metaheuristic is based on the fundamentals of cooperation of ants:

1. Big population: The existence of a big set of simple, not selfish, entities
2. Distributedness: No global control of each entity or the tasks done
3. Self-organization: Some communication channels must exist between entities

These three properties enable insect societies to accomplish cooperatively complex tasks, without the need of any control agent.

In particular, ACO was inspired by the way real ant colonies forage for food: ants first try random paths to explore the area near them. Once a food source is found, some food is collected and they return back to the nest. While moving, ants leave pheromone trails on the ground. As the ants returning through the shortest paths will arrive earlier, much more pheromone will be left on these paths. Hence, the ants leaving the nest will, in probability, choose those paths more than the longer ones. Furthermore, the number of ants choosing short paths will increase and, hence, the pheromone trails on them will increase faster at the same time that evaporation leaves other paths with low pheromone concentration levels. In essence, the indirect communication established via pheromone trails (*stigmergy* [18]) allows ant colonies to find shortest paths between their nest and food sources ([12]). In Figure 2.1 a

sketch of this behaviour is shown.

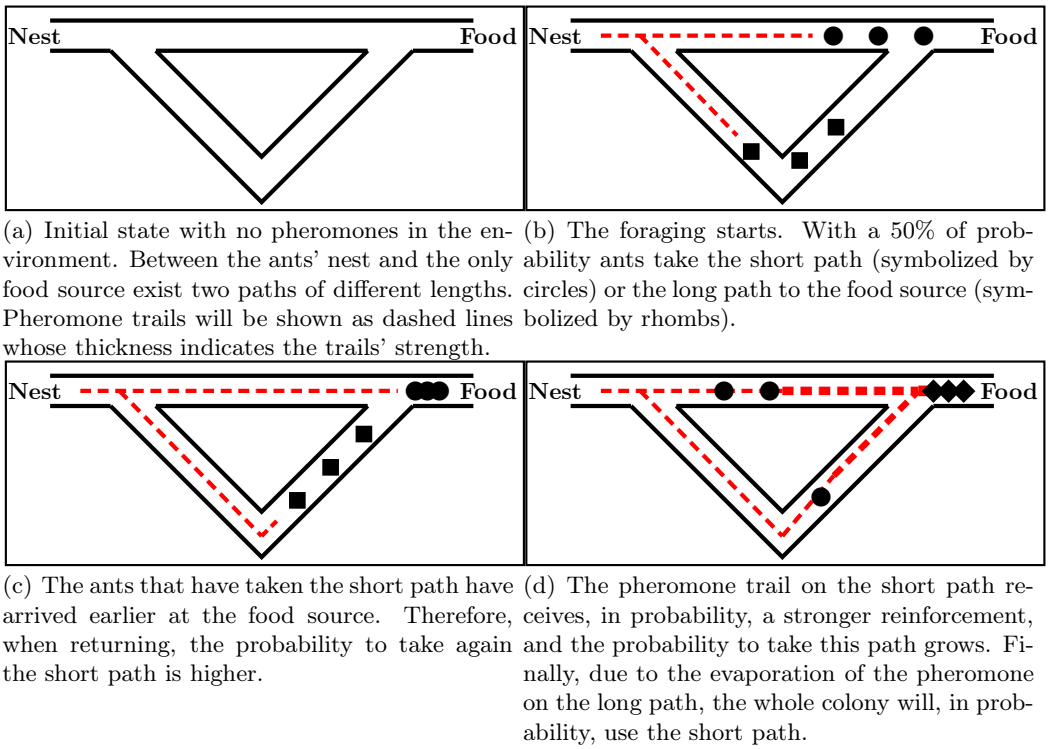

(a) Initial state with no pheromones in the environment. Between the ants' nest and the only food source exist two paths of different lengths. Pheromone trails will be shown as dashed lines whose thickness indicates the trails' strength.

(b) The foraging starts. With a 50% of probability ants take the short path (symbolized by circles) or the long path to the food source (symbolized by rhombs).

(c) The ants that have taken the short path have arrived earlier at the food source. Therefore, when returning, the probability to take again the short path is higher.

(d) The pheromone trail on the short path receives, in probability, a stronger reinforcement, and the probability to take this path grows. Finally, due to the evaporation of the pheromone on the long path, the whole colony will, in probability, use the short path.

Figure 2.1: Experimental setting that shows the shortest path finding capability of ant colonies.

This behaviour in nature of real ants is exploited in ACO in order to solve, for example, discrete optimization problems. The ACO metaheuristic is considered one of the most relevant developments in *Swarm Intelligence*, a branch of Computer Science, highly related to *Artificial Intelligence* that studies the algorithmic properties of the collective behaviour of social insects like ants, termites, bees, wasps and other animals suchs as flocks of birds or fish schools. Examples of swarm intelligent algorithms other than ACO are those for clustering and data mining inspired by ants' cemetery building behaviour [27, 45], those for dynamic task allocation inspired by the behaviour of wasp colonies [6], and particle swarm optimization [34].

In the ACO metaheuristic *ants* decide on the quantity of pheromone deposited, which may depend on an evaluation of the quality of the food source. With this additional evaluation and regulation skills, pheromone trails will guide other ants to the best food sources following, in some way, a collective criteria of all the ants working in the colony.

A useful property of ACO metaheuristic based algorithms relates to distributed computing. As the algorithm emulates the behaviour of several ants making the same task, this metaheuristic can be parallelized, at least, in a naive way, which consists in letting each processor emulate a different ant at the same time.

Our model of the foraging behaviour of real ants in Figure 2.1 can not be directly applied to combinatorial optimization problems because it only associates pheromone trails to

complete solutions of the problem. This way of modeling implies that the solutions to the considered problem are already known but in combinatorial optimization the objective is to find an unknown optimal solution. Thus, when CO problems are considered, solutions will be divided in several solution components and each one will have its own pheromone value associated. Each ant will choose one solution component at each step, until a full solution to the problem is assembled. Generally, the set of solution components is expected to be finite and of moderate size. $\mathcal{T}$ denotes the set of all pheromone values, more formally, $\mathcal{T} = \{\tau_i \mid c_i \text{ is a solution component}\}$.

One of the important facts in the development of an ACO based heuristic is to choose a good pheromone model and pheromone update method. While the pheromone model is highly related to each different problem, there are some well known pheromone update methods in the literature (Table 2.1). The choice among them may depend also on the problem characteristics.

Table 2.1: A selection of pheromone update systems

ACO variant	**Authors**	**Main reference**
Elitist AS (EAS)	Dorigo	[13]
	Dorigo, Maniezzo, and Colorni	[16]
Rank-based AS (RAS)	Bullnheimer, Hartl, and Strauss	[4]
$\mathcal{MAX}$–$\mathcal{MIN}$ Ant System ($\mathcal{MM}$AS)	Stützle and Hoos	[47]
Ant Colony System (ACS)	Dorigo and Gambardella	[14]
Hyper-Cube Framework (HCF)	Blum and Dorigo	[2]

The first pheromone update system, and also one of the simplest, is the *Ant System* (AS). The rules for the Ant Systemare:

- Pheromone update: $\tau_i \leftarrow (1-\rho) \cdot \tau_i$
- Reinforcement: $\tau_i \leftarrow \tau_i + \rho \cdot \sum_{\{s \in S_{iter} | c_i \in s\}} F(s)$

where $\rho \in [0,1]$ is the evaporation rate, S_{iter} is the set of solutions generated in the current iteration (being each solution a set of solution components) and F is the quality function $F : S \rightarrow \mathbb{R}^+$. Typically, when minimizing, $F(\cdot) = \frac{1}{f(\cdot)}$.

The complete ACO metaheuristic is shown in Algorithm 1. The rest of this chapter will be focused on the explanation of the pheromone update mechanism.

The first algorithm based on the ACO metaheuristic was one for solving the well known *Travelling Salesman Problem* (see Definition 1). An example for the TSP case is used here to explain the main steps in the construction of an ACO algorithm.

Definition 1 *In the TSP a completely connected, undirected graph $G = (V, E)$ with edge-weights is given. The nodes V of this graph represent the cities, and the edge weights represent the distances between the cities. The goal is to find a closed path in G that contains each node exactly once (henceforth called a tour) and whose length is minimal. Thus, the search space $\mathcal{S}$ consists of all tours in G. The objective function value $f(s)$ of a tour $s \in \mathcal{S}$ is defined as the sum of the edge-weights of the edges that are in s. The TSP can be modelled in many different*

Algorithm 1 ACO metaheuristic

```
1: INPUT: An instance I of a combinatorial problem P
2: InitializePheromoneValues(T)
3: while termination conditions not met do
4:    S_iter ← ∅
5:    for j = 1, ..., n_a do
6:       s ← ConstructSolution(T)
7:       s ← LocalSearch(s) [OPTIONAL]
8:       S_iter = S_iter ∪ {s}
9:    end for
10:   ApplyPheromoneUpdate(T)
11: end while
12: OUTPUT: The best solution found
```

ways as a discrete optimization problem. The most common model consists of a binary decision variable X_e for each edge in G. If in a solution $X_e = 1$, then edge e is part of the tour that is defined by the solution.

Concerning the AS approach, the edges of the given TSP graph can be considered solution components, i.e., for each edge $e_{i,j}$ a pheromone value $\tau_{i,j}$ is introduced. The task of each ant consists in the construction of a feasible TSP solution, i.e., a feasible tour. In other words, the notion of *task of an ant* changes from *"choosing a path from the nest to the food source"* to *"constructing a feasible solution to the tackled optimization problem"*. Note that with this change of task, the notions of nest and food source loose their meaning.

The solution construction procedure of each ant is as follows. First, one of the nodes of the TSP graph is randomly chosen as start node. Then, the ant builds a tour in the TSP graph by moving to a new city in each construction step, and adding the traversed edge to the solution under construction. When all nodes have been visited the ant closes the tour returning to the starting node of the solution construction. Each solution construction step is performed as follows. Assuming the ant to be in node v_i and T be the set of previously visited nodes in the current tour construction, the subsequent construction step conists in adding a node v_j, such that $v_j \notin T$, and an edge $e_{i,j}$ to the tour under construction. This step is done with probability

$$\mathbf{p}(e_{i,j}) = \frac{\tau_{i,j}}{\sum_{\{k \in \{1,\ldots,|V|\} | v_k \notin T\}} \tau_{i,k}} \quad ,\forall\, j \in \{1,\ldots,|V|\}, v_j \notin T \ . \tag{2.1}$$

For an example of such a solution construction see Figure 2.2.

Once all ants of the colony have completed the construction of their solution, pheromone evaporation is performed as follows:

$$\tau_{i,j} \leftarrow (1-\rho) \cdot \tau_{i,j} \quad ,\forall\, \tau_{i,j} \in \mathcal{T} \tag{2.2}$$

Then the ants perform their return trip. Hereby, an ant that has constructed a solution s leaves the following pheromone trails in each $e_{i,j} \in s$:

$$\tau_{i,j} \leftarrow \tau_{i,j} + \frac{C}{f(s)} \ , \tag{2.3}$$

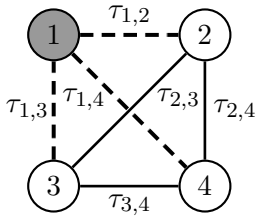

$$\mathbf{p}(e_{1,j}) = \frac{\tau_{1,j}}{\tau_{1,2} + \tau_{1,3} + \tau_{1,4}}$$

(a) First step of the solution construction.

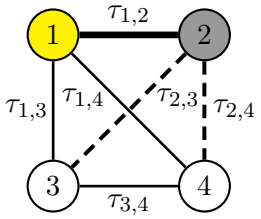

$$\mathbf{p}(e_{2,j}) = \frac{\tau_{2,j}}{\tau_{2,3} + \tau_{2,4}}$$

(b) Second step of the solution construction.

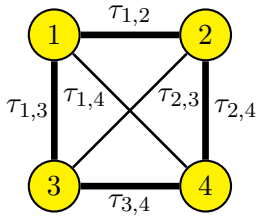

(c) The complete solution after the final construction step.

Figure 2.2: Example of the solution construction for a TSP problem consisting of 4 cities (modelled by a graph with 4 nodes; see Definition 1). The solution construction starts by randomly choosing a start node for the ant; in this case node 1. Figures (a) and (b) show the choices of the first, respectively the second, construction step. Note that in both cases the current node (i.e., location) of the ant is marked by dark gray color, and the already visited nodes are marked by light gray color (yellow in the online version). The choices of the ant (i.e., the edges she may traverse) are marked by dashed lines. The probabilities for the different choices (according to equation (4)) are given underneath the graphics. Note that after the second construction step, in which we exemplary assume the ant to have selected node 4, the ant can only move to node 3, and then back to node 1 in order to close the tour.

where C is a positive constant and $f(s)$ is the objective function value of the solution s. As it can be seen in the ACO metaheuristic description (Algorithm 1), n_a ants per iteration will performe these tasks until a stopping condition (e.g., a time limit) is satisfied.

Even though the AS algorithm proved that the ants foraging behaviour could be transferred into an algorithm for discrete optimization, it was generally found to be inferior to state-of-the-art algorithms. Fortunately, over the years several extensions and improvements of the original AS algorithm were introduced (see Table 2.1). In the next chapter, and for the development of our algorithms, the *Hyper-Cube Framework* (HCF) by Blum and Dorigo [2] is used and explained.

Chapter 3

ACO for the MEM/MEB problem

In previous chapters both the MEM/MEB problem and the Ant Colony Optimization metaheuristic have been introduced. In this one, with the target of solving the MEM and MEB problems with omnidirectional or directional antennas, new ACO algorithms will be developed. Hence, four different problems will be studied. Table 3.1 shows the four different algorithms that will be introduced in this chapter

Table 3.1: Problems studied in Chapter 3.

	MEM	**MEB**
Omnidirectional antennas	ACO	MACO
Directional antennas	D-ACO	D-MACO

Although in this chapter only one ACO algorithm for the four problems will be detailed, differences between the MEM or MEB problems when omnidirectional or directional antennas are considered can be used to obtain improved implementations for each particular problem. In fact, the main difference when choosing the antenna model is that when using omnidirectional antennas the inclusion of a new node in a partial solution consists in an increment of the emission power if the new connected node is the child that is furthest away from the father. On the other hand, in the directional antennas' case not only the distance to the father must be considered but also the increment in the beam width and the beam orientation necessary to reach the new node; similarly, differences between the algorithms for the MEM and MEB problems are tiny and will be explained in the corresponding points of its construction.

In addition to the ACO technique a local search procedure will also be developed. Local search will be based on the *r-shrink* procedure from Das et al. ([11]) but introducing some slight variations that enhance its performance. Although this algorithm was created to solve the MEB problem with omnidirectional antennas, its usage will be easily extended to the MEM problem with omnidirectional antennas and to the MEM/MEB problem with directional antennas. To apply this algorithm a *Variable Neighbourhood Descent* (VND) schema from [3] will be used.

Some definitions must be introduced in order to give a more formal description of the

r-shrink and other algorithms in this chapter.

Definition 2 *Given a directed graph $G = (V, E)$, where $V = \{v_1, v_2, \ldots, v_N\}$ is a set of nodes and E is a set of directed links, the **parents** of a node $i \in V$, denoted by $pa(i)$, is the set of nodes $\{j \mid (j, i) \in E\}$. The **children** of a node $i \in V$, denoted by $ch(i)$, is the set of nodes $\{j \mid (i, j) \in E\}$. Thus:*

$$j \in pa(i) \Longleftrightarrow i \in ch(j)$$

Remark 1 *Note that in a tree $T = (V, E)$ each node has at most 1 parent. That is:*

$$|pa(i)| \leq 1 \ \ \forall i \in V \tag{3.1}$$

Note that in the scope of this work, when talking about a tree, a directed tree is considered.

Example 1 *In Figure 3.1 $pa(5) = \{4\}$ and $ch(5) = \{6, 7, 8\}$.*

Definition 3 *Given a directed tree $T = (V, E)$, where $V = \{v_1, v_2, \ldots, v_N\}$ is a set of nodes and E is a set of directed links, a **directed path** between two nodes $i, j \in V$ is a sequence $< i, \alpha_0, \alpha_1, \ldots, \alpha_n, j >$ of distinct nodes such that $(\alpha_{k-1}, \alpha_k) \in E$, for all $1 \leq k \leq n$. $i \rightarrow j$ denotes that a directed path between nodes i and j exists.*

Example 2 *In Figure 3.1 $< 1, 2, 4, 5, 8 >$ is a directed path between nodes 1 and 8, however, $< 8, 5, 4, 2, 1 >$ is not a directed path between nodes 8 and 1.*

Definition 4 *Given a directed tree $T = (V, E)$, where $V = \{v_1, v_2, \ldots, v_N\}$ is a set of nodes and E is a set of directed links, the **descendants** of a node i in a tree, denoted by $de(i)$, is the set containing all nodes j, such that a directed path from i to j exists. Thus:*

$$de(i) \triangleq \{j \mid i \rightarrow j\}$$

*The **non-descendants** of a node i, denoted by $nd(i)$, is defined as:*

$$nd(i) \triangleq V \backslash \{i \cup de(i)\}$$

Example 3 *In Figure 3.1 $nd(4) = \{1, 2, 3\}$ and $de(4) = \{5, 6, 7, 8\}$.*

Definition 5 *Given a directed graph $G = (V, E)$, where $V = \{v_1, v_2, \ldots, v_N\}$ is a set of nodes and E is a set of directed links, The **indegree** of a node i, denoted by $d_{in}(i)$, and the **outdegree** of a node i are defined as follows.*

$$\begin{array}{rcl} d_{in}(i) & = & |pa(i)| \\ d_{out}(i) & = & |ch(i)| \end{array}$$

Example 4 *In Figure 3.1 $d_{in}(5) = 1$ and $d_{out}(5) = 3$.*

Remark 2 *Note that in a tree each node has indegree exactly 1 if it is not the source node and none otherwise, formally:*

$$d_{in}(i) = \begin{cases} 0, & \text{if } i = source \\ 1, & otherwise \end{cases} \ \ \forall i \in V \tag{3.2}$$

Definition 6 *Given a directed tree $T = (V, E)$, where $V = \{v_1, v_2, \ldots, v_N\}$ is a set of nodes and E is a set of directed links, a node is a* ***leaf node*** *(or simply a* ***leaf****) if its indegree is* 1 *and its outdegree is* 0*. Formally:*

$$\begin{aligned} |pa(i)| &= 1 \\ |ch(i)| &= 0 \end{aligned} \tag{3.3}$$

Example 5 *In Figure 3.1 node* 6 *is a leaf node. But node* 5 *is not a leaf node.*

A complete example of the properties of the nodes in a directed tree is given in Figure 3.1 and Table 3.2. Table 3.2 shows the properties of all the nodes of the directed tree T drawn in Figure 3.1.

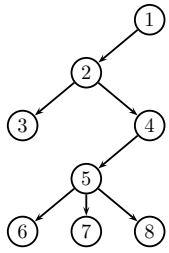

Figure 3.1: Example of a directed tree $T = (V_T, E_T)$.

Table 3.2: Table of properties for the directed tree $T = (V_T, E_T)$ in Figure 3.1.

i	$ch(i)$	$pa(i)$	$de(i)$	$nd(i)$	$d_{in}(i)$	$d_{out}(i)$	leaf?
1	$\{2\}$	$\emptyset$	$\{2,3,4,5,6,7,8\}$	$\emptyset$	0	1	*NO*
2	$\{3,4\}$	$\{1\}$	$\{3,4,5,6,7,8\}$	$\{1\}$	1	1	*NO*
3	$\emptyset$	$\{2\}$	$\emptyset$	$\{1,2,4,5,6,7,8\}$	1	1	*YES*
4	$\{5\}$	$\{2\}$	$\{5,6,7,8\}$	$\{1,2,3\}$	1	1	*NO*
5	$\{6,7,8\}$	$\{4\}$	$\{6,7,8\}$	$\{1,2,3,4\}$	1	3	*NO*
6	$\emptyset$	$\{5\}$	$\emptyset$	$\{1,2,3,4,5,7,8\}$	1	0	*YES*
7	$\emptyset$	$\{5\}$	$\emptyset$	$\{1,2,3,4,5,6,8\}$	1	0	*YES*
8	$\emptyset$	$\{5\}$	$\emptyset$	$\{1,2,3,4,5,6,7\}$	1	0	*YES*

Now, the BIP algorithm and its derivates will be explained. In the rest of this chapter the Sweep procedure will be explained. Then, first the r-shrink procedure and the Variable Neighbourhood Descent procedure will be introduced. In the following section, a description of each algorithm component of an ACO algorithm for the MEM problem with directional antennas will be presented. Then the full ACO solution obtained will be showed. Interesting issues in the difference of algorithm implementations for the MEM and MEB problems will be pointed out. Finally, similar remarks on implementation changes when using omnidirectional antennas in both the MEM and MEB problems will also be pointed out. Results for all cases will be presented and explained in the next chapter.

Algorithm 2 The BIP procedure

1: INPUT: a network $G = (V, E)$ and a source node $s \in V$
2: $T := (\{s\}, \emptyset)$
3: **while** $V_T \neq V$ **do**
4: $\quad (i, j) := \mathsf{argmin}_{\{(i,j)\in E |\, i\in V_T\, , j\in V\setminus V_T\}}\{P(T' \oplus (i, j))\}$
5: $\quad T' := T' \oplus (i, j)$
6: **end while**
7: OUTPUT: T

3.1 BIP and derived algorithms

The *Broadcast Incremental Power* (BIP) heuristic was developed by Wieselthier et al. in [51] for finding solutions to the MEB with omnidirectional antennas problem exploiting the Wireless Multicast Advantage (see Section 1.2). The BIP algorithm is easy to describe. Given a network and a source node, it begins with a partial solution tree that only includes the source node and it adds a new node at each step until all nodes in the network appear in the partial solution. The criterion used for choosing among the nodes not yet in the partial solution is the cost of addition of that node (using the most suitable node from the partial solution). That is, BIP wants to minimize the increment of the consumed power in the partial solution while adding one node and, thus, chooses the node that holds this property.

Algorithm 2 shows a formal description[1] of the BIP algorithm for the MEB problem.

In Figure 3.2 an execution of the BIP algorithm is described.

The *Multicast Incremental Power* (MIP) heuristic was also developed by Wieselthier et al. in [51]. In this case, the algorithm is used for finding solutions to the MEM problem with omnidirectional antennas exploiting, again, the Wireless Multicast Advantage (see Section 1.2). The MIP algorithm constructs a broadcast tree using BIP. Then, to obtain a multicast tree, the broadcast tree is pruned by eliminating all transmissions that are not needed to reach the members of the multicast group. More specifically, nodes with no downstream destinations in the multicast set will not transmit and some nodes will be able to reduce their transmitted power (if their most distant child has been pruned from the tree).

In Figure 3.3, examples of the solutions resulting from the execution of BIP and MIP over a random network with 20 nodes are given. Note that nodes belonging to the multicast set are painted in gray (dark blue in the online version).

These ideas were used in [52] to develop similar algorithms for the MEM/MEB problem with directional antennas. Two approaches were considered:

1. First, construct the tree using an algorithm designed for omnidirectional antennas. Then, reduce each antenna beam to the minimum possible width that preserves solution feasibility.

[1] The operation $\oplus$ between a directed tree $T = (V_T, E_T)$ and an edge $e = (i, j)$ appearing in the description is definied such that $T \oplus (i, j) := T' = (V_{T'}, E_{T'})$ where $V_{T'} = V_T \cup \{j\}$ and $E_{T'} = E_T \cup \{(i, j)\}$.

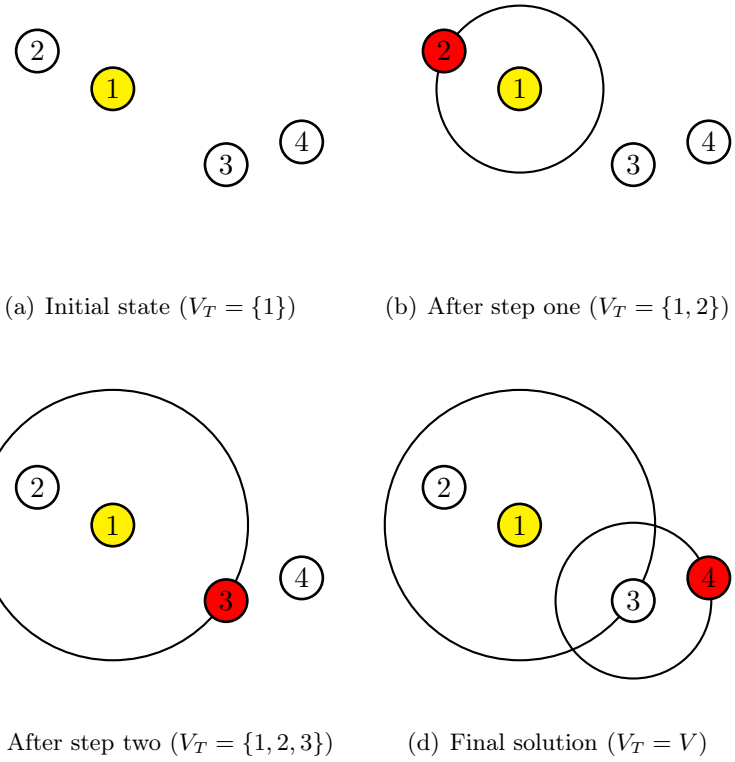

(a) Initial state ($V_T = \{1\}$) (b) After step one ($V_T = \{1, 2\}$)

(c) After step two ($V_T = \{1, 2, 3\}$) (d) Final solution ($V_T = V$)

Figure 3.2: Example of a BIP construction

2. Incorporate directional antenna properties into the tree construction process.

Note that antennas with a minimum beam width are considered and, hence, a new parameter $\theta_{\min}$ is considered given (see Section 1.1).

The *Reduced Beam BIP* (RB-BIP) and the *Reduced Beam MIP* (RB-MIP) just append a postprocessing phase to the construction of the BIP or MIP solution tree, respectively. This phase consists in reducing each node's antenna beamwidth to the smallest possible value that provides coverage of the node's downstream neighbours subject to the constraint $\theta_{\min} \leq \theta \leq 360$. Thus, the tree structure is independent of $\theta_{\min}$.

The *Directional BIP* (D-BIP) and the *Directional MIP* (D-MIP) algorithms are variations of the BIP and MIP algorithms, respectively. The only difference is that, in these algorithms, when calculating the required transmission powers, beam width and beam angle must be considered in addition to the transmission distance. However, using the definitions of required transmission power from Section 1.3 this problem is reduced to using the $P_d(\cdot)$ function for calculating required power of all nodes in the solution instead of the P_o function when deciding which is the node that minimally increments the solution's required power. It must be noticed that in the description of these algorithms the authors provide a fast way of calculating these required powers incrementally at each step. In our implementation these techniques are

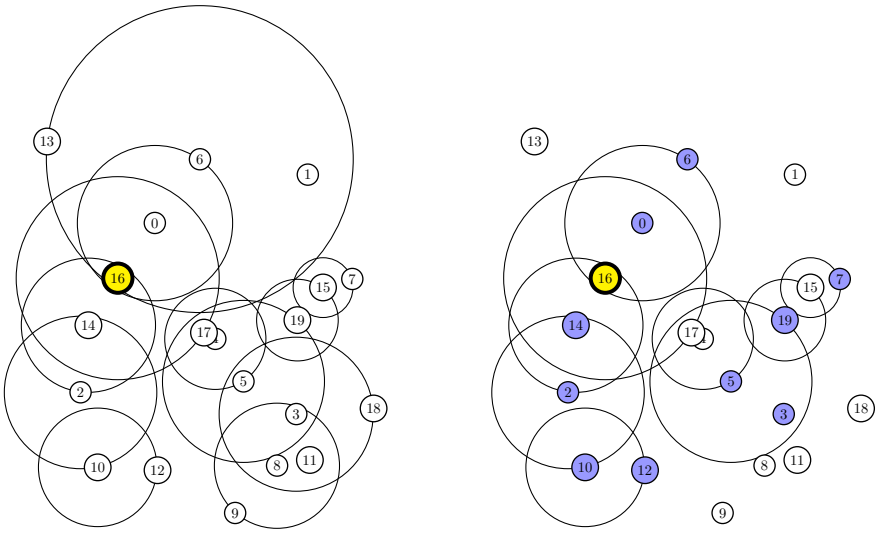

(a) BIP solution for network G (b) MIP solution for network G

Figure 3.3: Solutions found by BIP and MIP for a random network G of 20 nodes. Node 16 is the source node. To define the MEM instance an additional random multicast set M of 10 nodes is given.

adopted.

It is interesting to remark that when the minimum beam width is $\theta_{\min} = 360°$ (i.e. omni-directional antennas are considered), both the RB-BIP and the D-BIP behave exactly as the BIP does.

In Figure 3.4, examples of the schemas resulting from the execution of RB-BIP and D-BIP when using directional antennas with $\theta_{\min} = 30°$ over a random network with 20 nodes are given.

In Table 3.3 a classification (in terms of the problem they are designed for) of the BIP derived algorithms introduced in this section is shown. For further information and references see Section 1.3.

Table 3.3: Classification of the BIP family of algorithms for the MEM/MEB problem.

	MEB	**MEM**
Omnidirectional antennas	BIP	MIP
Directional antennas	RB-BIP	RB-MIP
	D-BIP	D-MIP

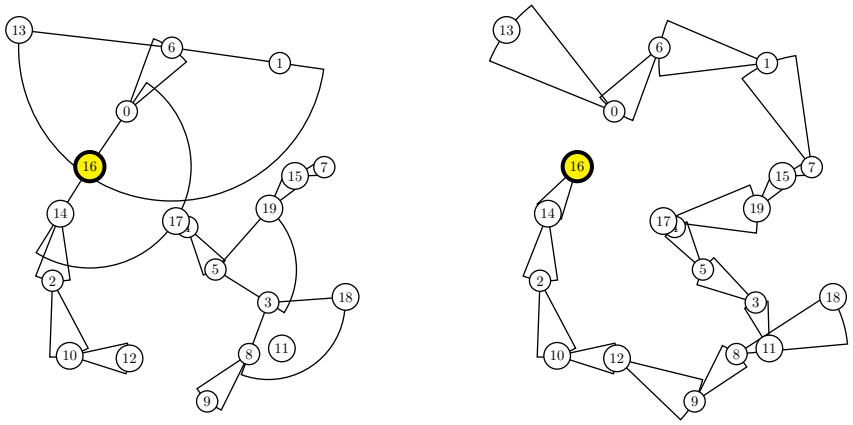

(a) RB-BIP solution for network G (b) D-BIP solution for network G

Figure 3.4: Solutions found with RB-BIP and D-BIP for a random network G of 20 nodes. Node 16 is the source node.

Finally, note that all algorithms in the BIP family are deterministic. Table 3.4 shows a comparison of time complexities for the different versions.

Table 3.4: Comparison of the BIP family of algorithms for the MEM/MEB problem.

Algorithm	**MIP/BIP**	**RB-MIP/RB-BIP**	**D-MIP/D-BIP**
Time complexity	$\mathcal{O}(n^3)$	$\mathcal{O}(n^3)$	$\mathcal{O}(n^3 \log n)$

3.2 Sweep

Given a solution $T = (V_T, E_T)$ to the MEB problem, the *Sweep* procedure from [51, 53] discovers and eliminates redundant transmissions generating energy savings. Sweep was designed to improve solutions of the BIP [51, 53] algorithm. The use of the Sweep operation was shown to provide modest improvement in energy efficiency in networks that use omnidirectional antennas. Typically, a single application of the Sweep operation can reduce total tree power by about 5%; small further improvements can often be obtained by a second application of this procedure, but little improvement has been found by additional applications.

The Sweep procedure for the MEB problem is summarized as follows. Emitting nodes (no leaf nodes are considered) in the solution tree are examined in ascending ID order (an arbitrary order), i.e. from 1 to N. If the transmission by node i reaches all neighbours of any other non-leaf node j (different than the source), then node j can be turned off improving energy efficiency and maintaining the property of a solution, that is, all nodes in the network are still reachable. An example of a Sweep application on a broadcast tree is shown in Figure 3.5.

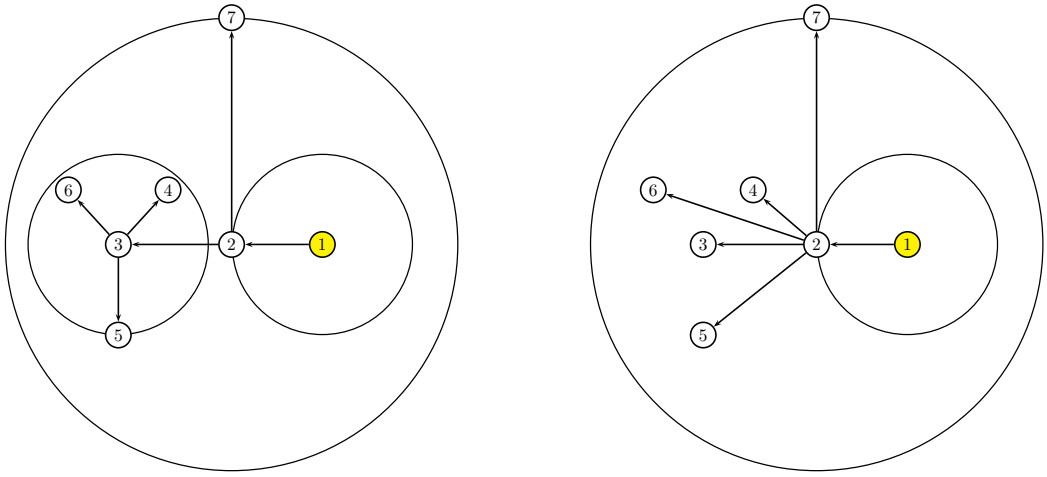

(a) Before the Sweep application

(b) After the Sweep application

Figure 3.5: Sweep in a broadcast tree with omnidirectional antennas. Nodes 4, 5, 6 and 7 are leaves. Nodes 1 and 3 do not reach any non leaf node neighbours. Node 2 reaches the set $ch(3)$ and, thus, node 3 can be turned off and its children can be assigned the new parent 2 (i.e., $ch(2) := ch(2) \cup ch(3)$).

The sweep algorithm can be easily modified to work as well with multicast trees. It is enough to restrict the set of examined nodes to those in the solution tree instead of visiting all nodes in the network. An example of a Sweep application on a multicast tree is shown in Figure 3.6.

However a fundamental characteristic of Sweep makes it unattractive in the case of directional antennas. In omnidirectional applications (and, hence, when reduced beam versions of tree-constrcution algorithms like *RB-BIP/RB-MIP* [52] are used[2]) the Sweep often results in an increase in the number of children of one or more transmitting nodes. In consequence, there is often an increase in the required angle of coverage needed by the antenna (beam width) of certain nodes and, thus, an increase in those nodes' required power, and possibly in the overall tree power.

However, when working with algorithms that obtain at each step partial solution trees directly with reduced beam widths (like *D-BIP/D-MIP* [52] or the ACO algorithms introduced in this work), this problem does not arise. Unfortunately, in the solutions generated by these algorithms there are fewer situations in which the Sweep will be useful (because the small beam widths make the requirements of a Sweep application difficult to happen).

Therefore, Sweep will not be applied to any of the algorithms presented in this work for the MEM/MEB problem with directional antennas.

[2]Here the application of the Sweep algorithm is supposed to be done between the tree construction and the beam width reducing phases.

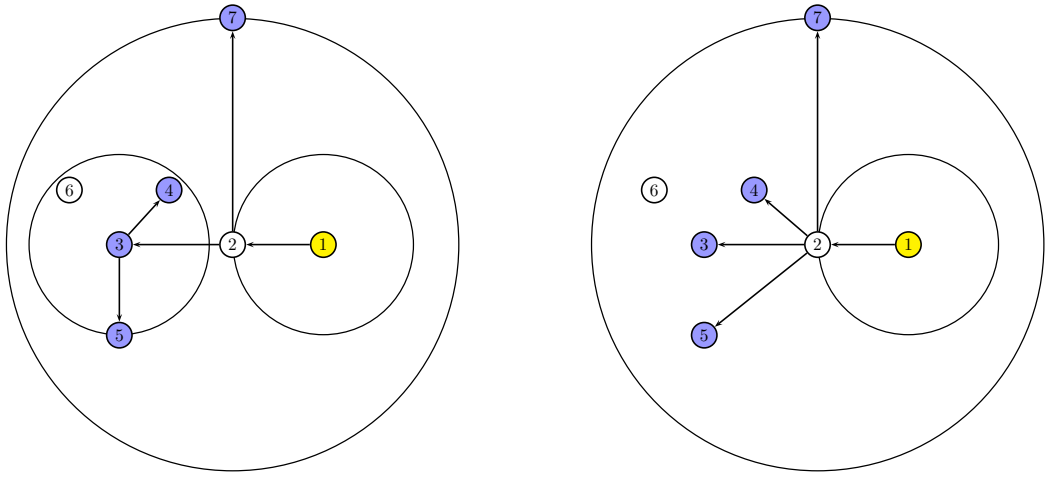

(a) Before the Sweep application

(b) After the Sweep application

Figure 3.6: Sweep in a multicast tree with omnidirectional antennas. Although node 2 is not in the multicast set, it is in the solution tree and, hence, it is a candidate for the Sweep algorithm.

3.3 r-shrink

The local search procedure r-shrink was originally developed in [11] for solving the MEB problem with omnidirectional antennas. The original version works in the following way. Given a solution $T = (V_T, E_T)$ and a parameter $r \leq |V| - 2$ as input, r-shrink works as follows. First, a permutation of all nodes is produced.[3] Nodes with $k \geq r$ children are treated as explained in the following, in the order given by the permutation. Exceptionally, if the source node is going to be explored, it needs to have $k > r$ children to be treated because if it is left with no children ($ch(source) = \emptyset$), the tree will become a non-connected graph and, therefore, the broadcast/multicast signal will remain isolated. Formally, for a r-shrink operation on node i to be allowed, $cut_{\max}(i) \geq r$ must hold, with:

$$cut_{\max}(i) = \begin{cases} d_{out}(i) - 1, & \text{if } i = source \\ d_{out}(i), & \text{otherwise} \end{cases} \tag{3.4}$$

When a node i is treated, first, the children of i are ordered in decreasing distance from i, say $j_1, \ldots, j_k$, where j_1 is the child with the greatest distance from i. In Figure 3.7 an example of such an ordered list is shown.

Then the first r children (that is, the r most distant children) are disconnected from i, and the algorithm tries to reconnect them to any of their non-descendants in the best way possible, that is, in a way that is least energy consuming. In Figure 3.8, a small example of the application of the 1-shrink algorithm is shown.

[3]Note that this is a slight variation to the original proposal in which nodes are treated in a bottop-up manner.

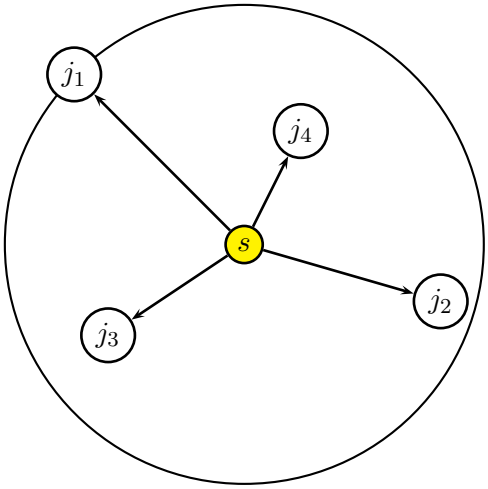

Figure 3.7: Nodes in $ch(s)$ ordered by distance to node s. Note that $d(s, j_1) \geq d(s, j_2) \geq d(s, j_3) \geq d(s, j_4)$.

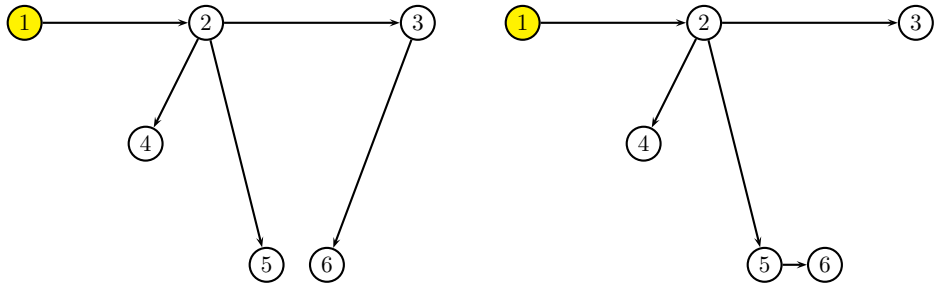

(a) Tree before 1-shrink operation on node 3 (b) Tree after 1-shrink operation on node 3

Figure 3.8: Example of one operation of a 1-rshrink on node 3

One additional definition is convenient to formally describe the r-shrink procedure:

Definition 7 *Given a solution $T = (V_T, E_T)$, the set of **foster parents** of node i, denoted by $fpa(i)$, is the set of the non-descendants of i excluding its current parent. Formally:*

$$fpa(i) \triangleq nd(i) \backslash pa(i) \tag{3.5}$$

Example 6 *In Figure 3.1 $nd(5) = \{1, 2, 3, 4\}$ and $pa(5) = \{4\}$, hence, $fpa(5) = \{1, 2, 3\}$.*

For what concerns r-shrink, extensions from the MEB to the MEM problem and from the omnidirectional to the directional case can be easily explained.

At each iteration of the original r-shrink procedure used for the MEB with omnidirectional antennas case, given a source node i the r most distant nodes from i in $ch(i)$ are removed and

properly reassigned another father. The election of the furthest nodes is consistent with the idea of eliminating nodes that (typically) will enable power reduction because, in the omnidirectional case, the Wireless Multicast Advantage (see Section 1.2) implies that the required emitting power of any given node is equal to the power required for the transmission to the furthest node from i in $ch(i)$.

To extend this algorithm to the case of directional antennas the way in which children of a node are ordered is redefined. In the directional case, although removing the furthest node from the children set of any node will (typically) enable power reductions, another way of generating savings is possible. Reducing the beam width also reduces the required transmission power as the area of coverage of the antenna beam becomes smaller. In the r-shrink procedure for the MEB problem with directional antennas these two methods of reducing energy required by nodes are combined and, when removing a child, the node which enables the biggest decrease in the consumed power will be chosen. The new ordering criterion is now the emission power reduction achieved by disconnecting a node. There is no priority or preference in using one of the two modes before the other. $D = [d_1, \ldots, d_l]$ will denote the list of nodes $d_j \in ch(i)$ ordered decreasingly following this last criterion. Notice, also, that in some cases the removal of a certain node can produce advantages for both the length and the width of the beam.

To extend the algorithm to the MEM problem case the set of foster parents has been restricted to be a subset of the nodes occurring in the initial solution to which the r-shrink is applied. In addition, before the application all leaves in the solution tree that are not nodes of the multicast set are deleted.

Algorithm 3 shows a high level description[4][5][6] of the new version of r-shrink used in this work for the MEM problem with directional antennas. It must be noticed that by the parametrization of the r parameter the r-shrink procedure defines not only one algorithm but a family of them, one for each possible $r \leq |V| - 2$.

Note that this algorithm is desgined for the MEM problem with directional antennas, that is the most general case of the four treated in this work and, thus, it can be directly used in algorithms solving any of the special cases. In fact, it is enough to specify the multicast set M to content all the nodes in the network (i.e., $M = V_T$) to have an r-shrink routine for the MEB problem with directional antennas. Furthermore, if $\theta_{\min} = 360°$ then the antennas used will be restricted to be omnidirectional.

One implementation issue must be remarked. When creating a r-shrink routine for the

[4]The operation $\ominus$ between a directed tree $T = (V_T, E_T)$ and a set of nodes $\{u_1, u_2, \ldots, u_m\}$ appearing in the description is definied such that $T \ominus \{u_1, u_2, \ldots, u_m\} := T' = (V_{T'}, E_{T'})$ where $V_{T'} = V_T$ and $E_{T'} = E_T \setminus \{(i,j) \mid i \in V_T \wedge j \in V_T \setminus \{u_1, u_2, \ldots, u_m\}\}$.

[5]Note that function $P(\cdot)$ is only defined for directed trees. In Algorithm 3 a definition of $P(\cdot)$ for directed forests (roughly, a directed graph containing different directed trees) is required. Let $F = (V_F, E_F)$ be a directed forest and $s \in V_F$ a node, we define $P(V_F, s) := P(T')$ where $T' = (V_{T'}, E_{T'})$ is a directed tree, with $V_{T'} = \{s\} \cup de(s)$ and $E_{T'} = E_F \cap \{(i,j) \mid i, j \in \{s\} \cup de(s)\}$ (that is, the connex component of F rooted at s)

[6]The operation $\oplus$ is also extended to directed forests. The operation $\oplus$ between a directed forest $F = (V_F, E_F)$ and an edge $e = (i,j)$ appearing in the description is definied such that $F \oplus (i,j) := F' = (V_{F'}, E_{F'})$ where $V_{F'} = V_F$ and $E_{F'} = E_F \cup \{(i,j)\}$.

Algorithm 3 The r-shrink procedure for the MEM problem with directional antennas

1: INPUT: the network $G = (V, E)$, a source node $s \in V$, a tree $T = (V_T, E_T)$ in G rooted in s, a parameter $r \leq 1$, and a multicast set $M \subseteq V$
2: Create a random permutation π of nodes in T
3: **for** $i \in V_T$ following the order in π **do**
4: **if** $cut_{\max}(i) \geq r$ **then**
5: $f_{ini} := P(T)$
6: $D := [d_1, \ldots, d_l]$
7: $F := T \ominus \{d_{l+1-r}, \ldots, d_l\}$
8: **for** $j \in D$ **do**
9: $k^* := \mathsf{argmin}_{k \in fpa(i) \cap V_T}\{P(F \oplus (k, j), s)\}$
10: $F := F \oplus (k^*, j)$
11: **end for**
12: $f_{end} := P(F)$
13: **if** $f_{ini} > f_{end}$ **then**
14: $T := F$
15: **end if**
16: **end if**
17: **end for**
18: OUTPUT: T (The best solution found)

MEM/MEB problem with omnidirectional antennas the ordering criterion used in the construction of the list $[d_1, \ldots, d_l]$ for a given node i can be, as in the original r-shrink algorithm, the distance from i to each of the nodes.

In [11] only the 1-shrink procedure was experimentally evaluated. In contrast, in this work the general r-shrink procedure is utilized within a *Variable Neighborhood Descent* (VND) algorithm [28], which is outlined in Algorithm 4. Note that $P()$ stands either for $P_o()$ (in the case of omnidirectional antennas) or $P_d()$ (in the case of directional antennas). The VND algorithm requires the maximum integer $r_{\max}$ for which the r-shrink procedure is executed as an input parameter. The idea for considering more algorithms than the 1-shrink is based on the fact that the r parameter may play a key role in the performance of the algorithm, because different r values can lead to different algorithms which may find different result trees with the same input. In Section 4.1 we experimentally select a value for the $r_{\max}$ parameter.

3.4 ACO for the MEM/MEB problem

The specific ACO algorithm implemented for the MEM/MEB problem is a $\mathcal{MAX}$–$\mathcal{MIN}$ Ant System (MMAS) in the Hyper-Cube Framework [2]. It works roughly as follows. At each iteration $n_a = 10$ artificial ants construct a tree rooted at the source node s. Local search is applied to each of these trees. The pheromone model $\mathcal{T}$ used by our ACO algorithm contains a pheromone value τ_e for each link $e \in E$. After the initialization of the variables T^{bs} (i.e., the best-so-far solution), T^{rb} (i.e., the restart-best solution), and cf (i.e., the convergence factor), all the pheromone values are set to 0.5. At each iteration, after the generation of solutions,

Algorithm 4 Variable Neighborhood Descent (VND)

INPUT: the network $G = (V, E)$, a source node $s \in V$, a tree $T = (V_T, E_T)$ in G rooted in s, a parameter $r_{\max}$
$r := 1$
while $r \leq r_{\max}$ **do**
  $T' := r$-shrink(T)
  if $P(T') < P(T)$ **then**
    $T := T'$
    $r := 1$
  else
    $r := r + 1$
  end if
end while
OUTPUT: a (possibly) improved tree T

Algorithm 5 ACO for the MEM problem with directional antennas

INPUT: the network $G = (V, E)$ and a source node $s \in V$, and a multicast set $M \subseteq V$
$T^{bs} :=$ NULL, $T^{rb} :=$ NULL
$cf := 0$, $bs\_update :=$ FALSE
forall $e \in E$ **do** $\tau_e := 0.5$ **end forall**
while termination conditions not satisfied **do**
  for $j = 1$ to n_a **do**
    $T^j :=$ ConstructTree(G,s,M)
    $T^j :=$ LocalSearch(T^j)
  end for
  $T^{ib} :=$ argmin$\{f(T^1), \ldots, f(T^{n_a})\}$
  Update(T^{ib},T^{rb},T^{bs})
  ApplyPheromoneUpdate(cf,bs_update,$\mathcal{T}$,T^{ib},T^{rb},T^{bs})
  $cf :=$ ComputeConvergenceFactor($\mathcal{T}, T^{rb}, T^{bs}$)
  if $cf \geq 0.99$ **then**
    if $bs\_update =$ **true then**
      forall $e \in E$ **do** $\tau_e := 0.5$ **end forall**
      $T^{rb} :=$ NULL
      $bs\_update :=$ **false**
    else
      $bs\_update :=$ **true**
    end if
  end if
end while
OUTPUT: T^{bs}

some of them are used for updating the pheromone values. The details of the algorithmic framework shown in Algortihm 5 are explained in the following.

ConstructTree(G,s,M): A solution construction starts with the partial solution $T = (V_T, E_T)$

where $V_T := \{s\}$ and $E_T := \emptyset$. Remember that s is the source node of the multicast tree to be constructed. Henceforth we denote by $\overline{V_T}$ the set of nodes which are not included in T, that is, $\overline{V_T} := V \setminus V_T$. At each construction step, one link (and one node) is added to T. The set E_{add} of potential links that can be added to T is defined as follows:

$$E_{\text{add}} := \{(i,j) \in E | i \in V_T, j \in \overline{V_T}\} \tag{3.6}$$

In words, E_{add} consists of those links whose source node is in T and whose goal node is not in T. From these links, one link is chosen according to the following probabilities:

$$\mathbf{p}(e) := \frac{\tau_e \cdot \eta(e)}{\sum_{e' \in E_{\text{add}}} \tau_{e'} \cdot \eta(e')} \ , \tag{3.7}$$

where $\eta(e)$ is the heuristic information of a link $e = (i,j)$ which is computed as follows: $\eta(e) := 1/(P(T') - P(T))$, where $T' = (V_T \cup \{j\}, E_T \cup \{e\})$. In words, the heuristic information accounts for the increase of emission power spent by the partial solution when adding link e. After choosing a link $e = (i,j)$ for the expansion of the current partial solution T, all links of E_{add} (if any) that do not result in a further increase of emission power are also added to T (in addition to e). This concerns all links $e' = (i,l) \in E_{\text{add}}$ with $d(i,l) \leq d(i,j)$ the node l and within the beam implicitly defined by all links $e(i,*)$ that are already in T (including $e = (i,j)$). The solution construction process stops as soon as $M \subset V_T$. After the solution construction all unnecessary transmissions are removed from T.

As E_{add} might contain quite a lot of bad-quality links (especially at the beginning of the construction process) we decided to study also ways of restricting E_{add}. In the following we refer to the use of the unrestricted set E_{add} as *mode 1*. In contrast, *mode 2* works as follows. $\forall\, j \in \overline{V_T}$ let $E_{\text{add},j} := \{(*,j) \in E_{\text{add}}\}$, that is, $E_{\text{add},j}$ contains all links of E_{add} with goal node j. Moreover, let $b(E_{\text{add},j}) := \text{argmax}_{e \in E_{\text{add},j}}\{\eta(e)\}$, that is, $b(E_{\text{add},j})$ is the link of $E_{\text{add},j}$ with the best heuristic information value. Given these definitions, the restriction of set E_{add} in *mode 2* is obtained as follows:

$$E^{\text{m2}}_{\text{add}} := \cup_{j \in \overline{V_T}}\{b(E_{\text{add},j})\} \ , \tag{3.8}$$

that is, only the best link to each node in $\overline{V_T}$ is considered. In the following, let $l := \text{argmax}_{j \in \overline{V_T}}\{\eta(b(E_{\text{add},j}))\}$. Note that l can be regarded as the *best node* in $\overline{V_T}$. Then, the restriction of set E_{add} in *mode 3* is obtained as follows:

$$E^{\text{m3}}_{\text{add}} := \{(*,l) \in E_{\text{add}}\} \ , \tag{3.9}$$

that is, $E^{\text{m3}}_{\text{add}}$ contains all the links of E_{add} that have l (the best node) as goal node.

In addition to the 3 modes outlined above a fourth modes obtained from assigning *mode 2* and *mode 3* each to half of the ants used by the algorithm has been tested.

Finally, a so-called candidate list strategy has been tested. It consists in the reduction of the options to the best ones available at each construction step. Formally, given a network $G = (V,E)$, a partial solution tree $T = (V_T, E_T)$ and a candidate list size c, for any construction mode $u \in \{1,2,3,4\}$ the candidate list C is a set holding the next three properties:

$$C \subseteq E^{\text{mu}}_{\text{add}} \tag{3.10}$$

$$|C| \leq c \tag{3.11}$$

$$\forall (i,j) \text{ where } i \in V_T \text{ and } j \in V \backslash V_T,\ \forall e \in E_T,\ \eta(e) \leq \eta((i,j)) \tag{3.12}$$

In particular, in addition to not using a candidate list, two different candidate list sizes have been tested: 4 and 8.

LocalSearch(T^j): As in the construction procedure some nodes from $V \backslash M$ may have been included in the solution tree and, at the end of the construction, they can remain unused (nodes in $V \backslash M$ are only useful as relay nodes), removal of leaf nodes of the tree not belonging to the multicast set can be a source of energy savings. Then, the VND algorithm as outlined in Section 3.3 is applied. As a result of the SWEEP and r-shrink applications, new leave nodes that do not belong to the multicast set may have appeared, hence, another unused leaf removal is done.

Update(T^{ib},T^{rb},T^{bs}): In this procedure T^{rb} and T^{bs} are set to T^{ib} (i.e., the iteration-best solution), if $P(T^{ib}) < P(T^{rb})$ and $P(T^{ib}) < P(T^{bs})$, respectively.

ApplyPheromoneUpdate(cf,bs_update,$\mathcal{T}$,T^{ib},T^{rb},T^{bs}): Our ACO algorithm may use three different solutions for updating the pheromone values: (i) the iteration-best solution T^{ib}, (ii) the restart-best solution T^{rb} and, (iii) the best-so-far solution T^{bs}. Their influence depends on the convergence factor cf, which provides an estimate about the state of convergence of the system. To perform the update, first an update value ξ_e for each link $e \in E$ is computed:

$$\xi_e := \kappa_{ib} \cdot \delta(T^{ib}, e) + \kappa_{rb} \cdot \delta(T^{rb}, e) + \kappa_{bs} \cdot \delta(T^{bs}, e) \ ,$$

where κ_{ib} is the weight of T^{ib}, κ_{rb} the weight of T^{rb}, and κ_{bs} the weight of T^{bs} such that $\kappa_{ib} + \kappa_{rb} + \kappa_{bs} = 1.0$. The δ-function is the characteristic function of the set of links in the tree, i.e., for each solution tree $T = (V_T, E_T)$:

$$\delta(T,e) \ = \ \begin{cases} 1 & : \ e \in E_T \\ 0 & : \ \text{otherwise} \end{cases}$$

Then, the following update rule is applied to all pheromone values τ_e :

$$\tau_e := \min\left\{\max\{\tau_{\min}, \tau_e + \rho \cdot (\xi_e - \tau_e)\}, \tau_{\max}\right\} \ ,$$

where $\rho \in (0,1]$ is the evaporation (or learning) rate. In this work a constant value of $\rho = 0.1$ is used in all cases. The lower and upper bounds $\tau_{\min} = 0.01$ and $\tau_{\max} = 0.99$ keep the pheromone values always in the range $(\tau_{\min}, \tau_{\max})$, thus preventing the algorithm from converging to a solution. After tuning, the values for κ_{ib}, κ_{rb} and κ_{bs} are chosen as shown in Table 3.5.

ComputeConvergenceFactor($\mathcal{T}$, T^{rb}, T^{bs}): This function computes, at each iteration, the convergence factor as

$$cf := \frac{\sum_{e \in E(T^{rb})} \tau_e}{|E_{T^{rb}}| \cdot \tau_{\max}} \ , \ \text{if } bs\_update = \text{FALSE} \tag{3.13}$$

or

Table 3.5: The schedule used for values κ_{ib}, κ_{rb} and κ_{bs} depending on cf (the convergence factor) and the Boolean control variable bs_update.

	$bs\_update = \text{FALSE}$			$bs\_update = \text{TRUE}$
	$cf < 0.7$	$cf \in [0.7, 0.9)$	$cf \geq 0.9$	
κ_{ib}	2/3	1/3	0	0
κ_{rb}	1/3	2/3	1	0
κ_{bs}	0	0	0	1

$$cf := \frac{\sum_{e \in E(T^{bs})} \tau_e}{|E_{T^{bs}}| \cdot \tau_{\max}} \quad , \text{ if } bs\_update = \text{TRUE} \tag{3.14}$$

Here, $\tau_{\max}$ is the upper limit for the pheromone values. The convergence factor cf can therefore only assume values between 0 and 1. The closer cf is to 1, the higher is the probability to produce the solution T^{rb} (or T^{bs} analogously).

Even though the ACO algorithm described above has been developed to tackle the MEM problem with directional antennas (the most general problem), all four considered problems can be solved (MEM/MEB problem with omnidirectional/directional antennas). The reason is that a MEB instance can be considered as a MEM instance with multicast set $M = V$ and that omnidirectional antennas can be considered as directional antennas with $\theta_{\min} = 360°$ (as explained at the end of Section 3.3). However, the differences between these problems can allow some implementation benefits when working with the most particular ones. In fact, four different algorithms have been implemented to solve the four different problems. The main implementation issues are:

- The computation of the power of a node is much simpler in the omnidirectional antennas case, where a bijection between emission distance and emission power can be established.
- The computation of the correct beam-width and the correct angle of emission are not necessary when working with omnidirectional antennas.
- Several set intersections with the multicast set can be removed if the MEB problem is considered because the multicast set used when emulating the broadcast behaviour includes all nodes in the network and, hence, intersecting one subset of the nodes in the network with it becomes the identity function.
- When considering the MEB problem, no leaf-removal can be done because all nodes must be reached (remember that the multicast set M used when emulating the broadcast behaviour with a multicast request is $M = V$).
- Particular implementation issues of the r-shrink algorithm should also be considered (see Section 3.3).

Chapter 4

Results

In the previous chapter an algorithm for the MEM/MEB problem with omnidirectional, respectively directional antennas, has been developed. In the following we present an experimental evaluation of these algorithms. Four different programs have been implemented taking in account the implementation issues explained in Chapter 3, one for each of the four considered problems.

For testing purposes several algorithms, some developed in this work and others from the related literature, have been developed. Table 4.1 summarizes all implemented algorithms.

Table 4.1: Algorithms implemented with evaluation purposes.

Algorithm name	Description in
BIP/MIP (+VND)	Section 3.1 (Section 3.3)
D-BIP/D-MIP (+VND)	Section 3.1 (Section 3.3)
RB-BIP/RB-MIP (+VND)	Section 3.1 (Section 3.3)
MILP	Section 1.3
ACO	Section 3.4
MACO	Section 3.4
D-ACO	Section 3.4
D-MACO	Section 3.4

Algorithms have been implemented in ANSI C++ using GCC 3.2.2 for compiling the software. Experimental results were obtained on a cluster of PCs with an AMD64X2 4400 processor and 4 GB of memory.

The set of benchmark instances is based on the set of instances in [1, 55]. This set consists of 30 MEB instances with 20 nodes each, and further 30 MEB instances with 50 nodes. Each instance consists of the positions of the n nodes (inside a 1000×1000 plane) and the indication of which node is the source node. This set has been extended with 30 random instances with 100 nodes and, also, with 30 random instances with 200 nodes.

In addition, 30 random multicast sessions for each size $n \in \{20, 50, 100, 200\}$ have been

created. 10 of these sessions have a multicast set of size $\lfloor \frac{n}{3} \rfloor$, 10 have a multicast set of size $\frac{n}{2}$ and 10 have a multicast set of size $\lceil \frac{2 \cdot n}{3} \rceil$. These sessions consist of the nodes in the multicast set and the source of the multicast instance. The idea is to combine each network of size n with the 30 different multicast sessions to obtain 30 different MEM instances for each of the 120 networks (using the positions provided by the network and the multicast set and the source node from the multicast session), obtaining 900 MEM instances for each considered size.

In all ACO executions, time limitations are specified as stopping criterion. Table 4.2 shows time limits given to ACO executions in terms of the network size considered.

Table 4.2: Time limits (in seconds) used for the ACO algorithm when working with an instance of size n.

n	20	50	100	200
Time limit (s)	5	20	100	500

4.1 Tuning of the $r_{\max}$ parameter

As a first step experiments for determining a value for the parameter $r_{\max}$ of the VND algorithm, the maximum value of r for any r-shrink application (see Algorithm 4 for details), were conducted. More specifically, the BIP algorithm was applied with a subsequent application of VND for $r_{\max} = 1, \ldots, |V|-2$ to the 30 problem instances with $n \in \{20, 50, 100, 200\}$ nodes.

Figure 4.1 shows, for $n \in \{100, 200\}$ the 30 results for different settings of $r_{\max}$ between 1 and $|V|-2$ in the form of boxplots. The following conclusions can be drawn. First, VND with $r_{\max} = 1$ (that is, repeating 1-shrink local searches until no further improvement is achieved) does nearly all the job. When $r_{\max}$ is increased, further improvements are obtained only occasionally for some instances. Moreover, it is hard to predict when these improvements will occur. However, performance was measured both with respect to the solution quality and the computation time, thus, the computation time that is spent by VND with the different settings of $r_{\max}$ was also measured. As improvements are obtained only occasionally for $r_{\max} > 1$, the computation time spent when $r_{\max} = |V| - 2$ is only slightly higher than the computation time spent with $r_{\max} = 1$. Therefore, the maximum possible setting $r_{\max} = |V| - 2$ is used for all further experiments.

It must be noticed that with values of r bigger than 1 huge and consistent objetive function reductions are obtained (mainly for $r < 10$). Therefore, the advantages of using the r-shrink with $r > 1$ are notable and, hence, its usage is justified.

Figure 4.1 shows how, even in the case of $n = 200$ in which the biggest trees are managed and the r-shrink aplication is slower, the objective function values obtained do not improve consistently for values of $r_{\max}$ bigger than 10. As it could be expected, execution times increase when r grows, but, even in the case of the bigger r's considered, these times are rather

small.

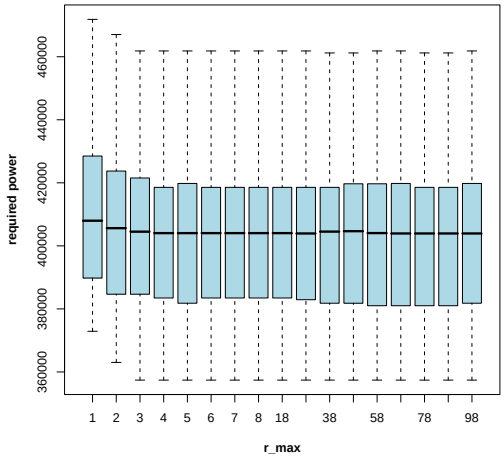

(a) $n = 100$, solution quality

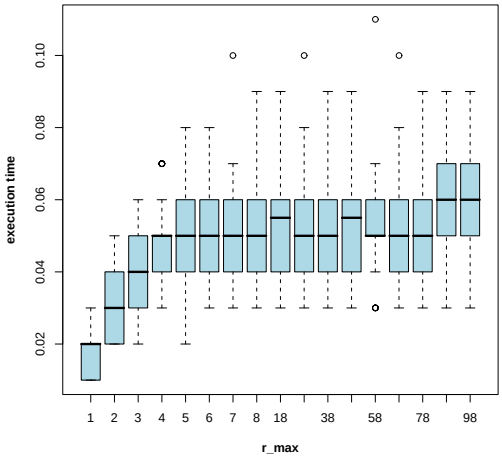

(b) $n = 100$, computation time in seconds

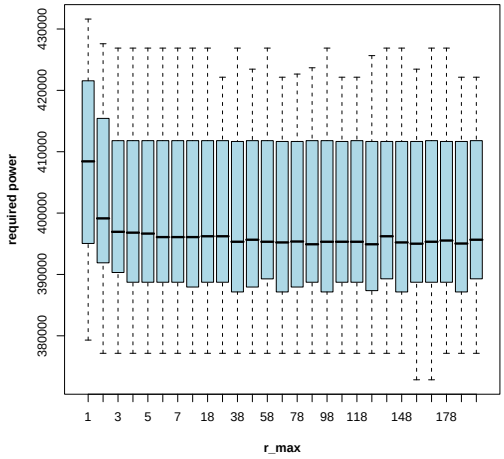

(c) $n = 200$, solution quality

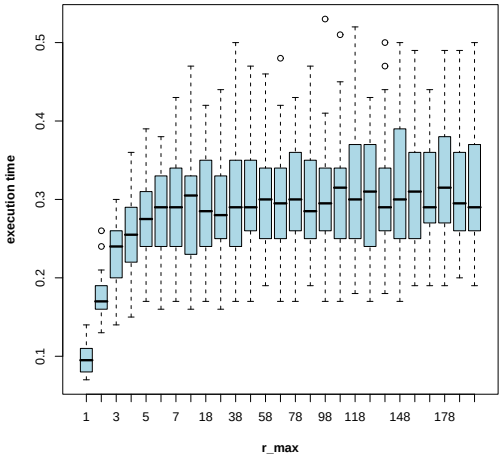

(d) $n = 200$, computation time in seconds

Figure 4.1: Tuning results concerning the parameter $r_{\max}$ of VND

Finally, Table 4.3 shows the values of $r_{\max}$ used for each considered network size n.

Table 4.3: $r_{\max}$ values used in the VND algorithm using the r-shrink. In all cases $r_{\max} = n-2$.

n	20	50	100	200
$r_{\max}$	18	48	98	198

4.2 Parameter selection for ACO

The ACO algorithm for the MEM/MEB problem with omnidirectional/directional antennas developed in Section 3.4 has two parameters: (1) solution construction mode and (2) candidate list size. Experiments regarding the setting of the solution construction mode and the candidate list size for omnidirectional antennas and directional antennas with $\theta_{\min} \in \{30°, 60°, 90°\}$ are presented here. Remember that four different solution construction modes (modes 1, 2, 3 and 4) are considered and, additionally, candidate list size restictions to $c \in \{4, 8, \text{all}\}$ are tested, where "all" means that no candidate list strategy is used. As we have four possible construction modes and three different candidate list strategies, this makes a total of 12 different algorithm settings.

For tuning purposes, the MEB problem with the four different antenna types considered (omnidirectional antennas and directional antennas with $\theta_{\min} \in \{30°, 60°, 90°\}$) were studied. For each instance and each antenna type 30 trials were executed. The ACO parameters were tuned to optimize the best value over all trials (followed by the highest number of best values found and the average value). The obtained parameters settings were also used for the MEM problem with the respective antenna types.

Tables in Appendix A show the results of the tuning. In all tables rows represent instances and columns the different ACO settings. For each considered network size and antenna type three different tables are provided, the first one showing the best values found, the second one showing the average values found and the third one showing the average times (in all cases results are over all corresponding trials). In addition, minimum values per row are presented in **bold**, that is, for each instance, the best performing parameters settings are indicated. Finally, a last row is added, where the number of minimum values in each column is shown, that is, for each parameters setting, the number of instances in which it is in the group of the best performing settings is shown. In fact, this value is used as the first criterion when choosing the best performing settings in each category.

A summary of this analysis is presented in Table 4.4, where the best performing parameter settings over all instances of all sizes for each of the four antenna types considered is shown. Further experiments with the ACO algorithm for both the MEB and the MEM problems will use these parameters settings for each antenna type.

Table 4.4: Parameter settings for the MEM/MEB by minimum beam width.

	$\theta_{\min} = 360°$	$\theta_{\min} = 30°$	$\theta_{\min} = 60°$	$\theta_{\min} = 90°$
Solution construction mode	3	1	1	3
Candidate list size	8	4	8	8

In Table 4.5 the number of instances in which the ACO/D-ACO algorithm with the chosen parameters settings is the best performing algorithm over all considered combinations of parameters is shown. Note that in the extreme cases ($\theta_{\min} = 30°$ and $\theta_{\min} = 360°$) the ACO/D-ACO algorithm has a parameters settings that perform very well for all network sizes, specially in the omnidirectional case where only in 5 instances of 200 nodes other configurations perform better.This contrasts with the $\theta_{\min} = 90°$ case in which best performing

configurations for different sized networks change.

Table 4.5: Number of instances in which the ACO/D-ACO algorithm with the chosen parameters settings is the best performing algorithm over all considered combinations of parameters.

n	$\theta_{\min} = 360°$	$\theta_{\min} = 30°$	$\theta_{\min} = 60°$	$\theta_{\min} = 90°$
20	30	30	30	30
50	30	30	29	26
100	30	27	25	18
200	25	14	7	10
total	115/120	101/120	91/120	84/120

4.3 Results for the MEB problem

With the final settings as outlined in the previous sections, the ACO algorithm was applied 30 times to each of the 30 instances of the 4 different network sizes (120 instances altogether).

In what refers to optimal results, notice that the MILP formulation from [25] (see also Section 1.6) can not be used to obtain signifcant results for all cases because its exponential execution time requirement is too large, even for 50 nodes instances. Therefore, the MILP model was executed with a time limit of 24 hours and for a restricted number of instances of the whole instance set. More in detail, results for instances with omnidirectional antennas for 20 and 50 nodes networks have been extracted from [55]. Results for 100 nodes networks with omnidirectional antennas after the 24 hours limit are around 3.5 times worse than results obtained with the ACO algorithm and, thus, are not presented in any table. Results for MEB instances of 20 nodes with all types of directional antennas have been calculated and, in most cases, solved to optimality within the 24 hours given. In all cases if values presented as optimal are not guaranteed to be optimal (because the solver has not had enough time or memory) they will appear marked with a $\leq$-sign.

Note, that due to the fact that only some of the optimal results are known, and also because for the 50 nodes instances with omnidirectional antennas results from some more sources than in the other cases exist, an additional special table (containing different columns than the other tables in this section) for this case will be presented. For this case, some additional results for 20 nodes instances can also be found in the literature, but are not presented in any table because the results obtained with the new ACO algorithm for networks of this size are optimal for all instances with computation times almost negligible what makes the table not very interesting.

4.3.1 Results for Omnidirectional Antennas

First of all, in Table 4.6, results of the ACO for the MEB problem instances with 50 nodes are shown in comparison to NP [1], ELS [55], ILS [33], and BIP + VND, respectively. The first table column contains the instance names. The second table column provides the values of the best solutions known. For algorithms NP, ELS, and ACO three values are provided: The column headed by **excess** gives the excess (in percent) of the average of the values of the best solutions found in 30 trials over the optimal (respectively, best known) value. The column with

heading **found** provides the number of trials in which the optimal (respectively, best known) value was found. Finally, the column titled **time (s)** contains the average computation times (in seconds) over 30 runs. For ILS the computation time is not provided as it was not given in [55]. For algorithm BIP + VND only the excess over the optimal (respectively, best known) solutions are provided. Finally, the last table row gives averages over all instances. Remember that in the rest of tables in this chapter only a subset of this columns is shown.

In the 50 nodes networks the results show that, first, the ACO algorithm outperforms all other algorithms in terms of solution quality. Only in 4 cases our algorithm is not able to find the optimal (respectively, best known) solution in all trials. On average it is found in 29.7 out of 30 trials. The second-best performing algorithm, ELS, only finds an optimal (respectively, best known) solution in 17.3 trials on average. Concerning computation times, the ACO is about one order of magnitude faster than ELS, even when we assume that the machine on which the experiments are performed is double as fast as the machine used to run ELS. Results for 50 nodes instances with omnidirectional antennas are summarized in Table 4.6.

Results for 20 nodes instances with omnidirectional antennas are summarized in Table 4.7. The format of this table and the rest of the tables in this section is as follows. The first column provides the instance name, the second and third columns the absolute result and time of BIP, the fourth column the deviation from BIP + VND to the BIP, and the remaining columns give the results of the ACO algorithm. Concerning ACO the following information is provided. The column with heading **deviation** provides the improvement over BIP (in percent), whereas the column titled **best** gives the value of the best solution found in 30 trials. The remaining columns provide the average of the best solutions found in 30 trials (plus standard deviation), and the average of the computation times over 30 trials (plus standard deviation). The last table row provides the average improvement (over 30 instances) over BIP + VND, the average emission power saving, and the average computation time over 30 instances.

Concerning the problem instances with 20 nodes the ACO algorithm produced an optimal solution for each instance in each run. On average our algorithm needed 0.00 seconds to find these solutions. The ELS algorithm published in [55] finds only in 24 cases (out of 30) an optimal solution in each run. Moreover, the average computation time needed by ELS is 0.43 seconds on a computer with a 2.8 GHz Pentium IV processor. Even assuming that our machine is double as fast, ACO is faster by two orders of magnitude. Clearly, the instances with 20 nodes are no challenge for the ACO algorithm.

The results for the problem instances with 50, 100 and 200 nodes are summarized (in comparison to BIP [52] and BIP + VND) in Table 4.8, Table 4.9 and Table 4.10, respectively. Remember that no optimal solutions will be presented in these cases. The BIP algorithm will be used as reference value, instead.

The results show that both for instances with 100 nodes and instances with 200 nodes the improvement of ACO over BIP is on average around 20%. The average computation times are higher than in the 20 and 50 nodes instances (28.70 seconds for the 100 nodes instances, and 296.00 seconds for the biggest instances considered). Note that in both cases the usage of the VND local search procedure causes an improvement of about 10% of the BIP solution.

In Figure 4.2 and Figure 4.3 a graphical representation of solutions found by BIP and ACO algorithms for MEB instances *p50.06* and *p100.25*, respectively, when omnidirectional antennas are considered is shown. Note that there is a huge difference in the structure of the solutions obtained with BIP and those obtained with ACO. For example, in Figure 4.2(b) one node's emission (node 14) covers 90% of the network nodes while in the solution in Figure 4.2(a) many more nodes are used as relay nodes but all with smaller transmission powers. It is interesting to note that the node covering 90% of the network in Figure 4.2(b) is even turned off in Figure 4.2(a).

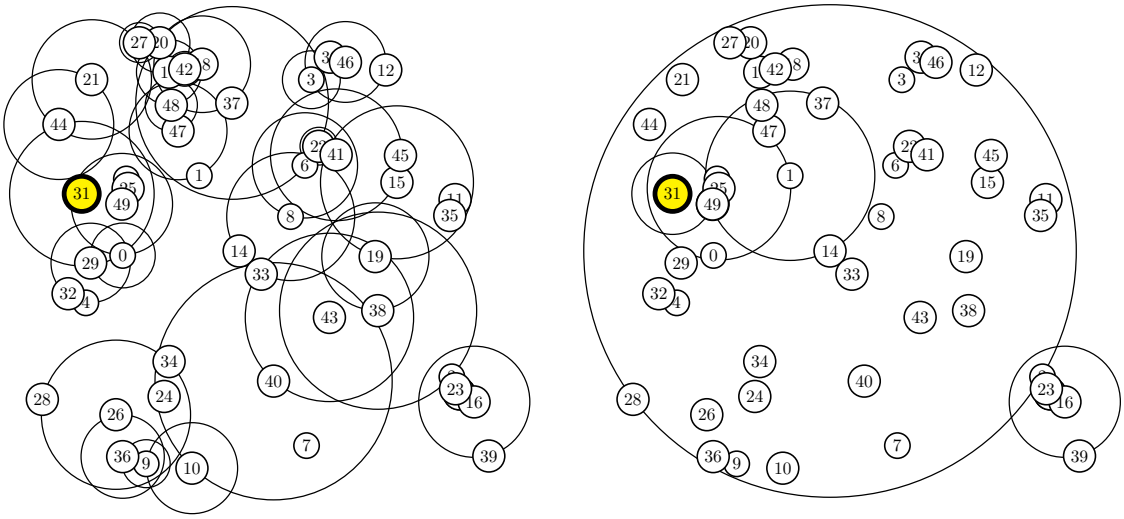

(a) BIP solution for instance *p50.06*. Required power: 504430.17.

(b) ACO solution for instance *p50.06*. Required power: 384438.46.

Figure 4.2: Solutions found for instance *p50.06* with BIP and ACO (when omnidirectional antennas are considered)

Table 4.6: Results for instances with 50 nodes (omnidirectional antennas).

Instance	Best known	NP			ELS			ILS		BIP + VND	ACO		
		excess	found	time (s)	excess	found	time (s)	excess	found	excess	excess	found	time (s)
p50.00	399074.64	6.22%	0/30	11.4	0.41%	15/30	57.0	3.31%	0/30	9.89%	0.00%	30/30	0.52
p50.01	≤ 373565.15	3.68%	0/30	7.1	0.16%	5/30	47.0	3.30%	0/30	22.79%	0.00%	30/30	1.97
p50.02	393641.09	10.11%	0/30	10.3	0.28%	13/30	46.0	12.06%	0/30	17.39%	0.00%	30/30	2.84
p50.03	316801.09	6.43%	0/30	6.1	1.71%	11/30	57.0	6.48%	0/30	18.43%	0.00%	30/30	0.36
p50.04	≤ 325774.22	5.22%	0/30	7.5	0.30%	25/30	40.0	7.22%	0/30	17.04%	0.00%	30/30	1.89
p50.05	382235.90	3.28%	1/30	10.9	0.83%	16/30	31.0	2.57%	0/30	7.69%	0.00%	30/30	3.42
p50.06	≤ 384438.46	1.19%	5/30	10.2	0.00%	30/30	29.0	0.14%	18/30	13.50%	0.00%	30/30	3.54
p50.07	≤ 401836.85	6.70%	0/30	8.9	0.54%	24/30	64.0	7.80%	0/30	11.50%	0.00%	30/30	0.54
p50.08	334418.45	0.10%	27/30	4.6	0.00%	30/30	29.0	0.00%	30/30	11.43%	0.00%	30/30	0.73
p50.09	≤ 346732.05	9.20%	0/30	12.9	3.29%	0/30	102.0	11.42%	0/30	15.22%	0.00%	30/30	1.88
p50.10	416783.45	2.14%	0/30	8.9	1.16%	13/30	40.0	2.05%	0/30	12.80%	0.00%	30/30	0.85
p50.11	≤ 369869.41	4.34%	0/30	7.7	2.87%	1/30	28.0	4.62%	0/30	9.99%	0.00%	30/30	4.47
p50.12	≤ 392326.01	3.18%	0/30	13.5	0.57%	7/30	66.0	0.44%	0/30	6.82%	0.00%	30/30	0.42
p50.13	≤ 400563.83	6.63%	0/30	11.2	0.04%	29/30	74.0	1.20%	0/30	21.16%	0.00%	30/30	1.38
p50.14	388714.91	0.08%	22/30	6.6	0.34%	3/30	11.0	0.00%	30/30	34.93%	0.00%	29/30	2.26
p50.15	371694.65	0.40%	0/30	8.1	0.20%	5/30	35.0	1.40%	0/30	9.62%	0.00%	30/30	1.12
p50.16	≤ 414587.42	5.28%	0/30	15.1	0.30%	26/30	81.0	6.06%	1/30	5.51%	0.00%	30/30	0.48
p50.17	355937.07	2.17%	1/30	11.9	1.88%	17/30	33.0	4.94%	2/30	9.00%	0.00%	30/30	0.38
p50.18	376617.33	5.96%	0/30	11.3	0.24%	8/30	65.0	0.98%	12/30	7.28%	0.00%	30/30	0.55
p50.19	335059.72	2.27%	5/30	9.8	0.00%	30/30	28.0	10.49%	1/30	33.60%	0.00%	30/30	0.39
p50.20	414768.96	3.14%	0/30	10.4	0.15%	0/30	35.0	6.33%	0/30	9.54%	0.00%	21/30	5.85
p50.21	≤ 361354.27	2.93%	2/30	10.4	0.00%	30/30	41.0	0.00%	30/30	9.01%	0.00%	30/30	0.29
p50.22	329043.51	0.00%	30/30	7.2	0.00%	30/30	14.0	4.61%	0/30	25.49%	0.00%	30/30	0.74
p50.23	383321.04	6.39%	0/30	11.1	0.00%	30/30	109.0	2.47%	0/30	10.95%	0.00%	30/30	1.06
p50.24	404855.92	5.69%	0/30	10.0	0.07%	17/30	37.0	0.87%	3/30	10.42%	0.00%	30/30	0.53
p50.25	363200.32	0.00%	30/30	3.2	0.00%	30/30	7.0	0.00%	30/30	24.65%	0.00%	30/30	0.45
p50.26	406631.51	9.59%	0/30	11.5	2.17%	2/30	60.0	11.63%	0/30	12.67%	0.00%	30/30	2.16
p50.27	451059.62	4.18%	0/30	9.5	0.18%	22/30	40.0	3.35%	0/30	9.09%	0.00%	30/30	1.50
p50.28	≤ 415832.44	4.48%	0/30	11.6	0.47%	23/30	78.0	0.28%	0/30	8.63%	0.00%	30/30	0.38
p50.29	380492.77	0.00%	30/30	5.9	0.08%	27/30	18.0	0.60%	0/30	14.62%	0.00%	30/30	1.92
		4.03%	**5.1/30**	**9.5**	**0.61%**	**17.3/30**	**46.0**	**3.89%**	**5.23/30**	**14.37%**	**0.00%**	**29.7/30**	**1.49**

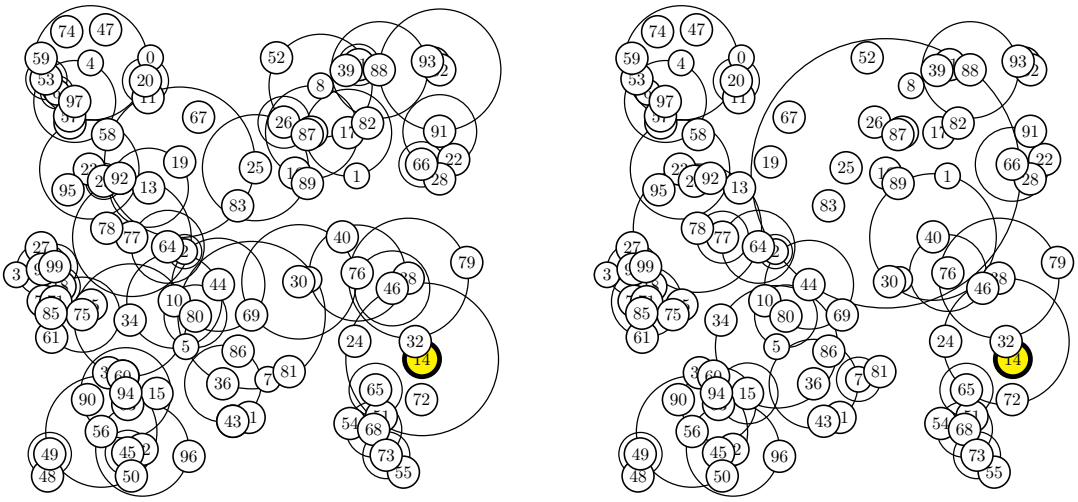

(a) BIP solution for instance *p100.25*. Required power: 436269.59.

(b) ACO solution for instance *p100.25*. Required power: 357934.45.

Figure 4.3: Solutions found for instance *p100.25* with BIP and ACO (when omnidirectional antennas are considered)

Table 4.7: Results for instances with 20 nodes with mode 3 and candidate list size of 8 (omnidirectional antennas).

Instance	MILP	BIP		BIP + VND		ACO					
		deviation	time (s)	deviation	time (s)	deviation	best	average	(std.)	time (s)	(std.)
p20.00	407250.81	31.15%	0.00	14.90%	-0.00	0.00%	407250.81	407250.81	(0.00)	0.01	(0.01)
p20.01	446905.52	31.40%	0.00	0.00%	0.00	0.00%	446905.52	446905.52	(0.00)	0.00	(0.01)
p20.02	335102.42	8.80%	0.00	0.00%	0.01	0.00%	335102.42	335102.42	(0.00)	0.00	(0.00)
p20.03	488344.90	9.38%	0.00	0.00%	0.00	0.00%	488344.90	488344.90	(0.00)	0.00	(0.00)
p20.04	516117.75	35.92%	0.00	14.75%	0.00	0.00%	516117.75	516117.75	(0.00)	0.01	(0.01)
p20.05	300869.14	42.08%	0.00	29.97%	0.01	0.00%	300869.14	300869.14	(0.00)	0.01	(0.01)
p20.06	250553.15	54.49%	0.00	32.91%	0.01	0.00%	250553.15	250553.15	(0.00)	0.00	(0.00)
p20.07	347454.08	14.15%	0.00	1.60%	0.01	0.00%	347454.08	347454.08	(0.00)	0.00	(0.01)
p20.08	390795.34	6.31%	0.00	0.00%	0.00	0.00%	390795.34	390795.34	(0.00)	0.00	(0.00)
p20.09	447659.11	14.82%	0.00	5.47%	0.01	0.00%	447659.11	447659.11	(0.00)	0.01	(0.01)
p20.10	316734.39	12.09%	0.00	0.00%	0.00	0.00%	316734.39	316734.39	(0.00)	0.00	(0.00)
p20.11	289200.92	57.28%	0.00	6.35%	0.01	0.00%	289200.92	289200.92	(0.00)	0.01	(0.01)
p20.12	314511.98	63.04%	0.00	10.98%	0.01	0.00%	314511.98	314511.98	(0.00)	0.00	(0.00)
p20.13	346234.51	50.03%	0.00	5.98%	0.00	0.00%	346234.51	346234.51	(0.00)	0.02	(0.02)
p20.14	301426.68	13.20%	0.00	0.00%	0.00	0.00%	301426.68	301426.68	(0.00)	0.00	(0.00)
p20.15	457467.93	21.01%	0.00	17.63%	0.01	0.00%	457467.93	457467.93	(0.00)	0.00	(0.01)
p20.16	484437.68	22.97%	0.00	9.21%	0.01	0.00%	484437.68	484437.68	(0.00)	0.00	(0.00)
p20.17	380175.41	18.11%	0.00	2.80%	0.00	0.00%	380175.41	380175.41	(0.00)	0.00	(0.00)
p20.18	320300.23	25.22%	0.00	6.48%	0.00	0.00%	320300.23	320300.23	(0.00)	0.01	(0.01)
p20.19	461267.52	11.60%	0.00	3.06%	0.00	0.00%	461267.52	461267.52	(0.00)	0.01	(0.01)
p20.20	403582.74	31.20%	0.00	5.39%	0.01	0.00%	403582.74	403582.74	(0.00)	0.00	(0.00)
p20.21	271958.28	54.40%	0.00	0.00%	0.01	0.00%	271958.28	271958.28	(0.00)	0.00	(0.00)
p20.22	328659.78	37.15%	-0.00	19.64%	0.00	0.00%	328659.78	328659.78	(0.00)	0.00	(0.00)
p20.23	326654.08	38.49%	0.00	20.04%	0.01	0.00%	326654.08	326654.08	(0.00)	0.00	(0.01)
p20.24	395859.67	22.81%	0.00	0.76%	0.01	0.00%	395859.67	395859.67	(0.00)	0.01	(0.01)
p20.25	453517.28	25.86%	0.00	6.30%	0.00	0.00%	453517.28	453517.28	(0.00)	0.01	(0.01)
p20.26	461547.18	26.56%	0.00	0.00%	0.00	0.00%	461547.18	461547.18	(0.00)	0.00	(0.00)
p20.27	389057.00	31.86%	0.00	29.14%	0.00	0.00%	389057.00	389057.00	(0.00)	0.00	(0.01)
p20.28	279251.95	56.10%	0.00	0.00%	0.01	0.00%	279251.95	279251.95	(0.00)	0.00	(0.00)
p20.29	299586.76	16.15%	0.00	14.86%	0.01	0.00%	299586.76	299586.76	(0.00)	0.00	(0.00)
		29.45%	0.00	8.61%	0.01	0.00%		373749.47	(0.00)	0.00	(0.01)

Table 4.8: Results for instances with 50 nodes with mode 3 and candidate list size of 8 (omnidirectional antennas).

Instance	BIP		BIP + VND		ACO					
	obj. function	time (s)	deviation	time (s)	deviation	best	average	(std.)	time (s)	(std.)
p50.00	513876.50	0.00	-14.65%	0.06	-22.34%	399074.64	399074.64	(0.00)	0.52	(0.61)
p50.01	516535.89	0.00	-11.74%	0.08	-27.68%	373565.15	373565.15	(0.00)	1.97	(1.31)
p50.02	538142.57	0.00	-14.13%	0.07	-26.85%	393641.09	393641.09	(0.00)	2.84	(3.03)
p50.03	400208.62	0.00	-6.25%	0.07	-20.84%	316801.09	316801.09	(0.00)	0.36	(0.12)
p50.04	421423.45	0.00	-10.38%	0.07	-22.70%	325774.22	325774.22	(0.00)	1.89	(1.52)
p50.05	463244.31	0.00	-11.14%	0.07	-17.49%	382235.90	382235.90	(0.00)	3.42	(3.47)
p50.06	504430.17	0.00	-11.63%	0.06	-23.79%	384438.46	384438.46	(0.00)	3.54	(3.49)
p50.07	491137.29	-0.00	-8.77%	0.06	-18.18%	401836.85	401836.85	(0.00)	0.54	(0.52)
p50.08	424060.62	0.00	-12.12%	0.07	-21.14%	334418.45	334418.45	(0.00)	0.73	(0.90)
p50.09	444904.00	0.00	-10.20%	0.06	-22.07%	346732.05	346732.05	(0.00)	1.88	(1.33)
p50.10	486360.14	0.00	-3.34%	0.06	-14.31%	416783.45	416783.45	(0.00)	0.85	(0.78)
p50.11	434358.88	0.00	-6.34%	0.07	-14.85%	369869.41	369869.41	(0.00)	4.47	(4.67)
p50.12	456808.49	0.00	-7.76%	0.06	-14.12%	392326.01	392326.01	(0.00)	0.42	(0.29)
p50.13	507644.12	0.00	-4.39%	0.06	-21.09%	400563.83	400563.83	(0.00)	1.38	(1.10)
p50.14	557299.19	-0.00	-5.89%	0.06	-30.25%	388714.91	388763.13	(264.14)	2.65	(3.27)
p50.15	432160.37	0.00	-5.71%	0.05	-13.99%	371694.65	371694.65	(0.00)	1.12	(1.48)
p50.16	497443.27	0.00	-12.06%	0.06	-16.66%	414587.42	414587.42	(0.00)	0.48	(0.23)
p50.17	428694.92	0.00	-9.50%	0.06	-16.97%	355937.07	355937.07	(0.00)	0.38	(0.11)
p50.18	448729.73	0.01	-9.96%	0.06	-16.07%	376617.33	376617.33	(0.00)	0.55	(0.42)
p50.19	489183.61	0.00	-8.49%	0.05	-31.51%	335059.72	335059.72	(0.00)	0.39	(0.25)
p50.20	527638.55	0.00	-13.89%	0.08	-21.39%	414768.96	414952.36	(284.94)	5.85	(5.72)
p50.21	452375.35	0.00	-11.16%	0.09	-20.12%	361354.27	361354.27	(0.00)	0.29	(0.16)
p50.22	467523.31	0.00	-11.68%	0.06	-29.62%	329043.51	329043.51	(0.00)	0.74	(1.37)
p50.23	485068.70	0.00	-18.19%	0.07	-20.98%	383321.04	383321.04	(0.00)	1.06	(0.96)
p50.24	525107.79	0.00	-14.86%	0.06	-22.90%	404855.92	404855.92	(0.00)	0.53	(0.15)
p50.25	523508.12	0.00	-13.52%	0.07	-30.62%	363200.32	363200.32	(0.00)	0.45	(0.75)
p50.26	518580.43	0.00	-11.65%	0.06	-21.59%	406631.51	406631.51	(0.00)	2.16	(1.72)
p50.27	547428.70	0.00	-10.11%	0.08	-17.60%	451059.62	451059.62	(0.00)	1.50	(1.81)
p50.28	520419.57	0.00	-13.19%	0.06	-20.10%	415832.44	415832.44	(0.00)	0.38	(0.26)
p50.29	516710.29	0.00	-15.60%	0.06	-26.36%	380492.77	380492.77	(0.00)	1.92	(2.90)
		0.00	-10.61%	0.07	-21.47%		379715.46	(18.30)	1.51	(1.49)

Table 4.9: Results for instances with 100 nodes with mode 3 and candidate list size of 8 (omnidirectional antennas).

Instance	BIP		BIP + VND		ACO					
	obj. function	time (s)	deviation	time (s)	deviation	best	average	(std.)	time (s)	(std.)
p100.00	450275.55	0.01	-12.75%	0.46	-24.30%	340869.27	340909.39	(122.41)	26.50	(23.98)
p100.01	434920.86	0.00	-12.45%	0.45	-18.31%	355284.77	355619.98	(256.40)	38.98	(30.25)
p100.02	467185.46	0.01	-9.77%	0.48	-19.27%	377145.59	377145.59	(0.00)	6.80	(6.31)
p100.03	445615.58	0.00	-14.59%	0.47	-19.90%	356942.53	357246.73	(186.58)	23.78	(24.25)
p100.04	465386.88	0.01	-9.03%	0.50	-17.39%	384446.36	384781.20	(170.28)	21.10	(25.65)
p100.05	517040.38	0.00	-10.68%	0.49	-19.40%	416758.58	416758.58	(0.00)	19.21	(17.45)
p100.06	478615.38	0.01	-14.88%	0.45	-21.35%	376408.49	379266.65	(1603.74)	34.61	(28.02)
p100.07	450138.55	-0.00	-10.24%	0.42	-23.62%	343798.46	343798.46	(0.00)	10.95	(9.77)
p100.08	468277.72	0.00	-11.34%	0.50	-20.51%	372254.06	373888.96	(743.65)	31.35	(25.12)
p100.09	468861.19	0.00	-7.68%	0.49	-21.73%	366993.89	366993.89	(0.00)	10.38	(11.91)
p100.10	407806.54	0.00	-6.57%	0.40	-17.96%	334579.00	334579.00	(0.00)	3.80	(1.33)
p100.11	456482.54	-0.00	-11.32%	0.46	-21.96%	356219.14	356219.14	(0.00)	12.28	(13.34)
p100.12	487388.96	0.00	-10.34%	0.46	-19.19%	393854.17	394305.00	(618.38)	33.81	(26.99)
p100.13	434600.54	0.00	-8.05%	0.53	-23.78%	331270.37	331270.37	(0.00)	11.89	(9.73)
p100.14	419692.94	0.00	-11.30%	0.51	-17.99%	344175.57	344883.10	(1013.85)	29.09	(25.15)
p100.15	416404.90	0.00	-8.31%	0.44	-15.25%	352884.55	352930.55	(76.34)	40.42	(25.45)
p100.16	413254.91	0.00	-9.16%	0.37	-18.04%	338713.69	339968.85	(1007.75)	43.65	(27.25)
p100.17	442166.58	0.00	-8.66%	0.48	-15.40%	374059.25	378223.85	(3362.87)	41.84	(29.52)
p100.18	397526.80	0.00	-10.09%	0.50	-16.50%	331926.13	337088.24	(2625.18)	23.70	(18.24)
p100.19	468763.42	0.00	-9.17%	0.54	-22.12%	365078.37	365078.37	(0.00)	13.18	(9.77)
p100.20	444943.92	0.01	-10.81%	0.45	-20.20%	355078.27	355874.33	(1538.21)	46.43	(24.11)
p100.21	443403.83	-0.00	-9.29%	0.49	-18.31%	362204.29	362251.54	(179.82)	22.39	(22.34)
p100.22	443943.48	-0.00	-6.44%	0.35	-17.53%	366125.96	366125.96	(0.00)	39.12	(21.13)
p100.23	523716.05	0.01	-13.53%	0.47	-21.89%	409062.55	409614.57	(1144.29)	42.10	(28.14)
p100.24	431005.17	-0.00	-9.69%	0.50	-16.99%	357772.11	358616.47	(827.94)	36.93	(26.40)
p100.25	436269.59	0.01	-11.57%	0.59	-18.13%	357191.63	358138.87	(708.06)	54.25	(25.86)
p100.26	454831.86	0.00	-8.39%	0.48	-22.58%	352148.02	352148.02	(0.00)	28.37	(22.36)
p100.27	444542.65	0.01	-8.69%	0.45	-16.76%	370033.07	371208.73	(991.17)	47.63	(29.74)
p100.28	448086.30	0.00	-15.48%	0.45	-22.14%	348889.36	349602.54	(1085.17)	35.84	(27.60)
p100.29	459516.13	0.01	-8.91%	0.48	-22.18%	357595.04	357862.43	(420.10)	30.67	(25.77)
		0.00	-10.31%	0.47	-19.69%		362413.31	(622.74)	28.70	(21.43)

Table 4.10: Results for instances with 200 nodes with mode 3 and candidate list size of 8 (omnidirectional antennas).

Instance	BIP		BIP + VND		ACO					
	obj. function	time (s)	deviation	time (s)	deviation	best	average	(std.)	time (s)	(std.)
p200.00	422258.91	0.01	-9.02%	3.39	-17.81%	347036.77	351102.20	(2114.95)	330.47	(125.50)
p200.01	452571.89	0.02	-12.95%	3.33	-22.29%	351705.57	352702.42	(720.14)	249.58	(114.17)
p200.02	415421.27	0.02	-10.25%	3.40	-20.32%	330988.87	331770.13	(939.23)	311.25	(107.49)
p200.03	444817.05	0.02	-5.82%	3.20	-21.52%	349108.32	357575.38	(4489.92)	371.23	(96.51)
p200.04	441075.09	0.02	-12.69%	3.95	-20.93%	348758.30	353498.45	(4658.25)	274.22	(135.21)
p200.05	443432.15	0.01	-11.56%	4.02	-20.65%	351858.81	354002.08	(537.34)	220.63	(127.22)
p200.06	433856.19	0.01	-11.77%	3.65	-21.80%	339294.50	346267.66	(3567.90)	339.00	(139.14)
p200.07	470339.65	0.02	-13.15%	3.87	-20.74%	372813.94	376500.66	(1941.33)	250.90	(137.65)
p200.08	435047.00	0.01	-11.94%	3.43	-21.03%	343546.05	344953.79	(740.57)	334.60	(109.31)
p200.09	454850.19	0.01	-8.77%	3.80	-20.26%	362684.81	365179.72	(1674.01)	249.22	(120.33)
p200.10	447286.66	0.01	-7.15%	3.67	-21.44%	351380.78	353397.12	(1971.09)	230.27	(114.93)
p200.11	425261.07	0.01	-6.54%	3.66	-20.49%	338112.06	344237.54	(1285.80)	289.61	(127.28)
p200.12	441498.14	0.01	-10.70%	3.30	-21.10%	348344.85	350881.98	(1673.52)	290.37	(111.30)
p200.13	442016.46	0.01	-10.76%	3.91	-19.76%	354679.27	356712.31	(1655.35)	262.89	(137.84)
p200.14	475573.55	0.01	-12.78%	3.76	-25.07%	356354.25	361403.06	(3776.67)	243.39	(135.75)
p200.15	465839.81	0.01	-11.60%	3.53	-21.36%	366330.34	369099.10	(2191.03)	399.72	(95.65)
p200.16	439282.84	0.02	-11.87%	3.50	-17.76%	361270.40	363541.37	(1545.00)	292.98	(129.81)
p200.17	446191.93	0.01	-10.15%	3.03	-20.95%	352707.79	354654.15	(997.96)	354.68	(95.60)
p200.18	415119.62	0.01	-7.65%	3.32	-16.27%	347564.54	348553.73	(633.94)	325.60	(110.95)
p200.19	449669.33	0.01	-6.32%	3.46	-19.97%	359863.22	360787.82	(1171.81)	316.29	(129.81)
p200.20	429835.30	0.01	-8.54%	3.48	-18.71%	349393.13	350192.66	(1039.87)	289.78	(116.20)
p200.21	467439.79	0.01	-9.58%	3.79	-22.77%	360997.52	361979.53	(1233.65)	335.59	(110.57)
p200.22	428361.42	0.01	-11.84%	3.33	-19.19%	346148.78	350803.29	(1838.01)	273.42	(116.68)
p200.23	430995.55	0.01	-8.08%	3.43	-15.97%	362165.31	363278.56	(806.56)	261.23	(148.40)
p200.24	478112.05	0.02	-14.57%	3.95	-24.59%	360546.83	362291.57	(1200.65)	362.32	(91.80)
p200.25	443306.12	0.03	-8.61%	3.64	-18.02%	363431.00	363433.11	(1.63)	221.70	(105.19)
p200.26	460091.26	0.01	-14.26%	3.83	-20.23%	367034.63	368593.91	(1279.39)	290.76	(120.82)
p200.27	457592.00	0.02	-10.04%	3.66	-20.03%	365931.63	369178.54	(2110.43)	296.49	(114.25)
p200.28	462195.02	0.01	-7.64%	3.74	-22.45%	358410.57	359727.38	(1296.98)	298.85	(130.13)
p200.29	430027.42	0.01	-9.23%	3.18	-14.40%	368120.26	371756.39	(1442.40)	313.10	(124.82)
		0.01	-10.19%	3.57	-20.26%		357268.52	(1684.51)	296.00	(119.34)

4.3.2 Results for Directional Antennas

Results for MEB instances with directional antennas are presented grouped by the $\theta_{\min}$ parameter of the antennas. Result tables have the same structure as in the omnidirectional antenna case. Remember that for 20 nodes networks an additional column with results from the optimal solver is included and used as reference. The last table row provides the average improvement (over 30 instances) over MILP for 20 nodes instances and over D-BIP for bigger instances, the average emission power saving, and the average computation time over 30 instances.

After presenting the results for the three different $\theta_{\min}$ values, an overall comparison (including omnidirecitonal antennas) is done in Section 4.3.2.4, showing the savings obtained using directional antennas instead of omnidirectional ones.

4.3.2.1 Directional antennas with $\theta_{\min} = 30°$

The results for the instances with 20 nodes are shown in Table 4.11, for the instances with 50 nodes in Table 4.12, for the instances with 100 nodes in Table 4.13, and for the instances with 200 nodes in Table 4.14.

The results show that for instances of all sizes the improvement of D-ACO over D-BIP is on average more than 10% (with a maximum average improvement of 11.66 obtained in the 50 nodes instances). The average computation times are very low for 20 nodes instances (0.09 seconds). However, in the 50 nodes instances (4.75 seconds) and 100 nodes instances (60.43 seconds) average times double the ones obtained in the omnidirectional case. On average, in the 200 nodes instances, times increase to 418.06 seconds, that is approximately 150% of those required for the same instances in the omnidirectional case. It is interesting to note that the computation times are higher than in the case of omnidirectional antennas. This accounts for the fact that the computation of the heuristic information is more complicated for directional antennas. It is also interesting to note that for all sizes, the average deviation of the D-BIP+VND algorithm in respect to the D-BIP is less than 1%, what may mean that the r-shrink local search procedure is of little use in this case.

In Figure 4.4 and Figure 4.5 a graphical representation of solutions found by D-BIP and ACO algorithms for MEB instances *p50.06* and *p100.25*, respectively, when directional antennas with $\theta_{\min} = 30°$ are considered is shown.

4.3.2.2 Directional antennas with $\theta_{\min} = 60°$

The results for the instances with 20 nodes are shown in Table 4.15, for the instances with 50 nodes in Table 4.16, for the instances with 100 nodes in Table 4.17 and for the instances with 200 nodes in Table 4.18.

The results show that the average improvement of D-ACO over D-BIP is for 20, 50 and 100 instances higher than 6%, while the average improvement in 200 nodes instances is of 5.83%. The average computation times are around 20% lower than in the $\theta_{\min} = 30°$ case: 0.05 seconds for 20 nodes instances, 3.77 seconds for 50 nodes instances, 50.00 seconds for 100 nodes instances and, 379.58 seconds for 200 nodes instances. Note that for all sizes, the average deviation of the D-BIP+VND algorithm in respect to the D-BIP is bigger than 1.5%,

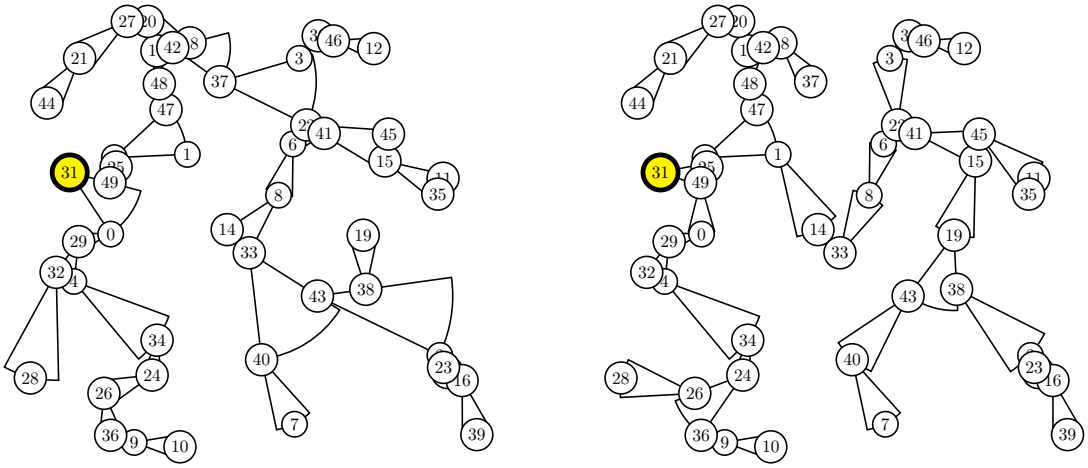

(a) D-BIP solution for instance *p50.06*. Required power: 62291.1.

(b) D-ACO solution for instance *p50.06*. Required power: 51440.2.

Figure 4.4: Solutions found for instance *p50.06* with BIP and ACO (when directional antennas with $\theta_{\min} = 30°$ are considered)

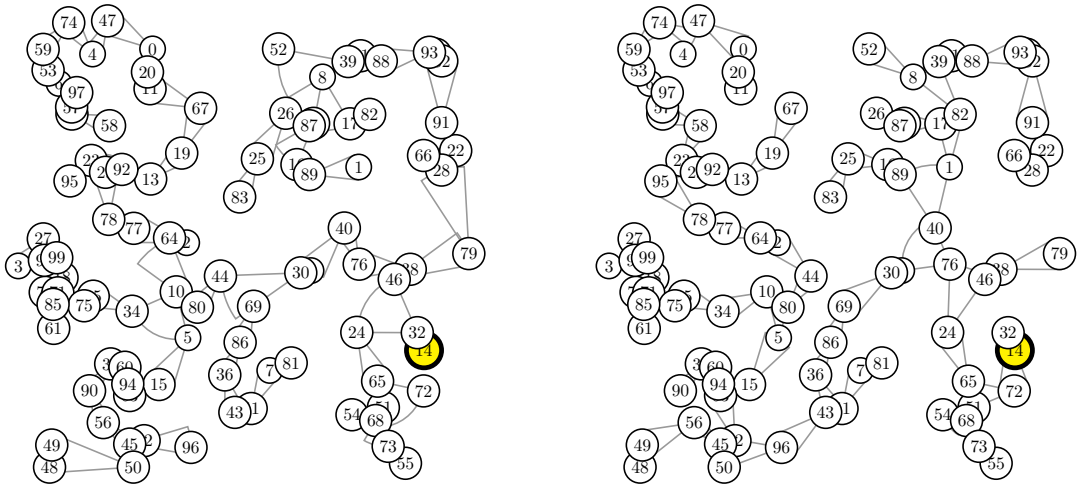

(a) D-BIP solution for instance *p100.25*. Required power: 61989.1.

(b) D-ACO solution for instance *p100.25*. Required power: 51238.0.

Figure 4.5: Solutions found for instance *p100.25* with D-BIP and D-ACO (when directional antennas with $\theta_{\min} = 30°$ are considered)

what suggests that the usage of the r-shrink local search procedure becomes more interesting when $\theta_{\min}$ grows.

In Figure 4.6 and Figure 4.7 a graphical representation of solutions found by D-BIP and

D-ACO algorithms for MEB instances *p50.06* and *p100.25*, respectively, when directional antennas with $\theta_{\min} = 60°$ are considered is shown.

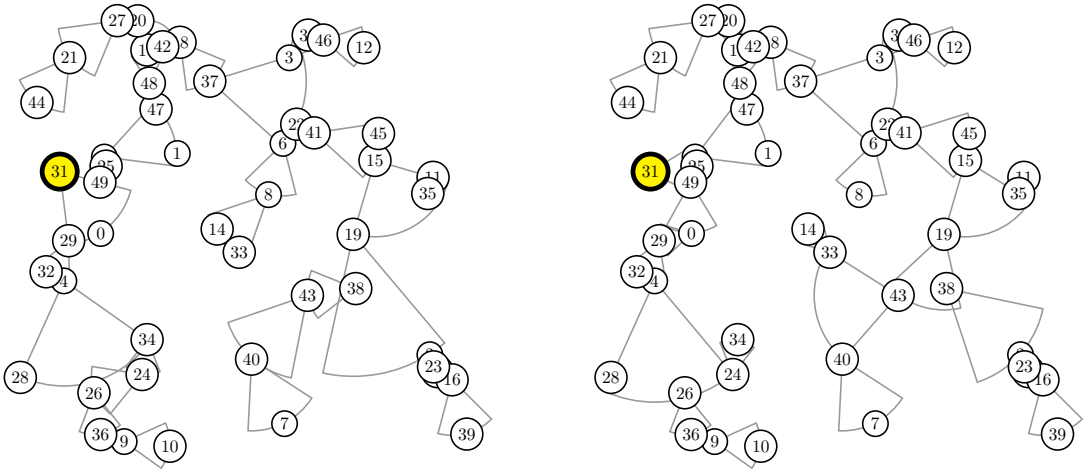

(a) D-BIP solution for instance *p50.06*. Required power: 98545.5.

(b) D-ACO solution for instance *p50.06*. Required power: 89382.8.

Figure 4.6: Solutions found for instance *p50.06* with D-BIP and D-ACO (when directional antennas with $\theta_{\min} = 60°$ are considered)

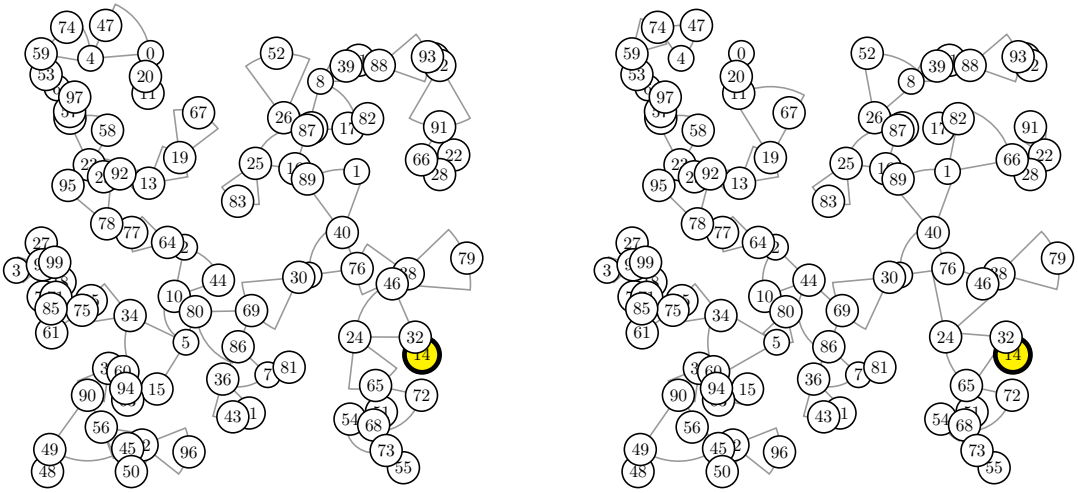

(a) D-BIP solution for instance *p100.25*. Required power: 90422.6.

(b) D-ACO solution for instance *p100.25*. Required power: 85111.6.

Figure 4.7: Solutions found for instance *p100.25* with D-BIP and D-ACO (when directional antennas with $\theta_{\min} = 60°$ are considered)

4.3.2.3 Directional antennas with $\theta_{\min} = 90°$

The results for the instances with 20 nodes are shown in Table 4.19, for the instances with 50 nodes in Table 4.20, for the instances with 100 nodes in Table 4.21 and for the instances with 200 nodes in Table 4.22.

The results show that for instances of all sizes the average improvement of D-ACO over D-BIP is higher than 8%. The average computation times are similar to the ones obtained in the $\theta_{\min} = 60°$ case: for 20 nodes instances 0.21 seconds (still very low), for 50 nodes instances 4.03 seconds, for 100 nodes instances 43.09 seconds and, for 200 nodes instances 357.31 seconds. Note that in this case, the average deviation of the D-BIP+VND algorithm in respect to the DBIP is around than 4% in all cases, what could mean that the usability of the r-shrink local search procedure increases when the $\theta_{\min}$ angle increases. Remember that in the omnidirectional case (i.e. $\theta_{\min} = 90°$) even a 10% improvent can be obtained by adding the VND to the D-BIP algorithm.

In Figure 4.8 and Figure 4.9 a graphical representation of solutions found by D-BIP and D-ACO algorithms for MEB instances *p50.06* and *p100.25*, respectively, when directional antennas with $\theta_{\min} = 90°$ are considered is shown.

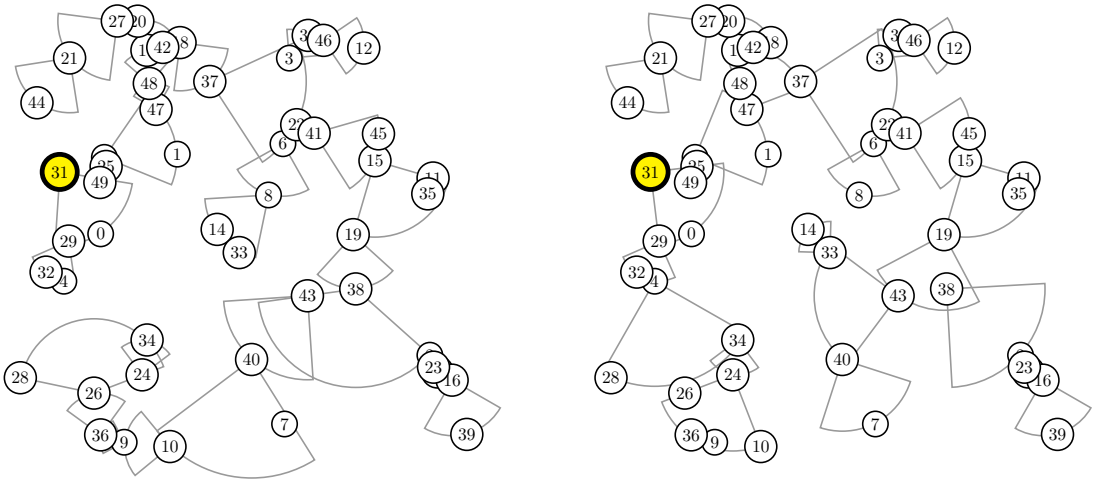

(a) D-BIP solution for instance *p50.06*. Required power: 136965.6.

(b) D-ACO solution for instance *p50.06*. Required power: 123376.6.

Figure 4.8: Solutions found for instance *p50.06* with D-BIP and D-ACO (when directional antennas with $\theta_{\min} = 90°$ are considered)

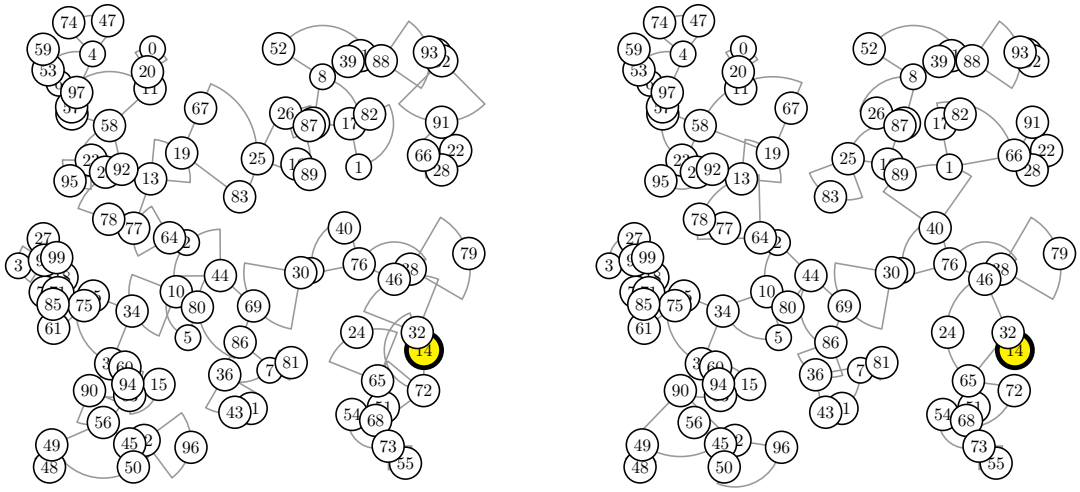

(a) D-BIP solution for instance *p100.25*. Required power: 125623.6.

(b) D-ACO solution for instance *p100.25*. Required power: 109975.6.

Figure 4.9: Solutions found for instance *p100.25* with D-BIP and D-ACO (when directional antennas with $\theta_{\min} = 90°$ are considered)

Table 4.11: Results for instances with 20 nodes with mode 1 and candidate list size of 4 (directional antennas with $\theta_{\min} = 30°$).

Instance	MILP	D-BIP		D-BIP + VND		D-ACO					
		deviation	time (s)	deviation	time (s)	deviation	best	average	(std.)	time (s)	(std.)
p20.00	63199.93	2.57%	0.00	2.57%	0.00	0.00%	63199.93	63199.93	(0.00)	0.03	(0.02)
p20.01	≤ 70824.64	7.14%	0.00	7.14%	0.00	-3.43%	68398.52	68398.52	(0.00)	0.02	(0.02)
p20.02	≤ 47978.29	18.19%	0.00	15.93%	0.01	-0.00%	47978.29	47978.29	(0.00)	0.10	(0.11)
p20.03	≤ 57673.25	13.77%	0.00	13.77%	0.00	-0.48%	57398.42	57398.42	(0.00)	0.02	(0.02)
p20.04	66887.32	4.42%	0.00	4.42%	0.00	-0.00%	66887.32	66887.32	(0.00)	0.01	(0.01)
p20.05	45238.84	19.92%	0.00	19.92%	0.01	0.00%	45238.84	45238.84	(0.00)	0.03	(0.03)
p20.06	≤ 51729.84	14.79%	0.00	14.79%	0.00	-0.00%	51729.84	51729.84	(0.00)	0.23	(0.22)
p20.07	≤ 55324.07	8.17%	0.00	1.03%	0.00	-6.78%	51571.88	51571.88	(0.00)	0.02	(0.01)
p20.08	≤ 49937.22	15.95%	0.00	15.95%	0.01	0.00%	49937.22	49937.22	(0.00)	0.05	(0.05)
p20.09	≤ 60836.59	6.29%	0.00	6.29%	0.00	-2.22%	59488.68	59488.68	(0.00)	0.02	(0.01)
p20.10	≤ 48060.81	30.54%	0.00	30.54%	0.00	0.00%	48060.81	48060.81	(0.00)	0.03	(0.03)
p20.11	≤ 52576.87	17.55%	0.00	17.55%	0.00	-0.00%	52576.87	52576.87	(0.00)	0.09	(0.10)
p20.12	≤ 46448.18	2.61%	0.00	2.61%	0.00	0.00%	46448.20	46448.20	(0.00)	0.01	(0.01)
p20.13	57650.44	48.71%	0.00	36.76%	0.01	-0.00%	57650.44	57650.44	(0.00)	0.04	(0.02)
p20.14	39342.53	23.14%	0.00	23.14%	0.01	-0.00%	39342.53	39342.53	(0.00)	0.07	(0.05)
p20.15	63346.56	0.38%	0.00	0.38%	0.00	-0.00%	63346.56	63346.56	(0.00)	0.01	(0.01)
p20.16	≤ 70879.81	19.24%	0.00	19.24%	0.00	-0.00%	70879.81	70879.81	(0.00)	0.07	(0.06)
p20.17	69089.46	35.14%	0.00	34.31%	0.01	-0.00%	69089.46	69089.46	(0.00)	0.11	(0.11)
p20.18	46477.60	2.17%	0.00	2.17%	0.00	-0.00%	46477.60	46477.60	(0.00)	0.02	(0.01)
p20.19	≤ 64922.68	4.60%	0.00	4.60%	0.01	-1.14%	64180.43	64180.43	(0.00)	0.06	(0.05)
p20.20	66069.30	16.39%	0.00	15.33%	0.00	0.00%	66069.32	66069.32	(0.00)	0.06	(0.07)
p20.21	43714.13	4.62%	0.00	4.62%	0.00	0.00%	43714.14	43714.14	(0.00)	0.01	(0.01)
p20.22	47693.55	14.43%	0.00	9.20%	0.00	0.00%	47693.55	47693.55	(0.00)	0.02	(0.03)
p20.23	51555.92	3.63%	0.00	3.63%	0.00	0.00%	51555.92	51555.92	(0.00)	0.02	(0.01)
p20.24	≤ 50855.85	12.44%	0.00	12.44%	0.00	-2.07%	49804.65	49804.65	(0.00)	0.23	(0.27)
p20.25	≤ 75655.67	27.02%	0.01	27.02%	0.00	-0.69%	75132.03	75149.49	(95.60)	0.89	(0.99)
p20.26	≤ 83211.94	11.67%	0.00	11.67%	-0.00	0.00%	83211.94	83575.58	(98.85)	0.23	(0.82)
p20.27	52136.27	28.39%	0.00	28.39%	0.00	0.00%	52136.30	52136.30	(0.00)	0.01	(0.01)
p20.28	≤ 57444.18	-4.21%	0.00	-4.21%	0.01	-7.92%	52897.18	52897.18	(0.00)	0.07	(0.06)
p20.29	52294.93	11.48%	0.00	11.48%	0.00	0.00%	52294.99	52294.99	(0.00)	0.09	(0.09)
		14.04%	0.00	13.09%	0.00	-0.82%		56492.43	(6.48)	0.09	(0.11)

Table 4.12: Results for instances with 50 nodes with mode 1 and candidate list size of 4 (directional antennas with $\theta_{\min} = 30°$).

Instance	D-BIP		D-BIP + VND		D-ACO					
	obj. function	time (s)	deviation	time (s)	deviation	best	average	(std.)	time (s)	(std.)
p50.00	66047.00	-0.00	-1.39%	0.04	-13.48%	57143.89	57145.34	(2.66)	7.11	(4.76)
p50.01	58532.79	0.00	-1.20%	0.04	-6.00%	55020.28	55020.28	(0.00)	5.74	(3.80)
p50.02	61867.92	0.00	0.00%	0.03	-10.14%	55592.02	55653.91	(85.09)	11.17	(5.60)
p50.03	49392.42	0.00	0.00%	0.04	-10.61%	44151.86	44151.86	(0.00)	0.52	(0.20)
p50.04	53559.60	-0.00	0.00%	0.04	-8.03%	49258.11	49277.80	(26.32)	5.59	(4.93)
p50.05	59443.10	0.00	0.00%	0.04	-8.11%	54624.04	54624.04	(0.00)	5.94	(5.05)
p50.06	62291.14	0.00	0.00%	0.04	-17.42%	51440.18	51440.18	(0.00)	2.23	(1.52)
p50.07	62862.27	0.00	-1.59%	0.04	-14.61%	53677.16	53677.16	(0.00)	0.52	(0.33)
p50.08	60839.79	0.00	0.00%	0.03	-11.38%	53915.98	53928.14	(46.28)	6.00	(5.65)
p50.09	55101.66	0.00	0.00%	0.04	-17.02%	45721.73	45721.73	(0.00)	3.10	(2.82)
p50.10	68045.17	0.00	-0.27%	0.04	-11.16%	60454.61	60480.04	(79.09)	8.85	(4.39)
p50.11	58739.78	0.00	0.00%	0.03	-13.79%	50641.36	50641.36	(0.00)	1.07	(1.42)
p50.12	56176.93	-0.00	0.00%	0.03	-6.78%	52365.95	52428.13	(109.35)	10.05	(4.81)
p50.13	53451.52	0.00	0.00%	0.04	-5.16%	50693.12	50693.12	(0.00)	1.44	(1.08)
p50.14	69956.37	0.00	-3.66%	0.04	-16.71%	58263.43	58263.43	(0.00)	5.14	(3.45)
p50.15	57492.23	0.00	0.00%	0.04	-17.12%	47647.14	47647.14	(0.00)	2.16	(2.48)
p50.16	60471.51	0.00	0.00%	0.04	-10.76%	53963.57	53963.57	(0.00)	1.83	(1.54)
p50.17	57460.78	-0.00	0.00%	0.04	-11.94%	50597.19	50597.19	(0.00)	3.66	(2.83)
p50.18	57112.83	0.00	0.00%	0.03	-6.83%	53211.01	53214.54	(19.29)	5.64	(5.07)
p50.19	57271.16	0.00	0.00%	0.04	-8.58%	52356.87	52356.87	(0.00)	3.70	(3.44)
p50.20	65220.16	0.00	-0.82%	0.04	-14.16%	55986.52	55986.52	(0.00)	1.76	(1.34)
p50.21	60390.51	-0.00	-6.05%	0.04	-15.38%	51102.38	51115.62	(29.96)	11.51	(6.04)
p50.22	58134.98	0.00	0.00%	0.03	-9.72%	52484.70	52488.10	(18.59)	6.28	(4.71)
p50.23	55642.81	-0.00	0.00%	0.04	-7.65%	51386.64	51388.28	(6.25)	7.29	(4.66)
p50.24	71031.93	-0.00	-0.05%	0.04	-18.58%	57834.24	57834.24	(0.00)	5.64	(4.36)
p50.25	69219.17	0.01	-3.53%	0.03	-12.78%	60369.77	60372.52	(15.06)	8.11	(5.05)
p50.26	65739.17	0.00	0.00%	0.03	-14.01%	56527.63	56539.00	(62.32)	6.39	(5.04)
p50.27	66783.83	0.00	0.00%	0.03	-11.16%	59330.71	59330.71	(0.00)	1.61	(1.37)
p50.28	62771.73	0.00	-1.54%	0.04	-11.35%	55646.64	55646.64	(0.00)	0.48	(0.33)
p50.29	60149.39	0.00	0.00%	0.04	-9.37%	54511.41	54511.41	(0.00)	1.91	(2.06)
		0.00	-0.67%	0.04	-11.66%		53537.96	(16.68)	4.75	(3.34)

Table 4.13: Results for instances with 100 nodes with mode 1 and candidate list size of 4 (directional antennas with $\theta_{\min} = 30°$).

Instance	D-BIP		D-BIP + VND		D-ACO					
	obj. function	time (s)	deviation	time (s)	deviation	best	average	(std.)	time (s)	(std.)
p100.00	56394.41	0.01	0.00%	0.28	-12.85%	49146.01	49321.35	(87.30)	77.84	(18.44)
p100.01	52077.90	0.01	-1.45%	0.34	-11.48%	46099.94	46516.89	(113.81)	69.91	(23.27)
p100.02	53254.80	0.00	-0.10%	0.33	-3.77%	51249.17	51290.96	(88.17)	70.35	(23.83)
p100.03	56728.01	0.00	-1.26%	0.25	-13.64%	48988.40	49153.76	(180.92)	74.11	(19.15)
p100.04	59388.88	0.01	-1.52%	0.28	-12.68%	51857.11	52329.05	(208.33)	77.93	(12.43)
p100.05	64686.46	0.00	0.00%	0.28	-13.52%	55942.81	55954.34	(43.43)	53.18	(21.99)
p100.06	57303.06	0.00	-0.49%	0.21	-5.42%	54197.69	54449.51	(132.70)	60.57	(30.64)
p100.07	56251.73	0.00	-1.06%	0.30	-11.34%	49872.89	50114.60	(190.54)	67.06	(26.31)
p100.08	57367.02	0.00	0.00%	0.26	-11.00%	51055.65	51147.34	(68.01)	62.98	(22.78)
p100.09	61647.84	0.00	-0.14%	0.32	-9.12%	56027.46	56217.21	(175.10)	66.72	(22.48)
p100.10	54923.13	0.00	0.00%	0.27	-12.01%	48325.42	48327.19	(9.69)	31.69	(21.76)
p100.11	54994.13	0.00	-0.17%	0.29	-10.46%	49239.39	49431.08	(86.49)	59.96	(23.84)
p100.12	61480.78	0.00	-1.18%	0.31	-15.32%	52063.53	52123.47	(33.36)	52.86	(25.32)
p100.13	53075.82	-0.00	0.00%	0.31	-5.35%	50237.86	50238.83	(0.59)	55.48	(25.34)
p100.14	49609.12	-0.00	0.00%	0.28	-6.94%	46167.07	46179.55	(37.00)	54.18	(27.05)
p100.15	54578.33	-0.00	-0.88%	0.26	-9.22%	49548.70	49587.11	(63.12)	61.80	(24.26)
p100.16	52367.90	0.00	0.00%	0.25	-10.45%	46894.55	46905.66	(13.43)	35.40	(21.23)
p100.17	61159.09	-0.00	0.00%	0.30	-11.68%	54018.40	54062.18	(44.10)	49.45	(28.54)
p100.18	50476.59	-0.00	-0.92%	0.34	-11.06%	44894.30	44899.49	(9.56)	33.68	(17.95)
p100.19	63936.22	0.01	-1.75%	0.31	-11.27%	56732.32	56875.26	(107.71)	68.94	(18.21)
p100.20	53130.16	0.01	0.00%	0.26	-8.07%	48842.43	48865.31	(61.92)	56.92	(27.78)
p100.21	60781.81	0.01	0.00%	0.26	-8.91%	55363.93	55397.09	(61.73)	63.76	(20.95)
p100.22	55227.65	0.00	0.00%	0.28	-14.07%	47456.42	47675.17	(167.75)	59.32	(24.84)
p100.23	66624.29	-0.00	0.00%	0.24	-11.41%	59024.03	59256.32	(153.94)	73.10	(18.85)
p100.24	64782.35	0.00	-3.42%	0.30	-18.03%	53099.30	53123.42	(19.27)	68.78	(22.22)
p100.25	61989.13	0.01	-0.73%	0.28	-17.34%	51238.00	51425.21	(124.03)	69.72	(21.94)
p100.26	59195.62	0.00	-0.14%	0.33	-11.40%	52448.92	52559.39	(41.83)	61.64	(22.75)
p100.27	53112.41	0.00	0.00%	0.27	-8.16%	48780.84	48815.29	(30.75)	48.59	(26.05)
p100.28	56245.31	0.00	0.00%	0.28	-10.58%	50295.28	50444.02	(90.17)	73.20	(22.87)
p100.29	52836.95	0.01	-0.07%	0.26	-7.20%	49033.45	49098.38	(84.74)	53.73	(26.64)
		0.00	-0.51%	0.28	-10.79%		51059.48	(84.32)	60.43	(22.99)

Table 4.14: Results for instances with 200 nodes with mode 1 and candidate list size of 4 (directional antennas with $\theta_{\min} = 30°$).

Instance	D-BIP		D-BIP + VND		D-ACO					
	obj. function	time (s)	deviation	time (s)	deviation	best	average	(std.)	time (s)	(std.)
p200.00	53790.35	0.01	-0.87%	2.43	-12.41%	47115.51	47382.98	(117.28)	428.55	(56.67)
p200.01	55274.42	0.01	-0.50%	2.33	-8.46%	50598.52	50816.87	(140.30)	422.18	(68.03)
p200.02	49336.10	0.01	-0.50%	2.31	-10.19%	44308.85	44585.52	(138.39)	424.59	(59.56)
p200.03	58187.05	0.01	-0.26%	2.25	-10.55%	52045.58	52298.08	(121.62)	410.88	(72.17)
p200.04	55740.61	0.01	-0.48%	2.46	-9.23%	50596.66	50752.69	(102.98)	436.09	(51.64)
p200.05	57280.31	0.01	0.00%	2.17	-11.91%	50456.55	50611.71	(88.66)	439.01	(45.61)
p200.06	55127.41	0.01	-1.10%	2.38	-9.03%	50149.92	50417.88	(128.41)	426.42	(78.08)
p200.07	58295.35	0.01	-2.24%	2.47	-12.78%	50843.91	51051.25	(140.27)	410.63	(73.76)
p200.08	54934.61	0.02	-1.44%	2.38	-9.92%	49485.06	49924.12	(201.56)	398.32	(70.12)
p200.09	57515.50	0.01	-2.12%	2.09	-10.07%	51723.47	51982.42	(126.36)	407.93	(67.17)
p200.10	54952.34	0.01	-0.65%	2.24	-9.23%	49882.63	50049.06	(96.50)	416.96	(60.11)
p200.11	52606.98	0.01	-0.72%	2.29	-11.14%	46746.72	46951.71	(138.36)	425.99	(59.80)
p200.12	54340.34	0.02	0.00%	2.25	-10.21%	48793.48	48940.17	(105.55)	385.90	(76.02)
p200.13	57277.99	-0.00	-0.73%	2.19	-9.93%	51591.26	51852.73	(144.65)	408.34	(104.96)
p200.14	55768.55	0.02	-0.16%	2.43	-9.22%	50626.23	50899.71	(144.39)	420.34	(57.89)
p200.15	57697.15	0.01	-0.95%	2.38	-9.94%	51961.62	52206.30	(162.68)	424.53	(62.53)
p200.16	56592.96	0.02	-1.03%	2.33	-12.15%	49716.45	50000.05	(143.95)	439.05	(67.33)
p200.17	54964.84	0.01	-0.36%	2.28	-11.57%	48606.15	48802.05	(95.43)	453.44	(47.18)
p200.18	49855.23	0.02	0.00%	2.26	-6.33%	46701.01	46989.25	(131.46)	424.52	(72.94)
p200.19	54997.09	0.01	-0.42%	2.46	-9.01%	50041.27	50497.09	(235.32)	427.12	(49.81)
p200.20	50092.96	0.01	-0.48%	2.62	-6.79%	46689.28	46835.76	(82.31)	400.36	(70.44)
p200.21	55873.69	0.02	-0.23%	2.34	-9.42%	50608.16	50853.92	(181.53)	405.60	(77.73)
p200.22	54025.16	0.01	-0.24%	2.27	-8.73%	49309.74	49476.53	(106.92)	400.72	(67.72)
p200.23	56710.90	0.02	-0.27%	2.28	-8.92%	51651.29	51932.56	(209.59)	418.15	(62.79)
p200.24	58130.15	0.01	-0.01%	2.43	-10.53%	52008.09	52275.84	(179.81)	382.90	(85.79)
p200.25	56705.28	0.01	0.00%	2.35	-8.74%	51751.22	52039.03	(168.60)	410.99	(63.11)
p200.26	59930.98	0.01	-0.19%	2.23	-12.43%	52478.73	52809.76	(238.88)	415.88	(62.09)
p200.27	60969.06	0.01	-1.06%	2.24	-12.07%	53612.82	53916.15	(133.34)	434.51	(59.37)
p200.28	55712.99	0.01	-0.25%	2.15	-11.68%	49207.32	49409.05	(154.32)	428.92	(47.84)
p200.29	53144.19	0.01	-0.08%	2.43	-8.96%	48384.95	48687.89	(120.55)	412.85	(57.93)
		0.01	-0.58%	2.32	-10.05%		50174.94	(142.67)	418.06	(65.21)

Table 4.15: Results for instances with 20 nodes with mode 1 and candidate list size of 8 (directional antennas with $\theta_{\min} = 60°$).

Instance	MILP	D-BIP		D-BIP + VND		D-ACO					
		deviation	time (s)	deviation	time (s)	deviation	best	average	(std.)	time (s)	(std.)
p20.00	107799.12	10.04%	0.00	8.91%	0.00	0.00%	107799.12	107799.12	(0.00)	0.02	(0.01)
p20.01	108600.28	24.48%	0.00	12.36%	0.01	0.00%	108600.28	108600.28	(0.00)	0.03	(0.02)
p20.02	77177.01	2.72%	0.00	2.72%	0.00	-0.00%	77177.01	77177.01	(0.00)	0.01	(0.01)
p20.03	$\leq$ 97480.94	8.72%	0.00	3.44%	0.00	0.00%	97480.94	97480.94	(0.00)	0.02	(0.02)
p20.04	125420.38	6.94%	0.00	6.02%	0.01	0.00%	125420.38	125420.38	(0.00)	0.02	(0.01)
p20.05	77162.35	7.71%	0.00	4.51%	0.01	0.00%	77162.35	77162.35	(0.00)	0.03	(0.02)
p20.06	$\leq$ 87639.56	11.01%	0.00	4.02%	0.00	-0.00%	87639.56	87639.56	(0.00)	0.13	(0.11)
p20.07	$\leq$ 91232.97	7.76%	0.00	7.76%	0.01	-0.20%	91046.44	91046.44	(0.00)	0.15	(0.18)
p20.08	82936.55	6.50%	0.00	0.54%	0.01	-0.00%	82936.55	82936.55	(0.00)	0.01	(0.01)
p20.09	83885.62	0.39%	0.00	0.00%	0.00	0.00%	83885.62	83885.62	(0.00)	0.01	(0.01)
p20.10	$\leq$ 75300.97	3.35%	0.00	0.00%	0.01	0.00%	75300.97	75300.97	(0.00)	0.01	(0.01)
p20.11	82591.95	3.51%	0.00	3.51%	0.00	0.00%	82591.95	82591.95	(0.00)	0.02	(0.01)
p20.12	90971.93	0.46%	0.00	0.46%	0.00	0.00%	90971.99	90971.99	(0.00)	0.02	(0.01)
p20.13	101468.12	19.53%	0.00	19.53%	0.00	0.00%	101468.13	101468.13	(0.00)	0.01	(0.01)
p20.14	64191.31	10.27%	0.00	10.27%	0.00	-0.00%	64191.31	64191.31	(0.00)	0.01	(0.01)
p20.15	107067.98	4.14%	0.00	4.14%	0.00	-0.00%	107067.98	107067.98	(0.00)	0.04	(0.02)
p20.16	$\leq$ 115907.83	9.99%	0.00	8.74%	0.00	-0.00%	115907.83	115907.83	(0.00)	0.10	(0.05)
p20.17	113576.40	10.77%	0.00	7.23%	0.01	0.00%	113576.40	113576.40	(0.00)	0.62	(0.56)
p20.18	80477.96	8.55%	0.00	8.18%	0.01	0.00%	80477.96	80477.96	(0.00)	0.01	(0.01)
p20.19	91112.59	0.98%	0.00	0.20%	0.00	0.00%	91112.59	91112.59	(0.00)	0.09	(0.05)
p20.20	104290.47	5.52%	0.00	5.22%	0.01	0.00%	104290.47	104290.47	(0.00)	0.01	(0.01)
p20.21	83771.26	2.50%	0.00	2.50%	0.01	0.00%	83771.26	83771.26	(0.00)	0.01	(0.01)
p20.22	83820.44	8.57%	0.00	4.68%	0.01	-0.00%	83820.44	83820.44	(0.00)	0.02	(0.02)
p20.23	87126.26	9.57%	0.00	8.20%	0.01	0.00%	87126.26	87126.26	(0.00)	0.01	(0.01)
p20.24	$\leq$ 86981.75	7.76%	0.00	3.77%	0.00	-1.02%	86091.65	86091.65	(0.00)	0.04	(0.02)
p20.25	$\leq$ 146489.77	5.93%	0.00	-7.70%	0.00	-15.94%	123134.14	123134.14	(0.00)	0.01	(0.01)
p20.26	123320.38	6.23%	0.00	6.23%	0.00	0.00%	123320.39	123320.39	(0.00)	0.05	(0.04)
p20.27	$\leq$ 94563.10	4.27%	0.00	2.93%	0.00	-0.00%	94563.09	94563.09	(0.00)	0.02	(0.02)
p20.28	$\leq$ 88243.77	2.76%	0.00	2.76%	0.00	-0.51%	87796.06	87796.06	(0.00)	0.01	(0.01)
p20.29	81302.68	5.02%	0.00	5.02%	0.00	0.00%	81302.68	81302.68	(0.00)	0.04	(0.02)
		7.20%	0.00	4.87%	0.00	-0.59%		93901.06	(0.00)	0.05	(0.04)

Table 4.16: Results for instances with 50 nodes with mode 1 and candidate list size of 8 (directional antennas with $\theta_{\min} = 60°$).

Instance	D-BIP		D-BIP + VND		D-ACO					
	obj. function	time (s)	deviation	time (s)	deviation	best	average	(std.)	time (s)	(std.)
p50.00	106484.24	0.00	-1.52%	0.05	-9.06%	96840.78	96840.78	(0.00)	3.60	(3.13)
p50.01	103404.52	-0.00	-3.29%	0.06	-7.84%	95300.75	95341.44	(222.88)	5.12	(4.57)
p50.02	99580.94	0.00	-2.37%	0.06	-2.64%	96950.00	97034.54	(108.30)	8.66	(5.46)
p50.03	78733.20	-0.00	-5.74%	0.06	-9.33%	71384.49	71384.49	(0.00)	0.19	(0.10)
p50.04	88360.18	0.00	-6.65%	0.05	-8.60%	80762.69	80895.72	(292.40)	6.87	(4.24)
p50.05	99158.27	0.00	-9.71%	0.06	-11.05%	88199.82	88199.82	(0.00)	2.70	(1.99)
p50.06	98545.48	0.00	0.00%	0.04	-9.30%	89382.78	89382.78	(0.00)	4.87	(3.50)
p50.07	108359.84	0.00	-7.30%	0.05	-13.78%	93426.77	93426.77	(0.00)	0.60	(0.45)
p50.08	90611.48	-0.00	0.00%	0.04	-1.95%	88846.94	88859.88	(44.33)	7.55	(5.29)
p50.09	84684.65	0.00	-1.67%	0.05	-4.72%	80683.59	80683.59	(0.00)	1.64	(1.07)
p50.10	113183.43	0.00	-0.08%	0.05	-10.21%	101627.66	101655.33	(18.42)	3.39	(4.23)
p50.11	93978.56	0.00	-2.91%	0.06	-6.41%	87951.94	87951.94	(0.00)	1.83	(1.67)
p50.12	91143.60	0.01	-1.94%	0.05	-5.00%	86588.96	86588.96	(0.00)	0.84	(0.42)
p50.13	93758.75	0.00	0.00%	0.05	-3.59%	90394.47	90394.47	(0.00)	5.35	(3.88)
p50.14	110331.80	0.00	-0.23%	0.05	-4.21%	105688.91	105763.29	(129.22)	10.00	(5.45)
p50.15	92663.15	0.00	-2.43%	0.05	-8.99%	84333.60	84411.57	(21.19)	3.98	(2.65)
p50.16	102584.40	0.00	-7.26%	0.06	-10.10%	92220.10	92220.10	(0.00)	0.39	(0.18)
p50.17	91532.48	0.00	-1.46%	0.05	-8.82%	83457.14	83708.41	(276.18)	8.15	(5.25)
p50.18	91147.39	0.00	-2.20%	0.05	-3.52%	87936.08	87936.08	(0.00)	0.36	(0.18)
p50.19	97338.98	0.00	-3.82%	0.04	-10.76%	86863.64	86863.64	(0.00)	0.61	(0.22)
p50.20	101949.83	0.00	-0.18%	0.05	-2.52%	99380.57	99490.72	(110.06)	7.58	(6.41)
p50.21	90794.92	0.00	0.00%	0.05	-4.58%	86635.42	86635.42	(0.00)	1.95	(2.72)
p50.22	91131.66	0.00	-0.18%	0.05	-5.96%	85701.01	85701.01	(0.00)	3.09	(2.93)
p50.23	94871.64	0.00	-4.25%	0.05	-11.36%	84095.11	84095.11	(0.00)	2.48	(1.07)
p50.24	103802.18	0.00	-1.01%	0.05	-1.01%	102749.46	102749.46	(0.00)	1.36	(0.83)
p50.25	100465.75	0.00	-2.47%	0.05	-4.92%	95526.70	95526.70	(0.00)	0.53	(0.57)
p50.26	104195.06	0.00	-0.84%	0.05	-5.47%	98497.39	98504.26	(15.62)	8.44	(5.38)
p50.27	114042.78	0.00	-3.05%	0.05	-6.01%	107188.84	107198.74	(37.70)	6.98	(5.31)
p50.28	103674.29	0.00	-1.16%	0.05	-5.72%	97743.01	97743.01	(0.00)	1.61	(1.33)
p50.29	95375.83	0.00	0.00%	0.04	-3.44%	92097.09	92097.09	(0.00)	2.52	(2.14)
		0.00	-2.46%	0.05	-6.70%		91309.50	(42.54)	3.77	(2.75)

Table 4.17: Results for instances with 100 nodes with mode 1 and candidate list size of 8 (directional antennas with $\theta_{\min} = 60°$).

Instance	D-BIP		D-BIP + VND		D-ACO					
	obj. function	time (s)	deviation	time (s)	deviation	best	average	(std.)	time (s)	(std.)
p100.00	90638.11	0.01	-0.81%	0.38	-5.99%	85204.36	85347.78	(183.63)	67.01	(24.61)
p100.01	86982.86	0.00	-3.03%	0.38	-8.75%	79371.57	79997.56	(402.92)	63.86	(26.46)
p100.02	89079.65	-0.00	-0.31%	0.35	-4.02%	85498.74	85511.13	(67.86)	39.04	(26.87)
p100.03	86821.55	0.00	-0.63%	0.35	-4.70%	82742.64	83063.40	(360.05)	58.18	(28.74)
p100.04	92430.38	-0.00	-0.65%	0.34	-7.57%	85430.76	85823.19	(410.75)	65.09	(23.32)
p100.05	105504.38	0.00	-0.74%	0.30	-7.99%	97071.56	97096.40	(28.00)	54.50	(28.11)
p100.06	96035.88	-0.00	-1.63%	0.33	-7.25%	89073.64	89852.56	(418.57)	67.74	(19.86)
p100.07	90582.99	0.01	-1.41%	0.42	-6.50%	84691.61	84936.24	(199.81)	64.46	(26.94)
p100.08	97239.22	0.01	-2.94%	0.45	-7.81%	89644.44	89740.81	(18.22)	41.33	(25.64)
p100.09	97152.20	0.01	-4.48%	0.36	-7.75%	89620.58	90486.94	(466.06)	54.41	(28.65)
p100.10	85506.29	-0.00	-4.00%	0.41	-9.04%	77776.52	77848.90	(147.23)	47.12	(24.27)
p100.11	87214.99	-0.00	-1.32%	0.40	-5.82%	82138.83	82440.01	(252.93)	46.46	(25.93)
p100.12	94828.06	0.00	-2.05%	0.47	-4.20%	90845.37	90946.20	(40.43)	25.24	(24.16)
p100.13	85301.21	0.00	-0.17%	0.41	-6.68%	79604.75	80033.47	(185.38)	58.82	(23.87)
p100.14	79414.95	0.00	-0.93%	0.40	-2.51%	77420.01	77427.16	(1.35)	13.17	(15.31)
p100.15	90950.23	-0.00	-2.21%	0.35	-6.94%	84635.42	84818.06	(103.57)	46.56	(26.50)
p100.16	84062.74	0.00	-1.56%	0.42	-5.90%	79105.27	79156.84	(46.00)	35.33	(23.06)
p100.17	96355.35	-0.00	-0.66%	0.36	-8.15%	88502.54	88569.10	(89.22)	58.70	(25.70)
p100.18	81529.79	0.01	-0.06%	0.36	-4.79%	77628.52	77662.89	(58.09)	63.46	(22.30)
p100.19	97701.52	0.00	-0.23%	0.41	-6.38%	91464.66	91781.89	(333.13)	46.45	(29.10)
p100.20	87543.96	0.00	-1.75%	0.36	-7.98%	80561.07	80561.07	(0.00)	17.74	(16.53)
p100.21	94360.20	-0.00	-0.95%	0.42	-7.86%	86941.66	86941.66	(0.00)	20.11	(14.25)
p100.22	87121.22	-0.00	-1.02%	0.37	-4.49%	83207.55	83358.10	(144.40)	51.33	(31.07)
p100.23	108187.05	-0.00	-4.14%	0.38	-10.72%	96587.64	97131.82	(342.83)	80.54	(17.18)
p100.24	95541.54	0.01	-2.34%	0.36	-8.38%	87539.37	87803.07	(258.27)	64.45	(25.81)
p100.25	90422.58	0.00	-1.44%	0.39	-5.87%	85111.60	85327.05	(142.58)	59.35	(26.33)
p100.26	91585.22	0.00	-1.67%	0.40	-5.23%	86794.00	86972.07	(184.78)	60.65	(22.06)
p100.27	81080.59	-0.00	0.00%	0.36	-1.78%	79636.18	79640.21	(15.33)	43.36	(23.45)
p100.28	89102.21	0.01	-3.97%	0.40	-7.00%	82867.41	82880.64	(3.38)	33.73	(23.76)
p100.29	88264.91	0.01	-1.93%	0.39	-8.31%	80934.07	81084.45	(92.44)	51.72	(27.64)
		0.00	-1.64%	0.38	-6.55%		85141.36	(166.57)	50.00	(24.25)

Table 4.18: Results for instances with 200 nodes with mode 1 and candidate list size of 8 (directional antennas with $\theta_{\min} = 60°$).

Instance	D-BIP		D-BIP + VND		D-ACO					
	obj. function	time (s)	deviation	time (s)	deviation	best	average	(std.)	time (s)	(std.)
p200.00	86893.63	0.02	-2.63%	3.28	-7.27%	80580.60	80847.25	(166.63)	401.63	(75.83)
p200.01	91701.01	0.01	-2.08%	3.00	-5.54%	86622.20	86831.34	(95.22)	358.09	(107.87)
p200.02	77173.06	0.01	-1.34%	2.90	-4.83%	73447.24	73712.61	(166.15)	343.30	(114.34)
p200.03	91040.93	0.01	-0.52%	2.98	-4.43%	87007.03	87350.07	(182.17)	395.70	(88.21)
p200.04	90277.31	0.01	-3.60%	3.41	-8.31%	82775.03	83006.54	(61.50)	374.00	(113.13)
p200.05	88885.97	0.01	-1.24%	3.03	-5.80%	83733.80	84135.73	(211.38)	389.54	(73.80)
p200.06	90102.98	0.01	-2.63%	3.20	-7.42%	83420.07	83482.94	(33.64)	348.89	(100.99)
p200.07	92258.34	0.01	-2.47%	3.09	-5.62%	87074.67	87247.48	(108.29)	372.65	(91.28)
p200.08	85676.20	0.01	-0.82%	3.06	-4.94%	81442.60	81799.81	(207.96)	319.19	(111.62)
p200.09	92707.38	0.01	-3.37%	2.69	-7.21%	86027.33	86371.21	(165.48)	361.93	(116.10)
p200.10	89964.60	0.01	-1.04%	2.96	-4.54%	85876.27	86517.35	(233.26)	356.21	(124.38)
p200.11	83784.45	0.02	-1.06%	3.02	-4.61%	79925.16	80052.90	(66.90)	396.89	(76.12)
p200.12	88333.04	0.01	-2.75%	3.02	-7.51%	81703.47	82051.24	(177.20)	423.87	(63.83)
p200.13	91219.68	0.01	-0.43%	3.18	-6.97%	84860.29	85307.90	(231.98)	361.85	(102.51)
p200.14	94166.75	0.01	-1.61%	2.93	-6.42%	88122.35	88373.28	(131.33)	393.93	(82.64)
p200.15	90753.52	0.01	-0.20%	2.66	-3.88%	87227.81	87452.20	(101.38)	355.47	(106.77)
p200.16	89491.45	0.01	-1.55%	3.04	-6.00%	84124.60	84280.72	(97.36)	377.14	(115.51)
p200.17	88779.44	0.01	-2.57%	3.01	-7.17%	82411.17	82615.13	(108.93)	392.16	(67.86)
p200.18	83654.40	0.02	-2.02%	3.04	-4.12%	80204.54	80467.08	(166.48)	406.31	(88.48)
p200.19	90255.00	0.02	-1.08%	3.08	-5.89%	84939.56	85348.84	(156.21)	396.40	(82.79)
p200.20	79419.05	0.02	-2.20%	3.20	-3.76%	76434.05	76535.62	(84.99)	349.21	(108.80)
p200.21	92766.40	0.02	-0.47%	3.07	-5.57%	87601.45	87943.28	(221.07)	373.35	(126.68)
p200.22	86925.68	0.01	-1.92%	3.22	-5.48%	82162.22	82467.90	(151.23)	376.00	(93.04)
p200.23	87958.01	0.01	-3.51%	3.19	-6.87%	81913.84	82138.23	(214.18)	373.01	(84.60)
p200.24	96218.14	0.01	-1.13%	2.72	-7.03%	89451.74	89938.41	(296.81)	392.09	(86.63)
p200.25	88662.32	0.01	-0.49%	2.90	-3.70%	85382.95	85939.48	(242.37)	385.39	(107.06)
p200.26	94577.78	0.02	-1.59%	3.20	-6.86%	88092.46	88260.95	(79.13)	396.48	(90.92)
p200.27	94435.64	0.01	-1.13%	2.83	-5.81%	88949.06	89419.36	(259.67)	412.70	(84.96)
p200.28	89871.86	0.01	-2.16%	3.33	-6.57%	83971.36	84176.52	(133.24)	408.42	(76.25)
p200.29	86943.60	0.02	-0.95%	3.03	-4.69%	82862.47	83174.99	(166.75)	395.62	(88.71)
		0.01	-1.69%	3.04	-5.83%		84241.55	(157.30)	379.58	(95.06)

Table 4.19: Results for instances with 20 nodes with mode 3 and candidate list size of 8 (directional antennas with $\theta_{\min} = 90°$).

Instance	MILP	D-BIP		D-BIP + VND		D-ACO					
		deviation	time (s)	deviation	time (s)	deviation	best	average	(std.)	time (s)	(std.)
p20.00	149269.03	1.83%	0.00	1.64%	0.00	0.00%	149269.03	149269.03	(0.00)	0.41	(0.40)
p20.01	149927.53	11.88%	0.01	5.71%	0.01	0.00%	149927.55	149927.55	(0.00)	0.02	(0.01)
p20.02	101073.24	4.58%	0.00	2.51%	0.00	0.00%	101073.24	101073.24	(0.00)	0.01	(0.01)
p20.03	126813.02	9.02%	0.00	0.59%	0.01	-0.00%	126813.02	126813.02	(0.00)	0.02	(0.01)
p20.04	168919.81	7.24%	0.00	0.17%	0.00	0.00%	168919.81	168919.81	(0.00)	0.02	(0.02)
p20.05	100251.75	12.27%	0.00	-0.00%	0.00	-0.00%	100251.75	100251.75	(0.00)	0.01	(0.00)
p20.06	112029.92	15.94%	0.00	14.25%	0.00	0.00%	112029.92	112029.92	(0.00)	1.05	(1.12)
p20.07	$\leq$ 112282.70	5.05%	0.00	1.46%	0.01	-0.29%	111954.48	111954.48	(0.00)	0.02	(0.02)
p20.08	110677.23	10.80%	0.00	4.54%	0.01	-0.00%	110677.23	110677.23	(0.00)	0.02	(0.01)
p20.09	118033.32	9.31%	0.00	0.00%	0.00	0.00%	118033.32	118033.32	(0.00)	0.02	(0.01)
p20.10	94753.92	4.38%	0.00	0.00%	0.01	0.00%	94753.93	94753.93	(0.00)	0.01	(0.00)
p20.11	107055.00	5.54%	0.00	3.10%	0.01	-0.00%	107055.00	107055.00	(0.00)	0.03	(0.02)
p20.12	114497.29	15.39%	0.00	3.75%	0.00	0.00%	114497.29	114497.29	(0.00)	0.03	(0.02)
p20.13	129068.95	19.64%	0.00	3.17%	0.01	0.00%	129068.95	129150.88	(54.55)	1.23	(1.48)
p20.14	88786.21	1.38%	0.00	-0.00%	0.01	-0.00%	88786.21	88786.21	(0.00)	0.01	(0.00)
p20.15	147031.13	5.01%	0.00	5.01%	0.00	0.00%	147031.13	147031.13	(0.00)	0.32	(0.21)
p20.16	$\leq$ 153059.44	3.68%	0.00	1.62%	0.01	0.00%	153059.60	153069.78	(38.76)	0.09	(0.11)
p20.17	133158.16	14.41%	0.00	0.72%	0.01	-0.00%	133158.16	133158.16	(0.00)	0.11	(0.12)
p20.18	103948.43	11.99%	0.00	1.73%	0.01	0.00%	103948.44	103948.44	(0.00)	0.02	(0.01)
p20.19	124745.01	1.76%	0.00	0.21%	0.01	0.00%	124745.01	124745.01	(0.00)	0.02	(0.02)
p20.20	144808.57	2.52%	0.00	2.19%	0.01	0.00%	144808.57	144808.57	(0.00)	0.47	(0.52)
p20.21	112268.71	10.46%	0.00	9.95%	0.00	0.00%	112268.71	112303.90	(192.76)	0.52	(0.41)
p20.22	112920.51	9.80%	0.00	5.49%	0.00	-0.00%	112920.51	112920.51	(0.00)	0.01	(0.01)
p20.23	118717.10	4.65%	0.00	4.65%	0.01	-0.00%	118717.10	118717.10	(0.00)	0.01	(0.01)
p20.24	$\leq$ 117601.39	10.33%	0.00	7.24%	0.00	-0.18%	117387.62	117481.38	(78.28)	1.27	(1.27)
p20.25	$\leq$ 156646.18	14.28%	0.00	10.58%	0.01	0.00%	156646.18	156646.18	(0.00)	0.16	(0.17)
p20.26	164076.55	2.13%	0.00	1.21%	0.00	-0.00%	164076.55	164076.55	(0.00)	0.15	(0.15)
p20.27	$\leq$ 136012.36	0.81%	-0.00	0.81%	-0.00	-1.28%	134276.62	134276.62	(0.00)	0.08	(0.06)
p20.28	$\leq$ 118160.51	9.91%	0.00	9.53%	0.00	0.00%	118160.51	118160.51	(0.00)	0.11	(0.11)
p20.29	102895.52	6.86%	0.00	0.43%	0.01	0.00%	102895.53	102895.53	(0.00)	0.02	(0.01)
		8.10%	0.00	3.41%	0.01	-0.06%		124247.73	(12.15)	0.21	(0.21)

Table 4.20: Results for instances with 50 nodes with mode 3 and candidate list size of 8 (directional antennas with $\theta_{\min} = 90°$).

Instance	D-BIP		D-BIP + VND		D-ACO					
	obj. function	time (s)	deviation	time (s)	deviation	best	average	(std.)	time (s)	(std.)
p50.00	143311.60	0.00	-5.46%	0.06	-8.92%	130526.46	130526.46	(0.00)	1.53	(1.35)
p50.01	137405.56	0.00	-3.68%	0.06	-6.29%	128769.59	129137.73	(162.31)	3.24	(4.84)
p50.02	140907.29	-0.00	-6.20%	0.06	-9.52%	127490.43	127855.45	(145.62)	2.59	(4.37)
p50.03	107864.79	-0.00	-6.73%	0.06	-9.26%	97871.58	97871.58	(0.00)	1.32	(0.68)
p50.04	118458.73	-0.00	-6.74%	0.07	-8.65%	108213.78	108213.78	(0.00)	1.53	(1.18)
p50.05	129844.41	0.01	-7.20%	0.07	-8.00%	119457.05	119457.05	(0.00)	1.40	(1.31)
p50.06	136965.62	-0.00	-4.23%	0.05	-9.92%	123376.60	123376.60	(0.00)	0.95	(0.79)
p50.07	136811.79	0.00	-6.26%	0.07	-11.34%	121298.68	121298.68	(0.00)	0.76	(0.30)
p50.08	121497.95	0.00	0.00%	0.05	-7.46%	112430.09	112914.96	(540.02)	8.98	(5.99)
p50.09	117045.62	-0.00	-3.27%	0.05	-5.06%	111126.19	111126.19	(0.00)	1.77	(1.52)
p50.10	149799.73	0.00	-1.53%	0.06	-10.46%	134131.66	134996.41	(254.82)	5.41	(4.04)
p50.11	120418.73	0.00	-1.83%	0.05	-7.94%	110859.51	110859.51	(0.00)	3.59	(2.88)
p50.12	123650.72	0.00	-4.05%	0.05	-5.24%	117171.47	117171.47	(0.00)	0.35	(0.21)
p50.13	130159.49	0.00	-0.69%	0.05	-6.05%	122280.80	122280.80	(0.00)	1.49	(0.56)
p50.14	150575.34	0.00	-3.79%	0.05	-6.59%	140657.12	140753.82	(43.98)	4.72	(3.59)
p50.15	121974.35	-0.00	-2.76%	0.06	-11.54%	107897.46	107901.39	(21.49)	5.25	(4.54)
p50.16	140617.25	-0.00	-9.37%	0.06	-13.05%	122265.49	122344.94	(37.15)	6.77	(4.94)
p50.17	124847.81	0.00	-5.36%	0.05	-12.22%	109588.74	110351.69	(540.63)	6.79	(4.84)
p50.18	121643.81	0.00	-3.83%	0.05	-6.69%	113500.80	113500.80	(0.00)	0.55	(0.20)
p50.19	134995.32	0.01	-7.70%	0.06	-16.69%	112470.24	112470.24	(0.00)	1.93	(1.68)
p50.20	146638.16	0.00	-4.22%	0.05	-5.20%	139012.08	139108.78	(54.26)	2.94	(3.74)
p50.21	128673.99	0.00	-2.42%	0.05	-11.07%	114428.01	114435.77	(6.90)	6.40	(5.61)
p50.22	126595.23	0.00	-2.88%	0.06	-8.40%	115960.12	116096.28	(25.72)	3.98	(3.93)
p50.23	118111.45	-0.00	-2.37%	0.06	-6.74%	110156.38	110501.66	(636.81)	6.81	(5.80)
p50.24	152346.39	0.00	-8.08%	0.06	-11.87%	134260.84	134260.84	(0.00)	1.00	(0.32)
p50.25	141142.72	0.00	-4.36%	0.06	-8.11%	129696.79	129946.33	(423.97)	7.87	(5.17)
p50.26	142556.10	0.00	-2.37%	0.06	-10.16%	128074.57	129266.72	(658.45)	9.33	(5.46)
p50.27	150151.89	0.00	-2.57%	0.05	-6.52%	140354.76	141203.26	(307.97)	9.02	(6.15)
p50.28	149443.02	0.00	-3.33%	0.06	-12.53%	130720.19	130974.22	(142.54)	3.98	(4.45)
p50.29	134114.98	0.00	-0.05%	0.04	-4.96%	127458.75	127515.65	(135.23)	8.76	(5.49)
		0.00	-4.11%	0.06	-8.88%		121590.64	(137.93)	4.03	(3.20)

Table 4.21: Results for instances with 100 nodes with mode 3 and candidate list size of 8 (directional antennas with $\theta_{\min} = 90°$).

Instance	D-BIP		D-BIP + VND		D-ACO					
	obj. function	time (s)	deviation	time (s)	deviation	best	average	(std.)	time (s)	(std.)
p100.00	122194.59	0.00	-5.87%	0.41	-9.83%	110184.68	110910.04	(750.52)	53.05	(28.38)
p100.01	118132.67	0.01	-4.92%	0.43	-7.19%	109639.91	109984.41	(65.55)	26.00	(23.09)
p100.02	124258.58	0.00	-1.15%	0.40	-6.18%	116579.50	116714.50	(162.06)	56.81	(24.29)
p100.03	121525.12	0.00	-5.51%	0.45	-11.38%	107692.64	108017.63	(183.98)	64.64	(25.21)
p100.04	120574.55	0.00	-2.72%	0.42	-5.44%	114020.39	114206.92	(190.10)	53.07	(22.74)
p100.05	142119.29	0.00	-3.22%	0.40	-6.88%	132345.16	132903.82	(405.00)	63.51	(24.72)
p100.06	134058.82	-0.00	-6.65%	0.45	-12.70%	117036.56	118054.86	(505.83)	64.69	(28.22)
p100.07	119025.84	-0.00	-2.96%	0.38	-4.51%	113660.52	113911.10	(280.54)	36.34	(27.66)
p100.08	128669.57	-0.00	-4.29%	0.38	-8.27%	118032.95	118757.78	(353.70)	56.94	(24.73)
p100.09	130471.93	-0.00	-5.21%	0.49	-6.92%	121443.75	121490.07	(108.02)	44.18	(23.20)
p100.10	112306.04	0.00	-4.08%	0.40	-7.16%	104266.98	104266.98	(0.00)	15.92	(9.00)
p100.11	121128.51	-0.00	-4.14%	0.40	-13.26%	105071.03	105131.57	(80.92)	52.41	(22.40)
p100.12	129685.28	0.01	-5.94%	0.40	-8.55%	118602.09	118621.83	(14.20)	44.58	(25.56)
p100.13	118208.67	-0.00	-3.26%	0.40	-9.59%	106868.73	106868.73	(0.00)	13.49	(4.76)
p100.14	112354.61	0.00	-2.35%	0.42	-8.83%	102428.75	103353.20	(747.93)	59.65	(25.77)
p100.15	117282.40	-0.00	-1.08%	0.42	-4.45%	112058.52	112173.80	(85.27)	56.08	(27.18)
p100.16	114246.47	-0.00	-3.09%	0.41	-8.80%	104196.65	104429.21	(131.76)	57.55	(24.22)
p100.17	126263.89	0.02	-1.92%	0.46	-6.96%	117471.24	117471.24	(0.00)	14.28	(6.48)
p100.18	108744.04	0.00	-1.88%	0.48	-4.59%	103751.44	103793.61	(21.44)	20.73	(24.42)
p100.19	130126.95	-0.00	-1.47%	0.47	-7.99%	119730.44	120115.81	(175.47)	41.44	(26.76)
p100.20	124081.90	0.00	-4.26%	0.43	-12.43%	108655.91	109540.08	(441.68)	68.35	(21.70)
p100.21	126118.49	-0.00	-3.76%	0.47	-8.42%	115504.13	115505.80	(9.18)	29.57	(24.43)
p100.22	122145.81	-0.00	-2.19%	0.39	-10.73%	109035.22	109113.58	(179.31)	49.76	(24.75)
p100.23	143264.47	0.01	-5.27%	0.52	-13.51%	123914.54	124529.85	(498.28)	54.34	(27.83)
p100.24	120812.46	-0.00	-3.26%	0.43	-4.94%	114845.82	114845.82	(0.00)	16.71	(8.26)
p100.25	125623.56	0.00	-6.27%	0.46	-12.46%	109975.55	110037.86	(12.17)	20.24	(18.16)
p100.26	123550.73	0.00	-5.20%	0.45	-7.79%	113924.55	113924.55	(0.00)	17.41	(9.60)
p100.27	117114.44	0.00	-2.83%	0.39	-6.51%	109494.48	109709.46	(207.71)	43.99	(29.19)
p100.28	117792.58	0.00	-2.91%	0.37	-6.05%	110668.55	110881.08	(132.48)	47.83	(25.81)
p100.29	118523.78	0.00	-4.10%	0.43	-5.66%	111811.70	111828.31	(10.16)	49.12	(27.83)
		0.00	-3.73%	0.43	-8.27%		113036.45	(191.78)	43.09	(22.21)

Table 4.22: Results for instances with 200 nodes with mode 3 and candidate list size of 8 (directional antennas with $\theta_{\min} = 90°$).

Instance	D-BIP		D-BIP + VND		D-ACO					
	obj. function	time (s)	deviation	time (s)	deviation	best	average	(std.)	time (s)	(std.)
p200.00	118740.64	0.01	-4.61%	3.33	-10.00%	106863.04	107221.10	(235.96)	390.46	(69.45)
p200.01	125849.55	0.01	-5.07%	3.40	-8.99%	114537.36	114993.85	(275.15)	329.21	(105.76)
p200.02	110673.48	0.01	-4.43%	3.14	-9.02%	100685.61	101187.35	(330.83)	378.30	(83.41)
p200.03	123242.13	0.01	-5.41%	3.60	-7.77%	113664.42	114138.10	(302.89)	385.30	(102.56)
p200.04	122223.14	0.01	-2.19%	3.33	-9.21%	110968.95	111360.16	(237.41)	270.85	(125.73)
p200.05	120915.02	0.01	-5.89%	3.61	-8.18%	111025.83	111663.81	(377.34)	375.68	(72.91)
p200.06	116086.78	0.01	-5.46%	3.43	-6.95%	108023.14	108441.47	(231.03)	253.93	(126.09)
p200.07	126897.97	0.02	-6.00%	3.46	-9.98%	114229.88	114711.48	(187.67)	378.81	(107.41)
p200.08	117518.14	0.01	-3.84%	3.45	-7.53%	108673.82	109138.10	(316.53)	350.57	(139.56)
p200.09	125795.42	0.01	-3.07%	3.27	-7.93%	115824.15	116309.24	(168.60)	352.74	(88.54)
p200.10	122108.61	0.01	-3.81%	3.45	-9.57%	110418.84	111280.47	(246.28)	321.78	(117.31)
p200.11	115113.12	0.01	-1.52%	3.31	-6.53%	107598.07	108364.09	(377.42)	373.25	(133.30)
p200.12	119767.65	0.02	-1.21%	3.19	-7.90%	110307.47	110889.81	(413.59)	335.12	(103.47)
p200.13	124092.78	0.01	-3.55%	3.47	-9.07%	112837.55	113439.75	(282.59)	335.77	(111.93)
p200.14	127752.94	0.02	-3.46%	3.45	-9.12%	116106.81	116731.76	(273.38)	384.82	(108.38)
p200.15	127846.20	0.01	-3.38%	3.19	-9.41%	115813.35	116300.74	(261.33)	394.81	(98.36)
p200.16	122331.81	0.01	-6.12%	3.54	-8.92%	111424.65	111672.17	(148.66)	366.99	(104.76)
p200.17	122107.61	0.01	-4.75%	3.43	-9.05%	111056.76	111300.64	(129.55)	405.72	(71.57)
p200.18	112877.53	0.02	-2.39%	3.29	-5.52%	106649.27	107237.23	(338.24)	354.94	(110.88)
p200.19	123902.20	0.01	-3.72%	3.50	-10.61%	110756.47	111226.03	(160.46)	362.79	(111.48)
p200.20	110711.93	0.01	-4.93%	3.35	-6.87%	103102.80	103523.89	(170.73)	376.46	(87.96)
p200.21	126752.00	0.01	-4.89%	3.97	-9.71%	114450.23	116003.18	(816.05)	354.85	(113.49)
p200.22	121109.39	0.01	-5.03%	3.43	-10.92%	107882.94	108479.54	(268.22)	415.68	(58.15)
p200.23	119482.10	0.01	-3.65%	3.45	-8.38%	109466.42	110416.33	(325.86)	343.22	(113.10)
p200.24	130993.60	0.01	-3.73%	3.26	-11.22%	116290.07	117327.47	(534.25)	362.31	(100.14)
p200.25	120880.96	0.02	-3.25%	3.46	-7.92%	111310.70	112837.47	(479.83)	344.39	(97.53)
p200.26	125730.51	0.02	-4.73%	3.68	-8.44%	115117.21	116155.53	(499.20)	325.12	(124.32)
p200.27	128336.18	0.01	-3.41%	3.24	-8.90%	116917.43	117534.48	(242.02)	363.59	(89.74)
p200.28	122197.49	0.01	-3.02%	3.37	-8.88%	111341.79	112241.58	(631.03)	359.59	(112.89)
p200.29	114958.99	0.01	-2.14%	2.95	-4.59%	109685.96	110473.07	(233.58)	372.33	(100.84)
		0.01	-3.96%	3.40	-8.57%		111753.33	(316.52)	357.31	(103.03)

4.3.2.4 Benefits of directional antennas

In Appendix B advantages of using directional antennas with $\theta_{\min} \in \{30°, 60°, 90°\}$ for each different instance size are shown comparing the average required power in these cases to the average required power when considering omnidirectional antennas. Average values over all considered network sizes are shown in Table 4.23. Moreover, results are summarized in Figure 4.10, where, for each different considered value of $\theta_{\min}$, a boxplot shows the average required energy over 30 different multicast sessions for each of the 120 MEB instances. In both cases the benefits of using directional antennas with $\theta_{\min} = 30°$ are clear. In fact, average energy saving for this case is 85.60%.

Table 4.23: Summary of best values of best results obtained for best performing ACO/D-ACO modes for all considered antenna types and instance sizes.

Size of instances	$\theta_{\min} = 360°$	$\theta_{\min} = 90°$		$\theta_{\min} = 60°$		$\theta_{\min} = 30°$	
	average	**energy saving**	**average**	**energy saving**	**average**	**energy saving**	**average**
20	373749.47	-66.30%	124240.37	-74.46%	93901.06	-84.70%	56479.72
50	379707.74	-67.99%	121383.54	-75.93%	91281.86	-85.86%	53530.67
100	361658.75	-68.81%	112763.75	-76.51%	84921.74	-85.91%	50938.04
200	354552.77	-68.66%	111101.03	-76.33%	83944.91	-85.92%	49923.08
	367417.18	-67.94%	117372.17	-75.81%	88512.39	-85.60%	52717.88

4.3.3 Importance of VND and pheromone update

In addition to the above experiments, an evaluation of the necessity of using the VND local search procedure and the pheromone update mechanism was done. All considered instances were evaluated with the best parameters found in each different scenario considered (one for each of the four different antenna types used) but disabling, first, the VND mechanism and, in second place, the pheromone update mechanism (but enabling again the VND). With these modifications, the effect of these two algorithmic components on the ACO/D-ACO algorithm is tested. Tables in Appendix D show the results of these tests. Results are summarized in Figure 4.11 where different boxplots show that, for instances of all considered sizes, results get worse when algorithm components are switched off. In fact, additional energy consumption can go, on average, up to 7.50% when disconnecting the VND and up to 4.92% when disconnecting the pheromone update mechanism. This means that both components are strictly necessary to obtain the results presented in previous sections.

4.4 Results for the MEM problem

For the experiments concerning the MEM problem the same parameters settings as determined for the MEB problem were used. The MACO algorithm was applied 30 times to each of the 30 networks. However, each of the 30 applications used a different multicast session and the average results over these 30 sessions are shown (see the beginning of this chapter for details).

Due to computation power limitations, we were not able to provide optimal values for all 30 multicast sessions. Note that calculating these results requires approximately 30 times

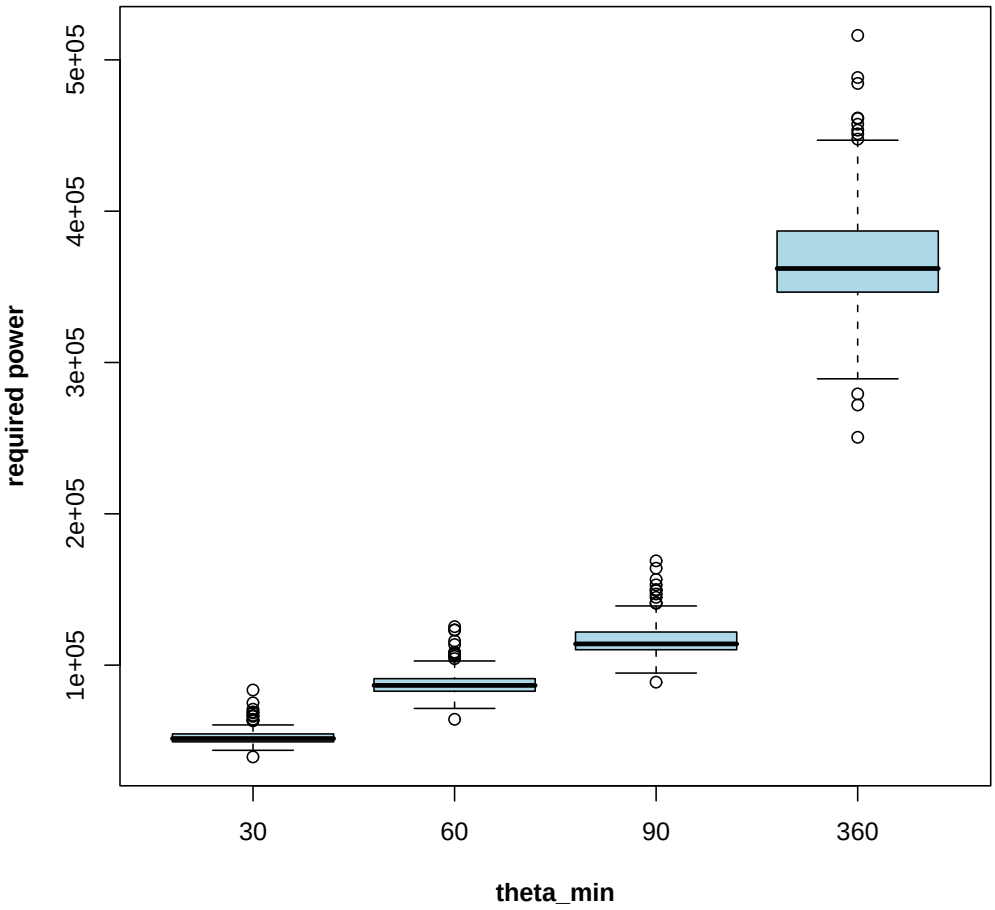

Figure 4.10: Comparison of the four considered antenna types $\theta_{\min} \in \{30°, 60°, 90°, 360°\}$.

more time than calculating the optimal value of one MEB instance.

4.4.1 Results for Omnidirectional Antennas

The results are summarized (in comparison to MIP [52] and MIP + VND) in Table 4.24, Table 4.25, Table 4.26 and Table 4.27, respectively. Remember that no optimal solutions will be presented in these cases, instead the MIP algorithm will be used as reference. The format of these tables is as follows. The first column provides the instance name, the second and third columns the absolute result and time of MIP, the fourth column the deviation from MIP + VND to the MIP, and the remaining columns give the results of the MACO algorithm. Concerning MACO the following information is provided. The column with heading **deviation** provides the improvement over MIP (in percent). The remaining columns provide the average of the best solutions found in the 30 sessions (plus standard deviation), and the average of the computation times over the 30 sessions (plus standard deviation). The last table row provides the average improvement (over 30 instances) of MIP+VND and MACO over MIP and the

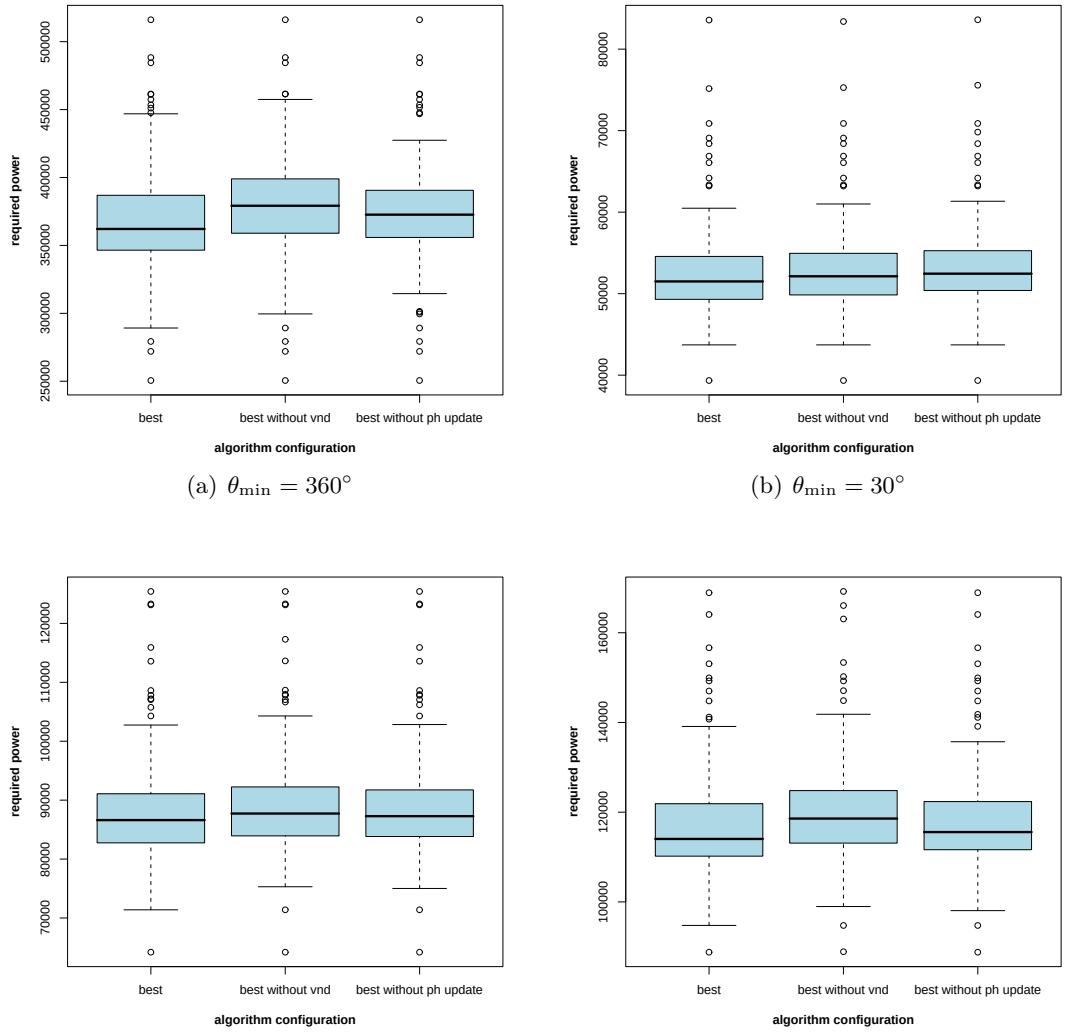

(a) $\theta_{\min} = 360°$ (b) $\theta_{\min} = 30°$

(c) $\theta_{\min} = 60°$ (d) $\theta_{\min} = 90°$

Figure 4.11: Comparison of full ACO/D-ACO with algorithms without VND and with VND but without pheromone update.

average computation time over 30 instances.

The results show that the average improvement obtained by MACO over MIP is 18.80% in 0.04 seconds for 20 nodes instances, 20.50% in 3.26 seconds for 50 nodes instances, 19.03% in 49.20 seconds for 100 nodes instances, and 19.54% in 378.88 seconds for 200 nodes instances. Note that in all cases the usage of the VND local search procedure causes an improvement of at least 8% in the MIP solution.

In Figure 4.12 and Figure 4.13 a graphical representation of solutions found by the MIP and MACO algorithms for MEM instance *p50.06* with a small and a large multicast set, respectively, when omnidirectional antennas are considered is shown. Note that nodes belonging

to the multicast set are painted in gray (dark blue in the online version).

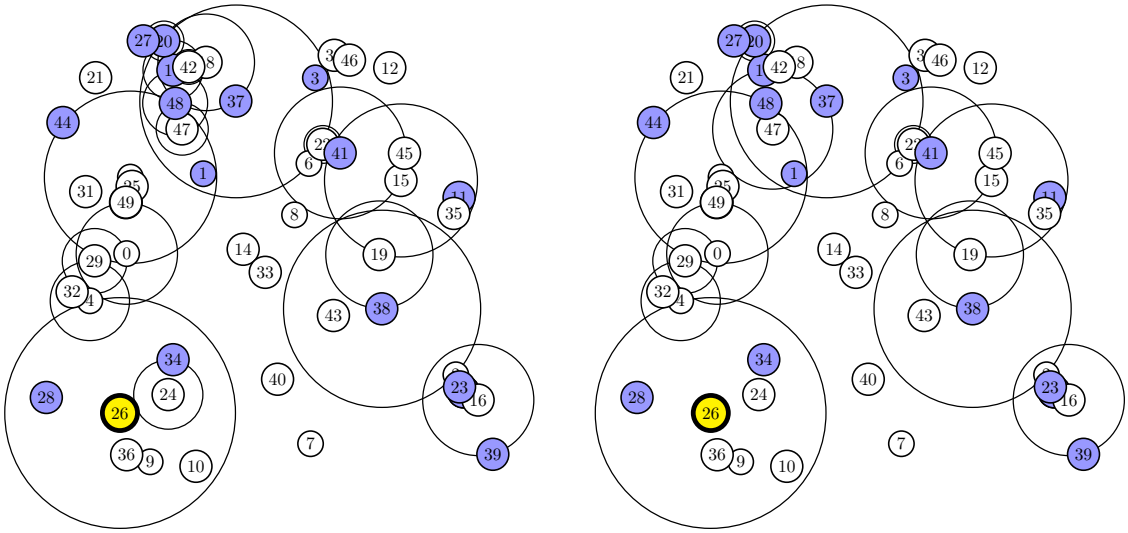

(a) MIP solution for instance *p50.06*. Required power: 342171.83.

(b) MACO solution for instance *p50.06*. Required power: 327499.30.

Figure 4.12: Solutions found for instance *p50.06* with a multicast set of size 16 with MIP and MACO (when omnidirectional antennas are considered)

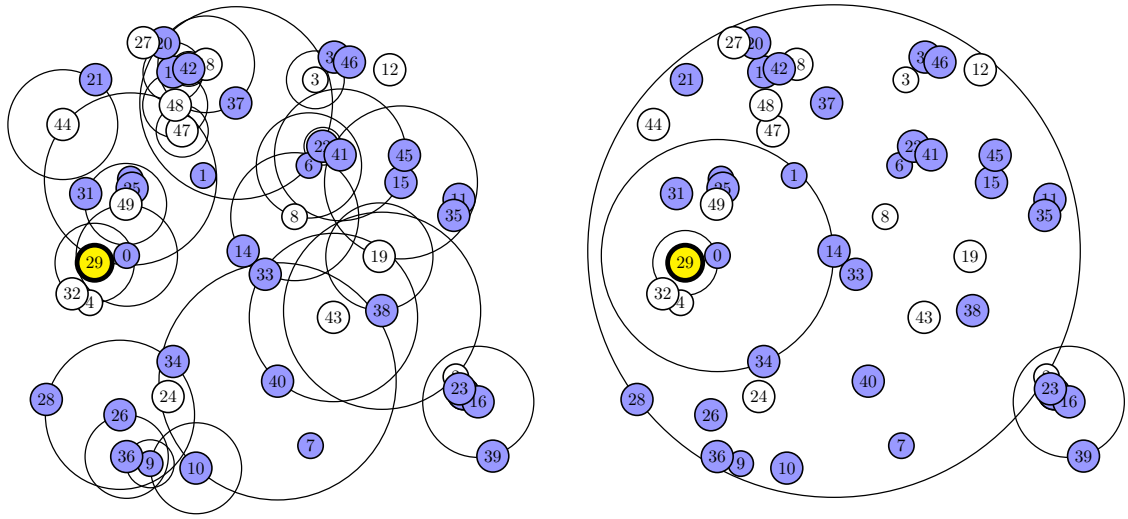

(a) MIP solution for instance *p50.06*. Required power: 478335.30.

(b) MACO solution for instance *p50.06*. Required power: 385351.83.

Figure 4.13: Solutions found for instance *p50.06* with a multicast set of size 34 with MIP and MACO (when omnidirectional antennas are considered)

Table 4.24: Results for instances with 20 nodes with mode 3 and candidate list size of 8 (omnidirectional antennas).

Instance	MIP		MIP + VND			MACO		
	average	time (s)	deviation	average	time (s)	deviation	average	time (s)
p20.00	450226.85	0.00	-7.67%	415674.26	0.11	-28.81%	320514.27	0.02
p20.01	484284.37	0.00	-11.44%	428894.51	0.08	-20.38%	385597.02	0.04
p20.02	316883.68	0.00	-9.30%	287423.73	0.09	-13.03%	275608.74	0.01
p20.03	465244.96	0.00	-7.14%	432018.23	0.10	-15.78%	391852.28	0.08
p20.04	563396.01	0.01	-9.92%	507492.94	0.17	-22.70%	435482.87	0.01
p20.05	308683.82	0.00	-11.69%	272606.64	0.13	-20.46%	245534.86	0.01
p20.06	317613.79	0.01	-13.48%	274804.68	0.10	-22.06%	247549.01	0.02
p20.07	332997.91	0.00	-6.32%	311938.61	0.07	-11.67%	294140.61	0.05
p20.08	311647.29	0.00	-6.22%	292261.19	0.14	-13.94%	268202.31	0.04
p20.09	434823.74	0.01	-2.95%	421979.62	0.16	-19.81%	348679.51	0.04
p20.10	325738.01	0.00	-9.75%	293966.51	0.13	-14.56%	278309.21	0.02
p20.11	347125.83	0.00	-7.58%	320809.31	0.10	-17.67%	285802.01	0.04
p20.12	393640.28	0.00	-15.07%	334303.41	0.11	-22.58%	304765.53	0.02
p20.13	412108.74	0.01	-20.66%	326957.64	0.15	-27.85%	297336.07	0.05
p20.14	296006.69	0.01	-6.36%	277170.25	0.13	-13.44%	256221.77	0.02
p20.15	455955.82	0.00	-6.79%	425006.25	0.11	-15.93%	383301.51	0.02
p20.16	442509.19	0.00	-9.10%	402230.10	0.10	-20.30%	352697.84	0.01
p20.17	399719.00	0.00	-7.58%	369400.97	0.13	-11.41%	354127.51	0.04
p20.18	330161.71	0.01	-13.16%	286726.90	0.11	-18.94%	267639.27	0.01
p20.19	443585.19	0.00	-10.36%	397630.51	0.12	-17.50%	365955.87	0.05
p20.20	479607.65	0.00	-11.87%	422691.58	0.14	-20.97%	379014.90	0.07
p20.21	382679.25	0.00	-2.73%	372236.66	0.09	-24.74%	288011.54	0.02
p20.22	365681.83	0.00	-7.60%	337882.49	0.10	-13.00%	318151.75	0.02
p20.23	381873.10	0.00	-7.05%	354939.69	0.12	-16.51%	318837.61	0.03
p20.24	373283.01	0.00	-9.77%	336811.36	0.09	-18.34%	304818.71	0.03
p20.25	487880.80	0.00	-11.97%	429471.56	0.11	-16.97%	405086.75	0.22
p20.26	590640.33	0.00	-4.17%	566039.82	0.11	-19.98%	472657.32	0.10
p20.27	406180.55	0.00	-7.80%	374497.71	0.09	-21.16%	320240.21	0.02
p20.28	397045.10	0.01	-14.18%	340735.91	0.12	-24.06%	301522.78	0.03
p20.29	302027.06	0.01	-11.10%	268501.10	0.08	-19.49%	243147.83	0.02
	399975.05	0.00	-9.36%	362770.14	0.11	-18.80%	323693.58	0.04

Table 4.25: Results for instances with 50 nodes with mode 3 and candidate list size of 8 (omnidirectional antennas).

Instance	MIP		MIP + VND			MACO		
	average	time (s)	deviation	average	time (s)	deviation	average	time (s)
p50.00	409720.40	0.02	-10.22%	367837.77	1.32	-19.38%	330300.58	3.12
p50.01	433992.12	0.00	-8.06%	399005.66	1.24	-22.34%	337045.18	3.85
p50.02	418585.92	0.00	-8.35%	383616.79	1.49	-27.63%	302929.55	2.74
p50.03	344505.01	0.00	-6.45%	322270.39	1.39	-19.45%	277510.65	2.61
p50.04	347840.08	0.02	-9.15%	316000.17	1.29	-19.30%	280696.57	3.97
p50.05	380462.66	0.00	-8.06%	349784.92	1.34	-20.60%	302102.97	3.15
p50.06	424615.48	0.01	-8.22%	389721.65	1.25	-22.52%	329012.34	2.80
p50.07	441314.95	0.00	-10.74%	393912.00	1.41	-22.11%	343753.84	3.41
p50.08	372097.64	0.00	-6.55%	347719.56	1.27	-18.31%	303954.85	4.95
p50.09	357629.76	0.01	-8.88%	325889.07	1.27	-18.99%	289699.20	4.54
p50.10	462204.21	0.02	-10.49%	413712.20	1.35	-19.72%	371049.56	2.16
p50.11	380429.35	0.02	-9.22%	345358.52	1.32	-20.73%	301562.28	3.27
p50.12	373792.67	0.01	-7.60%	345372.63	1.38	-15.10%	317368.40	2.97
p50.13	415113.67	0.00	-7.00%	386064.76	1.29	-21.95%	323985.05	3.44
p50.14	458916.84	0.00	-6.47%	429227.40	1.16	-23.12%	352825.48	2.69
p50.15	396283.70	0.02	-8.34%	363247.29	1.32	-17.58%	326600.33	2.71
p50.16	413079.77	0.01	-6.99%	384198.25	1.27	-15.07%	350808.55	2.94
p50.17	381734.17	0.02	-9.09%	347052.54	1.31	-16.02%	320575.49	3.08
p50.18	377066.65	0.00	-5.51%	356272.67	1.24	-17.49%	311099.47	2.21
p50.19	423725.37	0.01	-10.54%	379068.98	1.28	-22.61%	327931.49	4.41
p50.20	422071.46	0.00	-10.95%	375857.45	1.20	-22.46%	327290.27	3.74
p50.21	370509.20	0.00	-6.24%	347371.82	1.39	-17.91%	304154.57	3.70
p50.22	404741.16	0.03	-9.66%	365628.30	1.35	-20.98%	319825.77	2.44
p50.23	393425.56	0.02	-14.22%	337497.71	1.42	-25.20%	294290.06	2.72
p50.24	453209.94	0.00	-11.94%	399105.23	1.31	-19.16%	366379.47	3.50
p50.25	412412.62	0.01	-11.44%	365243.76	1.51	-18.96%	334199.28	3.31
p50.26	430732.06	0.02	-6.10%	404473.27	1.34	-22.07%	335673.23	4.03
p50.27	465694.34	0.01	-8.31%	427012.30	1.40	-23.93%	354266.05	2.37
p50.28	424492.49	0.03	-11.97%	373683.17	1.36	-20.27%	338450.58	2.80
p50.29	436589.65	0.04	-7.33%	404608.88	1.20	-24.13%	331242.92	4.17
	407566.30	0.01	-8.80%	371527.17	1.32	-20.50%	323552.80	3.26

Table 4.26: Results for instances with 100 nodes with mode 3 and candidate list size of 8 (omnidirectional antennas).

Instance	MIP		MIP + VND			MACO		
	average	time (s)	deviation	average	time (s)	deviation	average	time (s)
p100.00	375653.97	0.11	-10.40%	336595.02	9.62	-19.68%	301717.61	46.10
p100.01	382530.32	0.14	-10.69%	341637.56	9.67	-17.90%	314061.70	48.80
p100.02	393351.00	0.08	-8.35%	360488.58	9.65	-18.66%	319936.96	41.31
p100.03	363736.14	0.09	-11.82%	320735.75	10.06	-18.29%	297221.54	47.71
p100.04	383514.86	0.03	-7.71%	353950.79	9.39	-18.28%	313409.60	54.38
p100.05	430865.72	0.12	-6.70%	401989.20	9.31	-20.04%	344506.36	52.50
p100.06	427500.88	0.13	-10.20%	383883.06	9.67	-22.56%	331065.97	45.84
p100.07	392342.14	0.10	-8.89%	357480.23	9.12	-20.07%	313614.37	54.91
p100.08	414157.63	0.12	-9.98%	372831.48	9.83	-21.26%	326121.75	55.69
p100.09	433403.61	0.08	-7.29%	401798.66	9.29	-20.06%	346461.94	48.45
p100.10	339342.33	0.06	-6.84%	316138.24	9.49	-16.01%	285006.43	50.89
p100.11	377269.27	0.12	-8.35%	345777.62	9.70	-18.03%	309256.75	43.46
p100.12	412092.92	0.11	-9.85%	371501.48	9.86	-21.01%	325512.38	48.19
p100.13	378890.90	0.11	-7.44%	350712.28	9.63	-19.34%	305627.43	50.36
p100.14	355859.45	0.12	-7.32%	329828.22	9.87	-16.36%	297636.38	56.55
p100.15	362740.46	0.07	-7.64%	335031.54	8.47	-15.70%	305788.43	41.87
p100.16	357709.94	0.06	-6.73%	333628.88	8.70	-18.20%	292601.81	50.88
p100.17	377469.40	0.10	-6.86%	351589.17	9.07	-15.65%	318386.68	58.61
p100.18	349020.50	0.08	-7.64%	322339.43	10.31	-14.78%	297429.57	48.81
p100.19	388567.86	0.05	-7.24%	360434.57	9.67	-18.76%	315658.14	42.68
p100.20	368271.87	0.07	-9.09%	334797.82	9.51	-20.43%	293029.39	50.62
p100.21	380701.06	0.07	-9.14%	345905.15	9.81	-19.72%	305643.33	49.99
p100.22	388675.89	0.07	-6.88%	361950.44	9.35	-19.15%	314230.94	47.28
p100.23	432398.70	0.07	-10.68%	386225.92	10.32	-23.61%	330303.85	40.86
p100.24	378053.53	0.10	-7.64%	349185.78	10.04	-18.06%	309769.93	49.16
p100.25	379470.53	0.07	-8.86%	345844.48	9.76	-20.59%	301355.06	51.15
p100.26	409355.43	0.07	-8.83%	373220.44	9.72	-22.23%	318341.92	52.69
p100.27	367890.67	0.02	-8.31%	337305.81	9.46	-18.25%	300736.86	53.15
p100.28	371567.90	0.07	-9.26%	337149.78	10.03	-17.59%	306194.37	51.39
p100.29	396649.74	0.05	-6.84%	369506.72	9.02	-20.56%	315113.94	41.73
	385635.15	0.08	-8.45%	352982.14	9.58	-19.03%	311858.05	49.20

Table 4.27: Results for instances with 200 nodes with mode 3 and candidate list size of 8 (omnidirectional antennas).

Instance	MIP		MIP + VND			MACO		
	average	time (s)	deviation	average	time (s)	deviation	average	time (s)
p200.00	361750.38	0.35	-8.43%	331238.59	72.99	-17.99%	296686.21	342.80
p200.01	383532.76	0.37	-8.80%	349782.69	69.55	-18.65%	312012.57	398.65
p200.02	351814.84	0.39	-7.19%	326516.89	67.01	-16.77%	292833.08	397.50
p200.03	392717.09	0.41	-5.63%	370598.97	65.44	-20.56%	311970.34	386.08
p200.04	394470.09	0.38	-8.35%	361542.09	75.21	-19.09%	319177.09	380.25
p200.05	381332.11	0.39	-8.97%	347139.55	73.59	-19.37%	307485.31	362.79
p200.06	362585.69	0.38	-6.74%	338157.87	65.63	-18.30%	296228.14	403.21
p200.07	396094.80	0.40	-11.35%	351129.41	74.72	-20.05%	316660.63	373.65
p200.08	386858.17	0.33	-9.72%	349254.72	75.19	-21.87%	302265.74	369.38
p200.09	380599.24	0.38	-8.61%	347820.25	73.43	-18.32%	310886.49	410.15
p200.10	395870.59	0.36	-8.03%	364089.70	74.64	-21.93%	309063.33	387.24
p200.11	370837.33	0.33	-5.21%	351509.06	75.52	-19.25%	299438.77	372.74
p200.12	379009.06	0.45	-7.90%	349070.45	73.92	-20.56%	301082.17	393.03
p200.13	390033.35	0.39	-9.42%	353286.21	73.74	-20.46%	310235.59	352.36
p200.14	431794.47	0.35	-10.32%	387225.76	68.02	-25.11%	323388.29	372.48
p200.15	398357.60	0.38	-9.83%	359188.91	74.38	-20.51%	316652.57	396.34
p200.16	381151.04	0.40	-9.33%	345605.98	74.67	-15.80%	320922.82	347.58
p200.17	389550.47	0.42	-8.05%	358177.16	74.67	-20.11%	311214.09	382.42
p200.18	372695.72	0.43	-7.01%	346576.58	66.58	-15.86%	313583.29	383.87
p200.19	386673.72	0.33	-8.12%	355263.51	74.08	-20.07%	309076.23	358.85
p200.20	377069.11	0.43	-7.44%	348996.99	72.26	-17.92%	309486.35	394.87
p200.21	401406.12	0.34	-7.03%	373199.21	73.92	-21.26%	316076.30	390.60
p200.22	378211.31	0.36	-10.38%	338936.30	71.99	-18.14%	309598.58	363.61
p200.23	388829.48	0.41	-6.52%	363474.85	74.04	-17.68%	320080.18	366.44
p200.24	407649.81	0.41	-11.05%	362600.55	74.19	-23.13%	313353.42	350.23
p200.25	396143.90	0.39	-6.57%	370134.75	73.95	-18.91%	321246.80	397.06
p200.26	394114.39	0.40	-9.41%	357032.67	73.96	-21.27%	310282.30	385.29
p200.27	397613.45	0.39	-8.05%	365594.25	73.44	-19.94%	318327.08	406.25
p200.28	403124.30	0.37	-6.13%	378422.31	74.06	-21.21%	317631.37	404.85
p200.29	382332.82	0.33	-8.61%	349414.57	66.27	-16.07%	320885.86	335.96
	387140.77	0.38	-8.27%	355032.69	72.37	-19.54%	311261.03	378.88

4.4.2 Results for Directional Antennas

Results for MEM instances with directional antennas are presented grouped by the $\theta_{\min}$ parameter of the antennas (as in the case of the MEB problem results). Result tables have the same structure as the ones provided in the case of the MEM problem with omnidirectional antennas.

After the results for the three different $\theta_{\min}$ values considered, an overall comparison (including omnidirecitonal antennas) is done, showing the savings obtained using directional antennas instead of omnidirectional ones.

4.4.2.1 Directional antennas with $\theta_{\min} = 30°$

The results for the instances with 20 nodes are shown in Table 4.28, for the instances with 50 nodes in Table 4.29, for the instances with 100 nodes in Table 4.30 and for the instances with 200 nodes in Table 4.31.

The results show that for instances of all sizes the improvement of D-MACO over D-MIP is always higher than 15.42% (with a maximum average improvement of 20.25% obtained in the 20 nodes instances). The average computation times are very low for 20 nodes instances (0.14 seconds). However, in the 50 nodes instances (7.02 seconds) and 100 nodes instances (73.02 seconds) average times approximately increase the required times in the omnidirectional case between 10% and 20%, respectively. It is interesting to note that the computation times are higher than in the case of omnidirectional antennas. This may account for the fact that the computation of the heuristic information is more complicated for directional antennas (as it also happens in the broadcasting case). It is remarkable that for all sizes, the average deviation of the D-MIP+VND algorithm with respect to the D-MIP is at most 2.96%, what may mean that the r-shrink local search procedure is of little use in this case. However here it seems to be more adequate than in the MEB problem with directional antennas with $\theta_{\min} = 30°$, where the average benefit of the D-BIP+VND over the D-BIP was lower than 1%.

In Figure 4.14 and Figure 4.15 a graphical representation of solutions found by D-MIP and D-MACO algorithms for MEM instance *p50.06* with a small and a large multicast set, respectively, when directional antennas with $\theta_{\min} = 30°$ are considered is shown.

4.4.2.2 Directional antennas with $\theta_{\min} = 60°$

The results for the instances with 20 nodes are shown in Table 4.32, for the instances with 50 nodes in Table 4.33, for the instances with 100 nodes in Table 4.34 and for the instances with 200 nodes in Table 4.35.

The results show that the average improvement of D-MACO over D-MIP for 20, 50 and 100 nodes instances is higher than 11%, while the average improvement in 200 nodes instances is of 9.87%. The average computation times are similar to the ones obtained in the omnidirectional case: for 20 nodes instances 0.10 seconds, for 50 nodes instances 4.57 seconds, for 100 nodes instances 59.66 seconds and, for 200 nodes instances 409.82 seconds. Note that for all sizes, the average deviation of the D-MIP+VND algorithm with respect to the D-MIP is between 2% and 3% (similar to the previous case).

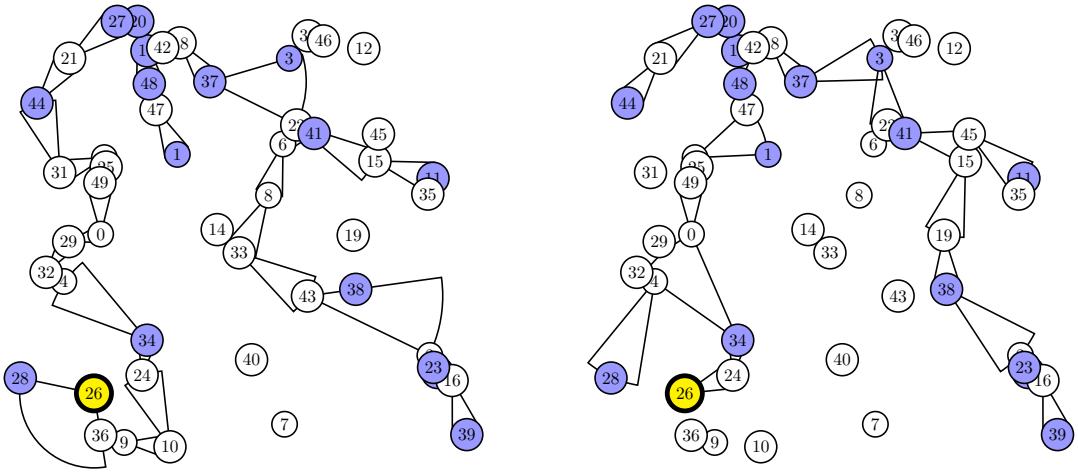

(a) D-MIP solution for instance *p50.06*. Required power: 54902.0.

(b) D-MACO solution for instance *p50.06*. Required power: 38742.7.

Figure 4.14: Solutions found for instance *p50.06* with a multicast set of size 16 with D-MIP and D-MACO (when directional antennas with $\theta_{\min} = 30°$ are considered)

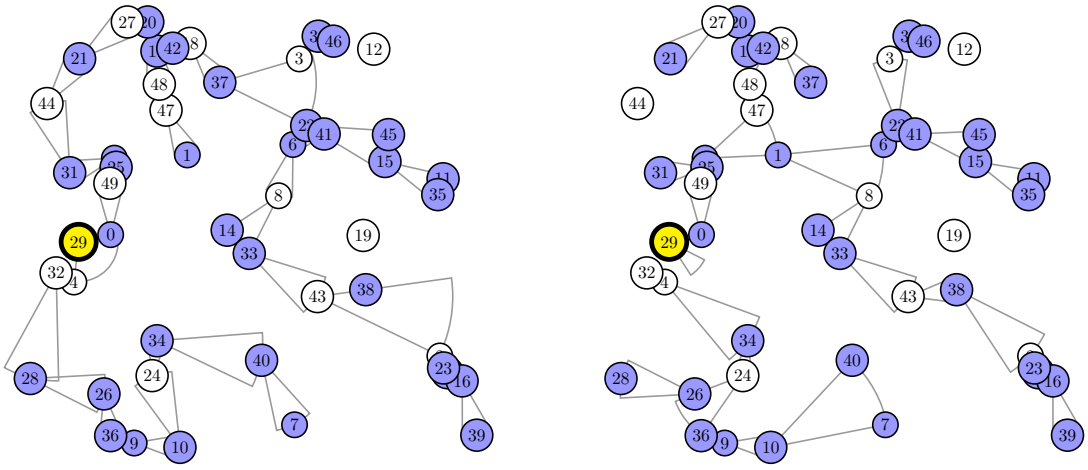

(a) D-MIP solution for instance *p50.06*. Required power: 58649.1.

(b) D-MACO solution for instance *p50.06*. Required power: 50456.1.

Figure 4.15: Solutions found for instance *p50.06* with a multicast set of size 34 with D-MIP and D-MACO (when directional antennas with $\theta_{\min} = 30°$ are considered)

In figures Figure 4.16 and Figure 4.17 a graphical representation of solutions found by D-MIP and D-MACO algorithms for MEM instance *p50.06* with a small and a large multicast set, respectively, when directional antennas with $\theta_{\min} = 60°$ are considered is shown.

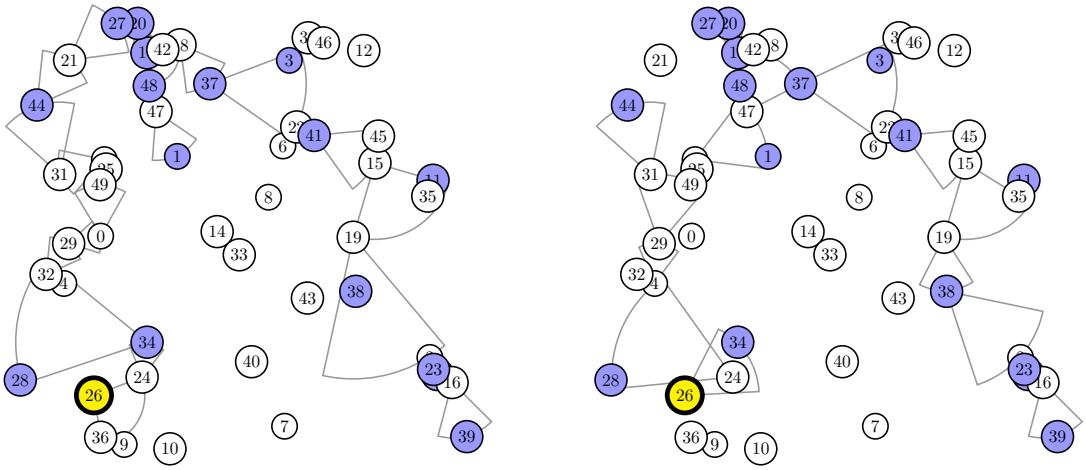

(a) D-MIP solution for instance *p50.06*. Required power: 80630.7.

(b) D-MACO solution for instance *p50.06*. Required power: 66793.2.

Figure 4.16: Solutions found for instance *p50.06* with a multicast set of size 16 with D-MIP and D-MACO (when directional antennas with $\theta_{\min} = 60°$ are considered)

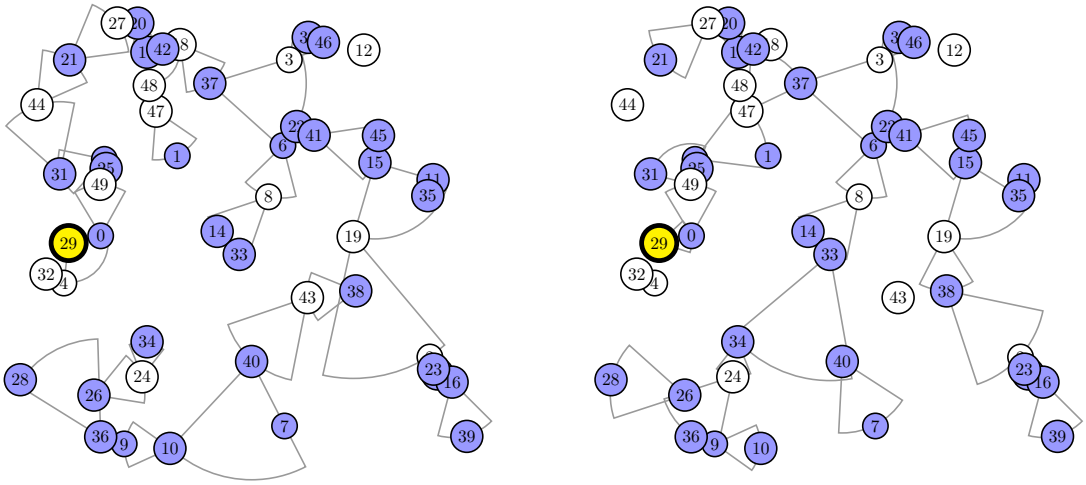

(a) D-MIP solution for instance *p50.06*. Required power: 102889.4.

(b) D-MACO solution for instance *p50.06*. Required power: 83540.9.

Figure 4.17: Solutions found for instance *p50.06* with a multicast set of size 34 with D-MIP and D-MACO (when directional antennas with $\theta_{\min} = 60°$ are considered)

4.4.2.3 Directional antennas with $\theta_{\min} = 90°$

The results for the instances with 20 nodes are shown in Table 4.36, for the instances with 50 nodes in Table 4.37, for the instances with 100 nodes in Table 4.38 and for the instances with 200 nodes in Table 4.39.

The results show that, as in the $\theta_{\min} = 90°$ case, the average improvement of D-MACO over D-MIP for all network sizes considered higher than 11%. The average computation times are similar to the ones obtained in the omnidirectional case: for 20 nodes instances 0.17 seconds, for 50 nodes instances 5.79 seconds, for 100 nodes instances 61.46 seconds and, for 200 nodes instances 397.04 seconds. Note that for all sizes, the average deviation of the D-MIP+VND algorithm in respect to the D-MIP is around 4%. Hence, it seems that like in the multicasting scenario, as well as in the broadcasting one, the VND usability increases when the $\theta_{\min}$ parameter does.

In Figure 4.18 and Figure 4.19 a graphical representation of solutions found by D-MIP and D-MACO algorithms for MEM instance *p50.06* with a small and a large multicast set, respectively, when directional antennas with $\theta_{\min} = 90°$ are considered is shown.

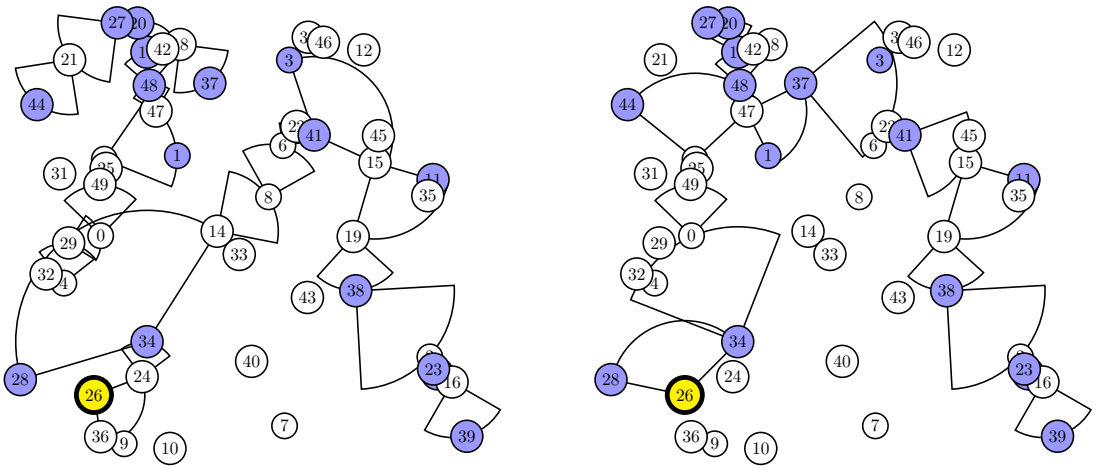

(a) D-MIP solution for instance *p50.06*. Required power: 114466.1.

(b) D-MACO solution for instance *p50.06*. Required power: 91303.7.

Figure 4.18: Solutions found for instance *p50.06* with a multicast set of size 16 with D-MIP and D-MACO (when directional antennas with $\theta_{\min} = 90°$ are considered)

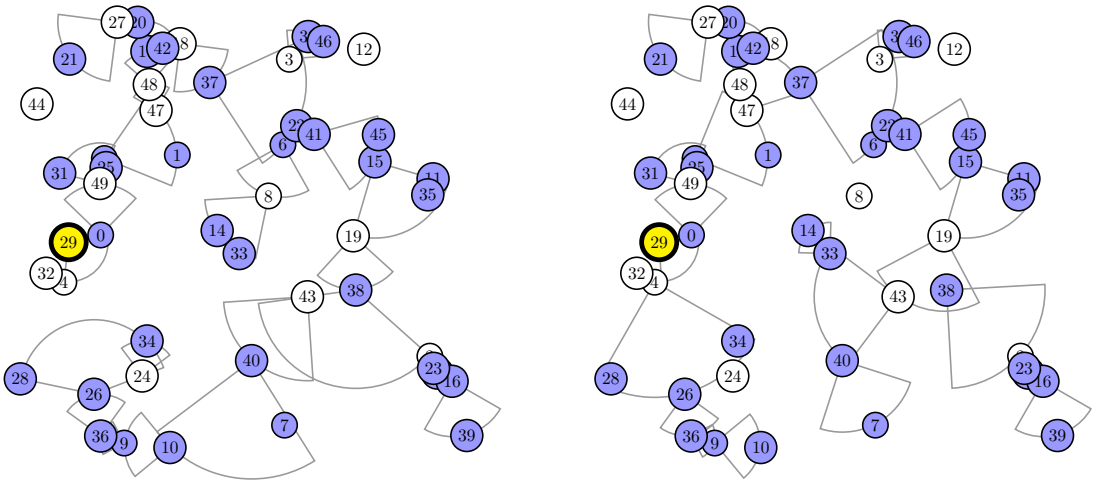

(a) D-MIP solution for instance *p50.06*. Required power: 130014.7.

(b) D-MACO solution for instance *p50.06*. Required power: 112415.2.

Figure 4.19: Solutions found for instance *p50.06* with a multicast set of size 34 with D-MIP and D-MACO (when directional antennas with $\theta_{\min} = 90°$ are considered)

Table 4.28: Results for instances with 20 nodes with mode 1 and candidate list size of 4 (directional antennas with $\theta_{\min} = 30°$).

Instance	D-MIP		D-MIP + VND			D-MACO		
	average	time (s)	deviation	average	time (s)	deviation	average	time (s)
p20.00	54391.82	0.01	-5.68%	51300.17	0.06	-20.42%	43287.13	0.17
p20.01	61190.17	0.00	-0.16%	61094.13	0.08	-15.63%	51626.20	0.06
p20.02	47144.40	0.01	-3.59%	45453.48	0.07	-18.28%	38526.96	0.13
p20.03	55010.26	0.00	-0.69%	54632.48	0.08	-19.12%	44493.87	0.06
p20.04	65303.39	0.00	-1.86%	64088.97	0.05	-12.24%	57309.53	0.17
p20.05	41322.14	0.01	-2.99%	40085.41	0.06	-22.26%	32122.14	0.09
p20.06	49448.57	0.00	-2.95%	47989.21	0.08	-24.21%	37477.74	0.24
p20.07	51696.93	0.00	-0.53%	51423.69	0.08	-14.76%	44068.89	0.12
p20.08	50010.27	0.00	-5.75%	47135.55	0.06	-27.70%	36157.48	0.11
p20.09	64597.97	0.00	-2.57%	62937.26	0.09	-22.30%	50189.75	0.12
p20.10	45537.04	0.00	-1.81%	44712.01	0.07	-15.82%	38335.14	0.11
p20.11	48609.16	0.00	-1.85%	47707.66	0.08	-24.51%	36694.93	0.03
p20.12	43663.90	0.00	-3.55%	42114.24	0.07	-17.07%	36211.97	0.10
p20.13	59673.36	0.01	-7.16%	55399.77	0.08	-28.41%	42722.98	0.09
p20.14	41550.50	0.00	-1.69%	40849.33	0.07	-21.14%	32766.20	0.17
p20.15	59910.46	0.01	-2.51%	58407.47	0.06	-20.93%	47373.93	0.15
p20.16	64464.88	0.00	-0.88%	63899.77	0.06	-24.15%	48897.45	0.11
p20.17	65006.06	0.00	-6.62%	60701.42	0.09	-29.13%	46069.82	0.21
p20.18	40056.02	0.00	-0.86%	39713.09	0.05	-13.10%	34808.24	0.06
p20.19	63862.81	0.00	-1.04%	63200.74	0.03	-17.75%	52526.67	0.05
p20.20	64553.01	0.00	-0.82%	64024.91	0.04	-21.01%	50988.65	0.12
p20.21	42847.73	0.00	-2.64%	41716.79	0.05	-19.10%	34665.36	0.08
p20.22	42090.65	0.00	-3.46%	40635.30	0.07	-16.28%	35236.82	0.09
p20.23	47730.37	0.00	-1.97%	46789.08	0.07	-11.71%	42139.66	0.07
p20.24	54163.97	0.00	-1.89%	53137.63	0.07	-24.74%	40762.17	0.18
p20.25	70205.05	0.01	-0.95%	69535.02	0.07	-21.91%	54825.06	0.28
p20.26	81865.02	0.00	-0.27%	81646.44	0.05	-17.80%	67289.42	0.35
p20.27	56903.29	0.00	-4.77%	54191.69	0.06	-26.41%	41876.85	0.18
p20.28	47079.24	0.00	-1.85%	46208.69	0.08	-17.71%	38743.84	0.05
p20.29	41973.89	0.00	-0.46%	41780.53	0.08	-21.81%	32821.06	0.31
	54062.08	0.00	-2.46%	52750.40	0.07	-20.25%	43033.86	0.14

Table 4.29: Results for instances with 50 nodes with mode 1 and candidate list size of 4 (directional antennas with $\theta_{\min} = 30°$).

Instance	D-MIP		D-MIP + VND			D-MACO		
	average	time (s)	deviation	average	time (s)	deviation	average	time (s)
p50.00	53468.48	0.01	-1.21%	52819.99	0.94	-18.00%	43846.13	8.48
p50.01	52677.74	0.01	-1.14%	52077.28	0.99	-16.82%	43816.00	5.30
p50.02	53545.02	0.01	-1.42%	52786.64	1.01	-20.39%	42626.45	7.94
p50.03	42707.51	0.02	-1.16%	42212.83	1.00	-17.85%	35084.95	6.89
p50.04	46633.45	0.00	-0.77%	46273.17	0.94	-21.10%	36794.08	8.50
p50.05	45648.80	0.02	-1.83%	44814.83	0.94	-13.78%	39357.81	7.52
p50.06	54356.95	0.00	-1.59%	53495.36	1.01	-20.50%	43213.46	5.77
p50.07	53231.12	0.02	-1.78%	52281.10	1.02	-18.23%	43528.37	8.23
p50.08	50651.49	0.00	-2.49%	49391.87	0.95	-19.39%	40830.74	6.04
p50.09	46011.03	0.00	-1.90%	45136.08	0.97	-19.86%	36873.86	6.91
p50.10	60324.68	0.00	-1.63%	59342.71	0.99	-17.39%	49836.98	7.18
p50.11	48908.04	0.00	-0.32%	48749.13	0.90	-19.87%	39189.64	6.00
p50.12	52289.50	0.04	-1.26%	51630.14	0.95	-17.28%	43255.01	7.21
p50.13	51133.81	0.02	-1.35%	50444.26	1.06	-18.66%	41593.82	6.17
p50.14	58625.53	0.01	-3.88%	56348.74	1.05	-21.60%	45964.68	8.11
p50.15	50843.67	0.00	-1.81%	49921.14	0.87	-20.17%	40589.52	5.16
p50.16	54868.13	0.01	-2.58%	53454.45	1.01	-15.90%	46142.07	7.93
p50.17	48125.86	0.01	-2.19%	47071.63	0.95	-19.44%	38771.78	4.96
p50.18	52391.90	0.02	-1.83%	51432.96	1.01	-18.50%	42700.22	7.03
p50.19	50829.99	0.03	-0.44%	50607.38	0.91	-19.67%	40829.62	7.11
p50.20	52627.37	0.01	-2.85%	51129.85	1.11	-21.54%	41290.55	7.59
p50.21	48224.98	0.02	-2.57%	46983.35	1.05	-17.91%	39590.06	8.26
p50.22	52578.42	0.03	-0.57%	52277.82	0.96	-21.15%	41458.10	7.52
p50.23	49422.93	0.01	-2.69%	48092.39	1.10	-21.93%	38584.01	6.51
p50.24	58596.88	0.00	-2.21%	57303.78	1.00	-22.72%	45282.11	6.76
p50.25	55771.34	0.02	-4.25%	53398.42	1.11	-18.59%	45405.14	7.30
p50.26	55661.40	0.00	-1.05%	55077.07	1.04	-21.54%	43670.44	7.33
p50.27	55152.30	0.00	-2.27%	53898.95	1.00	-17.61%	45437.64	6.77
p50.28	53882.90	0.00	-1.90%	52860.61	0.84	-16.59%	44941.68	8.04
p50.29	52120.24	0.03	-1.72%	51224.74	1.15	-16.99%	43262.65	5.95
	52043.72	0.01	-1.82%	51084.62	0.99	-19.03%	42125.59	7.02

Table 4.30: Results for instances with 100 nodes with mode 1 and candidate list size of 4 (directional antennas with $\theta_{\min} = 30°$).

Instance	D-MIP		D-MIP + VND			D-MACO		
	average	time (s)	deviation	average	time (s)	deviation	average	time (s)
p100.00	45963.43	0.03	-1.05%	45478.63	7.65	-15.38%	38893.65	78.77
p100.01	46002.99	0.07	-1.74%	45203.87	8.02	-16.69%	38325.90	73.15
p100.02	45063.52	0.05	-1.08%	44575.15	7.66	-12.59%	39389.16	67.27
p100.03	48496.76	0.06	-1.96%	47548.15	7.70	-19.85%	38871.90	79.38
p100.04	48541.76	0.05	-1.27%	47927.45	7.47	-17.59%	40002.32	75.89
p100.05	54387.71	0.05	-1.73%	53444.99	7.34	-19.80%	43618.49	76.84
p100.06	52911.79	0.07	-0.74%	52517.67	7.37	-17.79%	43496.87	73.00
p100.07	46596.60	0.06	-1.85%	45733.05	7.66	-14.38%	39895.62	70.14
p100.08	51517.83	0.04	-0.70%	51155.62	7.61	-20.10%	41162.40	65.95
p100.09	54050.14	0.07	-1.09%	53458.56	7.63	-18.62%	43985.62	79.05
p100.10	44667.04	0.06	-0.73%	44342.33	7.50	-17.28%	36949.02	72.75
p100.11	46785.60	0.05	-0.86%	46381.49	7.71	-17.59%	38557.87	68.11
p100.12	51784.17	0.06	-2.18%	50655.90	7.66	-20.26%	41294.65	71.43
p100.13	46085.41	0.04	-0.82%	45709.43	7.54	-13.76%	39743.84	65.61
p100.14	45339.96	0.07	-1.39%	44711.66	7.66	-18.48%	36959.55	72.87
p100.15	49327.38	0.05	-2.95%	47870.15	7.82	-20.49%	39220.41	74.24
p100.16	46888.14	0.04	-1.03%	46404.46	7.33	-21.00%	37043.02	68.11
p100.17	50814.21	0.07	-1.03%	50293.33	7.79	-17.03%	42162.36	73.41
p100.18	42808.37	0.06	-1.45%	42187.33	8.32	-16.80%	35615.84	75.71
p100.19	51319.77	0.07	-1.47%	50567.67	7.54	-19.19%	41471.24	77.01
p100.20	44779.91	0.07	-0.91%	44373.39	7.82	-14.62%	38232.03	69.93
p100.21	51170.57	0.08	-1.67%	50316.23	7.57	-19.54%	41170.08	67.87
p100.22	47089.77	0.08	-0.66%	46778.71	7.74	-16.67%	39239.03	71.39
p100.23	54453.38	0.07	-0.95%	53936.63	7.15	-18.81%	44210.90	76.35
p100.24	51318.06	0.08	-3.80%	49365.92	7.79	-21.49%	40290.41	76.06
p100.25	52041.40	0.09	-1.34%	51343.55	7.57	-22.28%	40447.40	79.14
p100.26	51822.58	0.06	-1.69%	50944.86	7.64	-15.37%	43857.25	68.59
p100.27	45282.54	0.11	-1.08%	44791.38	7.58	-18.11%	37083.19	70.07
p100.28	47147.68	0.06	-0.30%	47007.49	7.52	-16.44%	39394.87	74.52
p100.29	49347.69	0.07	-1.56%	48576.62	6.70	-16.39%	41257.79	77.93
	48793.54	0.06	-1.37%	48120.06	7.60	-17.81%	40061.42	73.02

Table 4.31: Results for instances with 200 nodes with mode 1 and candidate list size of 4 (directional antennas with $\theta_{\min} = 30°$).

Instance	D-MIP		D-MIP + VND			D-MACO		
	average	time (s)	deviation	average	time (s)	deviation	average	time (s)
p200.00	46630.03	0.42	-0.99%	46169.30	57.89	-19.06%	37740.62	425.45
p200.01	48115.10	0.38	-0.92%	47671.54	58.28	-14.86%	40965.76	437.00
p200.02	42769.92	0.36	-2.11%	41868.22	55.87	-16.30%	35796.45	435.53
p200.03	50615.44	0.38	-1.17%	50022.81	51.85	-18.33%	41337.94	419.22
p200.04	50214.82	0.37	-1.44%	49492.93	50.21	-17.93%	41211.72	423.64
p200.05	48504.51	0.35	-0.45%	48288.60	56.09	-18.09%	39728.78	422.36
p200.06	47167.72	0.41	-0.81%	46786.60	59.33	-15.74%	39743.30	428.17
p200.07	49428.00	0.34	-1.14%	48863.32	49.00	-18.22%	40423.01	411.47
p200.08	48470.33	0.34	-1.25%	47866.53	58.14	-17.55%	39962.94	426.50
p200.09	49608.24	0.37	-1.12%	49054.21	59.96	-17.10%	41127.20	426.37
p200.10	47589.60	0.42	-1.40%	46924.62	58.69	-14.56%	40658.54	426.27
p200.11	45445.69	0.36	-1.38%	44818.92	55.23	-16.51%	37942.91	426.11
p200.12	47031.37	0.38	-1.51%	46323.00	56.86	-16.25%	39387.87	427.36
p200.13	49325.17	0.37	-0.94%	48863.00	54.22	-17.07%	40904.70	428.30
p200.14	50596.65	0.39	-0.97%	50103.35	57.99	-17.69%	41645.71	430.09
p200.15	49079.24	0.30	-1.42%	48382.05	57.63	-15.99%	41231.38	437.40
p200.16	50282.01	0.40	-1.59%	49484.23	56.94	-17.69%	41388.63	416.13
p200.17	49185.75	0.36	-1.69%	48352.34	58.56	-18.76%	39957.14	432.24
p200.18	44627.62	0.36	-1.37%	44016.49	57.55	-13.31%	38689.90	433.69
p200.19	47036.85	0.30	-1.22%	46461.51	57.84	-14.13%	40389.10	431.99
p200.20	45518.08	0.33	-1.22%	44961.15	57.33	-15.35%	38531.79	422.39
p200.21	48974.18	0.37	-1.35%	48313.89	60.38	-16.82%	40737.32	434.98
p200.22	47664.44	0.34	-1.32%	47034.55	54.02	-15.72%	40170.09	429.71
p200.23	50251.92	0.36	-1.45%	49524.23	52.90	-16.88%	41767.42	425.69
p200.24	48503.14	0.38	-1.24%	47902.02	61.22	-14.31%	41560.49	426.87
p200.25	50260.22	0.37	-0.97%	49771.78	57.83	-15.72%	42358.77	423.80
p200.26	50068.31	0.38	-1.85%	49140.52	51.61	-19.77%	40167.69	430.00
p200.27	50853.89	0.40	-1.40%	50139.48	58.08	-16.88%	42271.57	429.13
p200.28	48642.17	0.40	-0.28%	48505.48	54.77	-17.47%	40142.17	429.79
p200.29	46931.01	0.40	-0.94%	46488.10	57.62	-14.65%	40056.86	409.82
	48313.05	0.37	-1.23%	47719.83	56.46	-16.62%	40266.59	426.92

Table 4.32: Results for instances with 20 nodes with mode 1 and candidate list size of 8 (directional antennas with $\theta_{\min} = 60°$).

Instance	D-MIP		D-MIP + VND			D-MACO		
	average	time (s)	deviation	average	time (s)	deviation	average	time (s)
p20.00	86354.92	0.00	-3.62%	83224.96	0.08	-12.68%	75407.76	0.04
p20.01	100978.05	0.01	-4.73%	96203.25	0.11	-15.29%	85540.94	0.09
p20.02	70315.74	0.00	-3.87%	67591.78	0.11	-10.88%	62663.00	0.02
p20.03	91341.51	0.00	-2.80%	88786.17	0.10	-9.70%	82479.06	0.25
p20.04	116573.15	0.00	-2.91%	113180.84	0.09	-14.02%	100230.57	0.16
p20.05	65075.16	0.01	-3.79%	62607.38	0.13	-15.19%	55187.16	0.14
p20.06	72104.59	0.00	-6.31%	67552.04	0.06	-15.44%	60975.01	0.05
p20.07	87853.80	0.00	-3.58%	84705.53	0.12	-9.64%	79387.29	0.42
p20.08	68855.31	0.01	-3.72%	66295.04	0.10	-10.75%	61453.23	0.05
p20.09	83533.34	0.01	-2.14%	81748.63	0.11	-10.51%	74750.33	0.03
p20.10	65763.95	0.00	-0.93%	65154.35	0.09	-5.38%	62226.83	0.07
p20.11	70329.45	0.00	-1.82%	69051.66	0.05	-10.55%	62913.13	0.05
p20.12	73074.20	0.00	-0.34%	72829.35	0.08	-4.00%	70150.28	0.04
p20.13	86614.63	0.00	-2.75%	84236.32	0.08	-16.58%	72250.21	0.03
p20.14	60906.40	0.00	-1.45%	60021.95	0.09	-8.92%	55476.23	0.03
p20.15	87308.62	0.02	-0.95%	86482.91	0.05	-7.82%	80483.11	0.10
p20.16	96205.57	0.00	-3.23%	93101.75	0.05	-12.60%	84080.61	0.08
p20.17	101294.06	0.00	-2.75%	98503.77	0.09	-22.30%	78707.00	0.30
p20.18	65163.70	0.00	-2.65%	63438.24	0.10	-9.90%	58712.38	0.02
p20.19	88557.73	0.00	-2.86%	86022.50	0.08	-10.41%	79336.27	0.15
p20.20	100320.98	0.00	-4.25%	96052.49	0.10	-15.24%	85033.22	0.02
p20.21	75517.76	0.00	-2.47%	73653.57	0.08	-16.67%	62930.95	0.06
p20.22	68414.27	0.00	-2.38%	66787.17	0.07	-6.22%	64158.17	0.06
p20.23	78601.09	0.00	-2.48%	76650.97	0.10	-11.56%	69515.78	0.03
p20.24	81714.72	0.00	-7.04%	75965.75	0.06	-14.67%	69730.09	0.09
p20.25	98794.69	0.01	-1.80%	97013.64	0.10	-7.97%	90921.57	0.06
p20.26	132583.86	0.00	-4.53%	126575.73	0.08	-18.28%	108349.68	0.13
p20.27	81580.96	0.00	-3.13%	79031.14	0.06	-11.66%	72066.75	0.04
p20.28	80577.55	0.01	-0.33%	80308.61	0.07	-11.84%	71038.15	0.11
p20.29	64138.73	0.00	-3.09%	62156.29	0.09	-11.41%	56817.31	0.34
	83348.28	0.00	-2.96%	80831.13	0.09	-11.94%	73099.07	0.10

Table 4.33: Results for instances with 50 nodes with mode 1 and candidate list size of 8 (directional antennas with $\theta_{\min} = 60°$).

Instance	D-MIP		D-MIP + VND			D-MACO		
	average	time (s)	deviation	average	time (s)	deviation	average	time (s)
p50.00	87322.57	0.00	-4.21%	83650.21	1.26	-14.53%	74631.05	4.66
p50.01	88165.53	0.01	-2.99%	85533.36	1.22	-12.97%	76734.08	3.97
p50.02	83846.53	0.02	-2.29%	81924.01	1.24	-14.77%	71459.37	4.55
p50.03	67475.91	0.00	-3.81%	64901.86	1.20	-11.79%	59523.05	4.19
p50.04	74209.07	0.00	-4.32%	71005.10	1.17	-16.12%	62244.30	4.80
p50.05	73865.60	0.02	-7.34%	68442.76	1.20	-11.33%	65493.82	4.67
p50.06	86386.79	0.02	-1.32%	85248.18	1.28	-14.54%	73828.43	3.75
p50.07	86795.27	0.01	-4.26%	83098.67	1.15	-13.26%	75282.68	3.93
p50.08	75515.87	0.02	-0.71%	74979.02	1.15	-9.69%	68195.21	3.57
p50.09	69758.68	0.03	-1.57%	68664.20	1.23	-8.13%	64088.06	6.38
p50.10	95535.52	0.05	-1.56%	94044.82	1.19	-11.54%	84510.49	4.42
p50.11	75781.11	0.01	-2.41%	73953.41	1.36	-9.07%	68909.44	4.14
p50.12	78928.41	0.00	-2.15%	77230.43	1.19	-7.65%	72887.78	4.87
p50.13	82717.82	0.02	-2.89%	80329.07	1.15	-11.96%	72825.81	4.58
p50.14	91745.12	0.02	-1.94%	89961.11	1.14	-11.65%	81055.13	7.12
p50.15	81723.16	0.00	-3.12%	79176.15	1.40	-11.15%	72613.62	5.44
p50.16	87010.07	0.01	-3.75%	83745.66	1.19	-10.97%	77468.24	2.41
p50.17	75736.62	0.03	-1.79%	74377.47	1.11	-10.20%	68009.32	4.22
p50.18	81401.96	0.01	-3.20%	78793.24	1.16	-12.98%	70836.41	2.80
p50.19	81370.80	0.02	-4.05%	78072.44	0.88	-14.01%	69972.44	5.09
p50.20	78455.45	0.01	-1.66%	77149.86	1.07	-8.50%	71788.05	5.46
p50.21	76950.40	0.00	-0.54%	76533.35	1.00	-10.40%	68947.06	4.83
p50.22	80377.92	0.03	-2.04%	78734.50	1.13	-11.90%	70816.05	3.82
p50.23	79066.88	0.02	-2.58%	77029.14	0.94	-15.54%	66780.10	4.86
p50.24	87526.49	0.02	-0.62%	86980.43	1.02	-8.48%	80107.13	4.13
p50.25	78937.68	0.01	-2.13%	77257.65	1.04	-6.15%	74079.85	2.49
p50.26	87661.08	0.01	-1.20%	86612.39	1.20	-11.80%	77321.14	4.62
p50.27	94083.39	0.00	-3.04%	91224.15	1.18	-13.11%	81745.87	7.65
p50.28	87875.25	0.01	-2.94%	85294.62	1.18	-11.56%	77712.67	5.33
p50.29	79877.47	0.01	-1.14%	78968.08	1.15	-6.86%	74400.53	4.31
	81870.15	0.01	-2.59%	79763.84	1.16	-11.42%	72475.57	4.57

Table 4.34: Results for instances with 100 nodes with mode 1 and candidate list size of 8 (directional antennas with $\theta_{\min} = 60°$).

Instance	D-MIP		D-MIP + VND			D-MACO		
	average	time (s)	deviation	average	time (s)	deviation	average	time (s)
p100.00	75726.64	0.06	-3.14%	73349.64	8.76	-11.94%	66685.08	57.02
p100.01	76655.31	0.06	-4.45%	73243.71	8.94	-13.51%	66297.59	65.76
p100.02	72900.38	0.07	-1.01%	72163.15	8.84	-7.21%	67644.62	45.22
p100.03	72796.92	0.05	-3.14%	70513.44	9.32	-10.82%	64920.97	64.12
p100.04	75534.24	0.05	-1.99%	74034.52	8.06	-10.73%	67428.86	65.84
p100.05	88809.77	0.06	-1.80%	87214.08	8.18	-14.81%	75655.52	68.66
p100.06	84027.09	0.06	-2.94%	81558.25	8.89	-14.57%	71784.61	64.96
p100.07	74997.19	0.06	-2.18%	73359.59	9.25	-10.11%	67417.90	68.88
p100.08	80377.24	0.08	-1.93%	78824.60	8.62	-9.71%	72572.15	66.80
p100.09	85139.46	0.10	-4.79%	81065.45	8.78	-14.01%	73209.99	65.27
p100.10	68723.67	0.09	-2.79%	66808.36	8.99	-9.75%	62025.09	51.59
p100.11	75303.17	0.08	-1.85%	73911.31	8.58	-12.87%	65611.67	72.22
p100.12	82236.82	0.08	-1.52%	80987.12	8.18	-11.09%	73118.93	69.39
p100.13	72751.83	0.07	-4.32%	69606.11	8.28	-10.13%	65385.31	48.78
p100.14	69965.90	0.10	-1.81%	68696.18	8.99	-9.58%	63261.31	41.19
p100.15	76738.40	0.08	-1.92%	75268.34	8.93	-12.83%	66894.89	54.49
p100.16	70143.03	0.09	-2.34%	68500.89	9.22	-9.75%	63303.18	53.58
p100.17	79176.99	0.10	-2.31%	77351.57	9.09	-11.62%	69980.22	68.59
p100.18	69110.81	0.12	-1.00%	68417.64	8.94	-9.93%	62248.90	61.00
p100.19	77222.73	0.14	-1.89%	75761.22	8.91	-9.88%	69592.56	57.47
p100.20	71388.85	0.07	-2.81%	69379.35	8.90	-9.73%	64445.60	52.07
p100.21	76917.50	0.08	-2.52%	74975.54	9.19	-11.74%	67887.02	45.84
p100.22	75270.97	0.06	-1.50%	74142.34	7.97	-9.95%	67783.95	55.49
p100.23	84713.74	0.06	-3.53%	81722.98	9.17	-12.30%	74291.19	68.53
p100.24	76726.39	0.07	-2.83%	74555.94	8.73	-11.31%	68045.63	58.18
p100.25	78053.75	0.06	-2.98%	75724.09	8.39	-12.99%	67911.83	64.71
p100.26	78893.82	0.09	-2.96%	76560.21	8.16	-8.90%	71874.61	61.71
p100.27	66849.52	0.09	-1.31%	65973.79	8.56	-6.62%	62423.72	55.94
p100.28	73081.54	0.07	-2.88%	70979.96	8.56	-8.48%	66880.90	56.51
p100.29	79430.84	0.07	-2.96%	77082.86	8.53	-13.26%	68900.09	59.97
	76322.15	0.08	-2.51%	74391.07	8.73	-11.00%	67849.46	59.66

Table 4.35: Results for instances with 200 nodes with mode 1 and candidate list size of 8 (directional antennas with $\theta_{\min} = 60°$).

Instance	D-MIP		D-MIP + VND			D-MACO		
	average	time (s)	deviation	average	time (s)	deviation	average	time (s)
p200.00	72048.35	0.35	-2.79%	70041.42	69.32	-9.63%	65109.56	411.08
p200.01	76141.83	0.39	-2.82%	73991.55	70.84	-8.49%	69674.57	401.80
p200.02	67457.44	0.38	-2.52%	65758.30	69.40	-9.24%	61225.14	383.44
p200.03	77534.08	0.43	-1.71%	76208.38	67.34	-10.11%	69699.17	420.58
p200.04	78789.62	0.43	-2.57%	76765.78	69.43	-12.89%	68634.74	423.73
p200.05	72013.24	0.47	-1.79%	70725.48	71.26	-8.31%	66028.86	398.71
p200.06	73544.54	0.42	-2.81%	71479.56	64.37	-10.79%	65607.26	422.40
p200.07	76382.36	0.37	-2.75%	74281.68	63.29	-8.78%	69673.50	413.48
p200.08	75357.68	0.40	-2.19%	73707.72	70.46	-10.66%	67327.59	408.04
p200.09	78778.77	0.39	-2.52%	76794.09	62.05	-12.76%	68728.34	397.23
p200.10	76398.34	0.44	-1.11%	75552.59	68.25	-8.42%	69966.92	423.60
p200.11	72324.81	0.36	-1.23%	71436.73	68.49	-9.58%	65393.30	399.94
p200.12	76078.97	0.40	-3.44%	73460.10	68.55	-12.25%	66756.15	418.49
p200.13	75698.02	0.40	-1.41%	74630.45	70.99	-9.73%	68330.33	395.03
p200.14	80941.49	0.40	-2.48%	78938.03	69.13	-10.39%	72533.63	403.64
p200.15	76147.46	0.42	-0.89%	75472.17	68.40	-8.80%	69447.17	416.62
p200.16	77499.16	0.43	-2.24%	75763.67	72.06	-9.30%	70295.11	436.37
p200.17	77252.70	0.36	-3.56%	74500.28	70.20	-11.52%	68356.68	399.55
p200.18	73151.65	0.42	-2.76%	71132.96	62.92	-8.79%	66722.63	420.02
p200.19	75437.40	0.32	-2.11%	73842.24	68.79	-9.74%	68091.88	379.40
p200.20	69863.19	0.34	-2.48%	68133.89	66.38	-6.22%	65515.97	390.09
p200.21	77638.24	0.37	-1.76%	76273.26	67.18	-9.32%	70404.57	408.36
p200.22	74430.15	0.39	-2.53%	72550.05	63.45	-9.39%	67439.94	417.15
p200.23	76057.67	0.38	-4.41%	72703.64	72.34	-9.34%	68952.55	423.70
p200.24	78778.60	0.36	-2.50%	76805.79	60.42	-10.44%	70550.20	423.37
p200.25	76893.58	0.38	-1.37%	75841.79	68.62	-8.25%	70548.10	396.07
p200.26	77668.83	0.37	-2.38%	75822.54	66.87	-10.95%	69167.82	408.55
p200.27	79953.36	0.36	-2.97%	77582.50	65.45	-11.19%	71006.41	410.24
p200.28	78192.47	0.42	-2.09%	76561.01	70.67	-12.33%	68549.47	425.89
p200.29	75659.93	0.34	-2.58%	73705.63	68.87	-8.61%	69145.98	417.95
	75803.80	0.39	-2.36%	74015.44	67.86	-9.87%	68296.12	409.82

Table 4.36: Results for instances with 20 nodes with mode 3 and candidate list size of 8 (directional antennas with $\theta_{\min} = 90°$).

Instance	D-MIP		D-MIP + VND			D-MACO		
	average	time (s)	deviation	average	time (s)	deviation	average	time (s)
p20.00	117061.05	0.01	-0.50%	116480.87	0.09	-12.10%	102902.12	0.12
p20.01	132349.92	0.00	-3.99%	127073.14	0.09	-11.45%	117196.18	0.07
p20.02	87971.55	0.00	-2.87%	85449.07	0.10	-6.32%	82415.86	0.08
p20.03	125646.93	0.00	-2.78%	122153.96	0.10	-9.69%	113470.02	0.19
p20.04	159473.37	0.00	-6.45%	149189.95	0.09	-14.89%	135732.35	0.24
p20.05	83708.27	0.00	-4.33%	80080.52	0.12	-10.69%	74763.72	0.22
p20.06	91461.53	0.00	-5.42%	86502.45	0.11	-12.18%	80324.60	0.08
p20.07	114412.98	0.00	-5.68%	107911.87	0.08	-14.32%	98025.78	0.09
p20.08	92636.89	0.01	-6.33%	86770.54	0.08	-11.97%	81548.61	0.14
p20.09	119245.34	0.00	-3.80%	114714.95	0.07	-12.86%	103905.24	0.20
p20.10	89798.15	0.00	-3.47%	86681.24	0.11	-9.32%	81427.87	0.02
p20.11	97157.28	0.01	-4.62%	92669.33	0.10	-11.87%	85621.23	0.18
p20.12	102389.58	0.00	-2.61%	99721.16	0.09	-11.02%	91107.72	0.30
p20.13	113027.40	0.00	-8.30%	103644.56	0.10	-17.56%	93181.41	0.16
p20.14	80794.02	0.00	-2.46%	78803.79	0.10	-4.89%	76844.83	0.11
p20.15	118053.65	0.01	-3.22%	114248.52	0.08	-9.20%	107192.74	0.06
p20.16	125212.10	0.00	-3.07%	121373.95	0.08	-11.19%	111203.40	0.08
p20.17	118323.15	0.00	-4.16%	113404.63	0.10	-10.12%	106348.02	0.34
p20.18	88932.95	0.00	-8.01%	81805.81	0.12	-13.06%	77320.49	0.04
p20.19	122543.29	0.00	-6.72%	114306.16	0.08	-12.09%	107723.44	0.26
p20.20	132556.67	0.00	-5.18%	125686.77	0.09	-13.58%	114556.99	0.08
p20.21	105069.20	0.00	-3.07%	101845.62	0.10	-17.74%	86427.00	0.29
p20.22	94614.34	0.00	-2.43%	92310.66	0.09	-4.77%	90098.94	0.07
p20.23	105298.37	0.00	-2.57%	102588.82	0.08	-11.48%	93208.40	0.08
p20.24	102843.17	0.00	-4.64%	98075.65	0.08	-10.00%	92556.00	0.06
p20.25	138294.66	0.00	-6.93%	128715.59	0.09	-12.90%	120450.65	0.34
p20.26	169598.11	0.00	-3.74%	163252.67	0.11	-14.12%	145651.24	0.38
p20.27	108535.71	0.00	-2.09%	106268.95	0.10	-9.63%	98085.63	0.10
p20.28	111873.12	0.00	-2.26%	109340.74	0.10	-16.52%	93393.02	0.09
p20.29	88009.68	0.01	-9.28%	79842.28	0.12	-15.14%	74681.32	0.52
	111229.75	0.00	-4.37%	106363.81	0.10	-11.76%	97912.16	0.17

Table 4.37: Results for instances with 50 nodes with mode 3 and candidate list size of 8 (directional antennas with $\theta_{\min} = 90°$).

Instance	D-MIP		D-MIP + VND			D-MACO		
	average	time (s)	deviation	average	time (s)	deviation	average	time (s)
p50.00	114895.09	0.01	-5.11%	109019.35	1.24	-14.30%	98466.39	6.20
p50.01	118074.12	0.00	-3.77%	113617.72	1.21	-12.96%	102774.93	5.72
p50.02	115214.75	0.00	-4.05%	110549.50	1.27	-18.75%	93612.91	6.90
p50.03	95115.24	0.01	-5.74%	89659.09	1.29	-13.91%	81880.54	6.55
p50.04	99288.97	0.01	-5.42%	93905.46	1.35	-15.13%	84263.06	6.92
p50.05	103074.07	0.00	-3.87%	99087.39	1.30	-12.22%	90479.32	6.59
p50.06	120912.43	0.01	-4.12%	115928.74	1.23	-16.97%	100393.37	5.08
p50.07	117732.12	0.03	-4.12%	112880.73	1.22	-14.49%	100673.93	4.77
p50.08	103426.75	0.00	-3.06%	100261.58	1.24	-11.96%	91053.33	6.74
p50.09	96117.91	0.01	-2.59%	93632.67	1.29	-9.18%	87294.48	6.81
p50.10	128838.44	0.00	-6.34%	120672.52	1.31	-12.77%	112387.52	6.57
p50.11	102716.94	0.00	-3.74%	98876.68	1.31	-11.89%	90505.01	5.32
p50.12	102664.46	0.02	-4.57%	97971.86	1.32	-7.70%	94757.37	3.45
p50.13	110603.24	0.00	-1.39%	109061.59	1.21	-9.20%	100426.39	4.75
p50.14	123596.59	0.01	-4.83%	117631.98	1.28	-10.50%	110619.61	7.47
p50.15	108259.98	0.01	-3.24%	104754.62	1.36	-10.93%	96421.97	7.22
p50.16	112212.20	0.00	-4.11%	107604.42	1.27	-8.85%	102275.92	5.71
p50.17	105089.23	0.02	-5.23%	99597.05	1.34	-12.33%	92130.99	7.29
p50.18	108236.95	0.01	-3.14%	104843.09	1.26	-13.25%	93890.63	6.03
p50.19	110717.32	0.03	-4.85%	105348.56	1.20	-15.21%	93879.80	5.29
p50.20	112689.97	0.01	-3.34%	108924.94	1.21	-13.13%	97898.19	5.38
p50.21	103379.97	0.00	-3.17%	100103.95	1.35	-12.43%	90525.46	4.60
p50.22	107109.37	0.04	-4.39%	102407.43	1.28	-10.47%	95890.11	5.27
p50.23	106534.53	0.00	-3.99%	102279.66	1.27	-14.75%	90816.17	5.18
p50.24	123631.31	0.01	-3.67%	119089.57	1.15	-13.78%	106592.60	3.84
p50.25	109466.79	0.01	-5.51%	103437.30	1.30	-8.41%	100260.60	4.61
p50.26	119842.35	0.01	-3.26%	115936.80	1.03	-14.85%	102043.60	6.96
p50.27	123872.97	0.00	-3.44%	119609.59	1.35	-12.89%	107911.26	6.14
p50.28	119185.18	0.01	-6.20%	111792.31	1.33	-12.97%	103724.79	5.53
p50.29	114159.88	0.00	-1.35%	112614.53	1.22	-12.28%	100135.51	4.74
	111221.97	0.01	-4.05%	106703.36	1.27	-12.62%	97132.86	5.79

Table 4.38: Results for instances with 100 nodes with mode 3 and candidate list size of 8 (directional antennas with $\theta_{\min} = 90°$).

Instance	D-MIP		D-MIP + VND			D-MACO		
	average	time (s)	deviation	average	time (s)	deviation	average	time (s)
p100.00	101098.31	0.06	-5.04%	96002.51	9.58	-11.66%	89309.83	63.05
p100.01	103059.60	0.12	-4.80%	98108.52	9.46	-11.08%	91639.80	63.32
p100.02	102234.71	0.06	-2.06%	100128.23	9.25	-7.70%	94363.71	65.29
p100.03	97047.62	0.08	-2.78%	94346.52	9.36	-9.64%	87692.04	63.44
p100.04	103091.79	0.05	-4.91%	98034.31	9.26	-12.14%	90572.63	75.19
p100.05	118451.40	0.08	-4.12%	113574.83	9.31	-12.66%	103453.11	60.12
p100.06	116112.84	0.06	-5.33%	109925.24	9.66	-16.64%	96786.11	55.25
p100.07	102028.63	0.06	-2.88%	99089.91	9.52	-10.27%	91546.63	64.89
p100.08	110877.56	0.15	-4.73%	105632.26	9.51	-12.50%	97019.80	57.42
p100.09	116166.48	0.05	-3.73%	111832.45	9.52	-13.50%	100484.20	63.11
p100.10	92959.26	0.04	-3.72%	89504.34	8.83	-9.88%	83773.57	67.86
p100.11	102765.13	0.07	-3.49%	99180.09	9.31	-14.97%	87384.64	66.16
p100.12	114070.17	0.05	-5.51%	107784.22	9.21	-14.84%	97146.21	60.94
p100.13	101487.24	0.05	-4.24%	97188.35	8.04	-11.37%	89943.10	59.76
p100.14	97094.78	0.05	-2.86%	94320.86	8.37	-11.07%	86343.10	67.29
p100.15	99674.19	0.06	-1.94%	97745.30	8.68	-9.49%	90219.38	57.64
p100.16	96957.07	0.05	-3.71%	93360.90	8.64	-11.92%	85402.75	62.22
p100.17	106394.88	0.07	-3.36%	102822.36	9.12	-11.81%	93833.29	57.26
p100.18	93714.83	0.06	-3.22%	90698.36	9.77	-8.99%	85286.51	54.74
p100.19	103186.13	0.07	-2.83%	100265.89	8.99	-9.50%	93383.86	61.69
p100.20	99635.96	0.05	-5.06%	94596.66	9.81	-11.70%	87977.94	64.48
p100.21	104538.91	0.05	-4.56%	99776.46	8.97	-12.58%	91383.67	61.51
p100.22	105775.27	0.07	-2.83%	102776.71	8.78	-14.24%	90715.56	57.52
p100.23	116304.32	0.05	-5.73%	109639.69	9.74	-15.55%	98220.78	62.61
p100.24	100242.40	0.05	-3.28%	96954.91	9.46	-8.54%	91677.92	54.38
p100.25	105949.76	0.05	-5.71%	99895.16	9.13	-15.07%	89985.09	58.61
p100.26	108678.66	0.04	-4.12%	104201.07	9.43	-9.85%	97975.87	62.57
p100.27	96635.62	0.05	-3.16%	93584.52	9.78	-10.51%	86478.17	57.48
p100.28	99218.28	0.07	-3.40%	95847.48	9.26	-9.54%	89755.85	60.71
p100.29	106773.56	0.08	-3.58%	102955.00	9.28	-11.74%	94237.06	57.28
	104074.18	0.06	-3.89%	99992.44	9.23	-11.70%	91799.74	61.46

Table 4.39: Results for instances with 200 nodes with mode 3 and candidate list size of 8 (directional antennas with $\theta_{\min} = 90°$).

Instance	D-MIP		D-MIP + VND			D-MACO		
	average	time (s)	deviation	average	time (s)	deviation	average	time (s)
p200.00	98887.46	0.44	-3.61%	95316.90	74.00	-10.11%	88893.58	379.39
p200.01	104924.55	0.41	-4.70%	99996.60	74.97	-11.98%	92359.33	415.85
p200.02	95044.19	0.43	-3.83%	91399.56	73.17	-10.82%	84759.93	400.04
p200.03	105957.13	0.40	-5.07%	100590.22	72.35	-12.82%	92378.00	412.91
p200.04	105308.92	0.39	-4.09%	100998.20	73.36	-11.15%	93565.26	369.04
p200.05	103064.46	0.39	-5.33%	97569.90	70.84	-12.47%	90209.89	421.82
p200.06	98386.04	0.47	-4.64%	93818.81	74.85	-11.02%	87543.73	341.05
p200.07	105266.01	0.43	-6.34%	98587.09	75.13	-11.54%	93117.42	408.58
p200.08	103770.04	0.36	-5.22%	98351.58	73.93	-12.82%	90469.48	405.48
p200.09	104852.42	0.42	-4.53%	100099.01	69.23	-12.22%	92042.80	404.09
p200.10	104757.30	0.43	-3.92%	100647.83	73.36	-11.55%	92658.04	399.16
p200.11	98419.46	0.34	-1.95%	96504.69	72.81	-9.66%	88914.85	379.17
p200.12	101376.63	0.41	-2.92%	98412.43	68.64	-11.12%	90105.91	397.50
p200.13	104489.57	0.40	-3.55%	100782.29	72.71	-11.49%	92479.12	382.58
p200.14	111381.18	0.38	-4.15%	106759.59	73.39	-12.36%	97614.31	364.76
p200.15	109298.28	0.41	-5.24%	103566.11	67.99	-14.78%	93142.18	410.36
p200.16	105197.41	0.38	-4.43%	100540.49	74.93	-9.97%	94713.82	406.63
p200.17	103726.35	0.37	-4.60%	98957.38	73.22	-11.30%	92005.83	417.56
p200.18	99607.46	0.40	-3.58%	96040.49	72.34	-8.00%	91643.34	384.99
p200.19	102194.60	0.39	-3.57%	98545.10	74.50	-10.76%	91195.16	381.10
p200.20	98225.63	0.42	-3.67%	94616.66	73.81	-9.14%	89251.37	389.32
p200.21	106838.62	0.39	-4.16%	102394.53	75.57	-11.89%	94132.72	420.37
p200.22	104414.16	0.38	-5.12%	99070.79	73.74	-13.13%	90706.94	408.25
p200.23	104217.76	0.42	-4.08%	99969.13	73.32	-9.93%	93873.71	412.83
p200.24	108101.64	0.36	-4.69%	103033.21	72.60	-12.67%	94405.15	406.39
p200.25	104472.92	0.39	-3.23%	101098.01	73.98	-10.01%	94018.93	398.53
p200.26	103844.61	0.39	-4.82%	98834.62	75.72	-11.36%	92044.78	411.93
p200.27	108286.66	0.34	-4.52%	103393.75	70.90	-13.09%	94117.26	392.75
p200.28	105740.41	0.33	-2.58%	103017.59	66.37	-12.18%	92862.04	393.22
p200.29	100839.50	0.38	-2.84%	97976.44	64.38	-7.35%	93429.92	395.57
	103696.38	0.40	-4.17%	99362.97	72.54	-11.29%	91955.16	397.04

4.4.2.4 Benefits of directional antennas

In Appendix C advantages of using directional antennas with $\theta_{\min} \in \{30°, 60°, 90°\}$ for each different instance size are shown comparing the average required power in these cases to the average required power when considering omnidirectional antennas. Average values over all considered network sizes are shown in Table 4.40 and are, additionally, summarized in Figure 4.20, where, for each different considered value of $\theta_{\min}$, a boxplot shows the average required energy over 30 different multicast sessions for each of the 120 MEB instances. In both cases the benefits of using directional antennas with $\theta_{\min} = 30°$ are clear. In fact, average energy saving for this case is 86.97%. Note that the use of directional antennas produces huge and similar energy savings in the broadcast and multicast scenarios.

Table 4.40: Summary of best values of best results obtained for best performing MACO/D-MACO modes for all considered antenna types and instance sizes.

Size of instances	$\theta_{\min} = 360°$	$\theta_{\min} = 90°$		$\theta_{\min} = 60°$		$\theta_{\min} = 30°$	
	average	**energy saving**	**average**	**energy saving**	**average**	**energy saving**	**average**
20	323693.58	-69.72	97912.16	-77.37	73099.07	-86.70	43033.86
50	323552.80	-69.98	97132.86	-77.61	72475.57	-86.98	42125.59
100	311858.05	-70.57	91799.74	-78.25	67849.46	-87.15	40061.42
200	311261.03	-70.46	91955.16	-78.06	68296.12	-87.06	40266.59
	317591.37	-70.18%	94699.98	-77.82%	70430.06	-86.97%	41371.87

4.4.3 Importance of VND and pheromone update

As in the MEB problem experiments, in addition to the above experiments, an evaluation of the necessity of using the VND local search procedure and the pheromone update mechanism was done. All considered instances were evaluated with the best parameters found in each different scenario considered (one for each of the four different antenna types used) but disabling, first, the vnd mechanism and, in second place, the pheromone update mechanism (but enabling again the VND). With these modifications, the real effect on the MACO/D-MACO algorithm of this two different components is tested. Tables in Appendix E show the results of these tests. Results are summarized in Figure 4.21 were different boxplots show that, for instances of all considered sizes, results get worse when algorithm components are switched off. In fact, additional energy consumption can go, on average, up to 27.54% when disconnecting the VND and up to 10.94% when disconnecting the pheromone update mechanism. This means that both components are strictly necessary to obtain the results for the MEM problem presented in previous sections and, hence, justifies its interest.

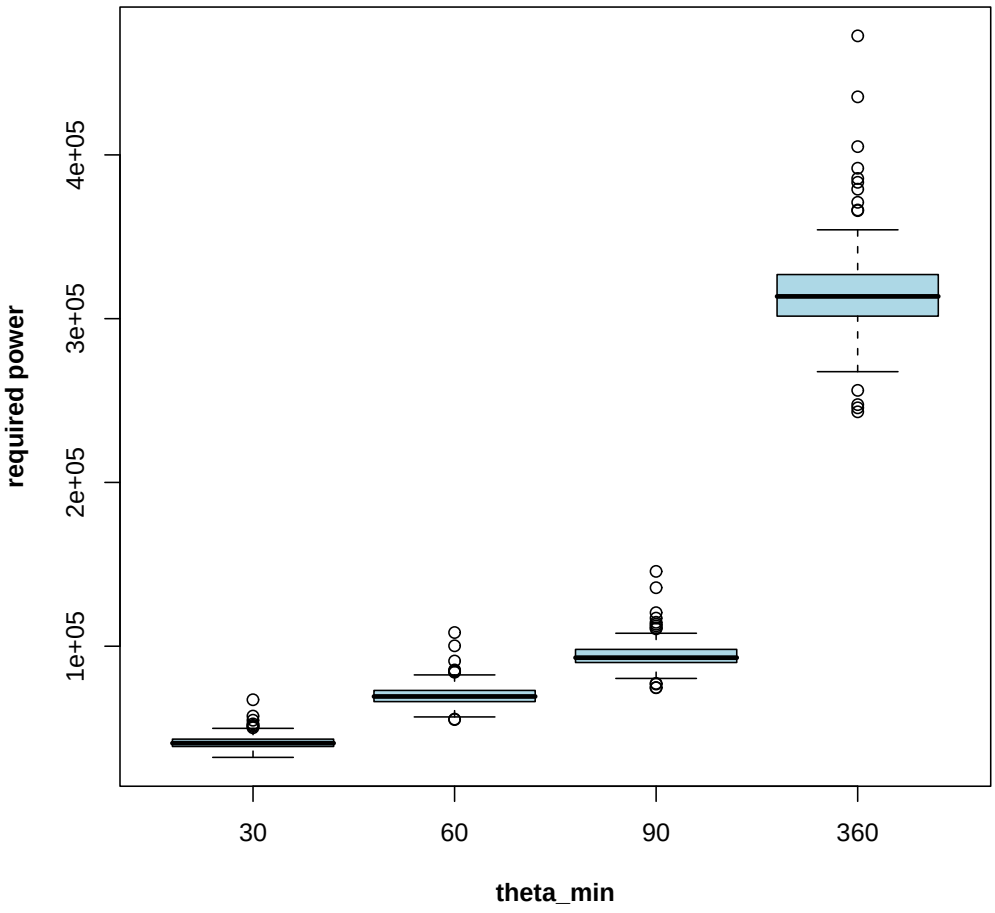

Figure 4.20: Comparison of the four considered antenna types $\theta_{\min} \in \{30°, 60°, 90°, 360°\}$.

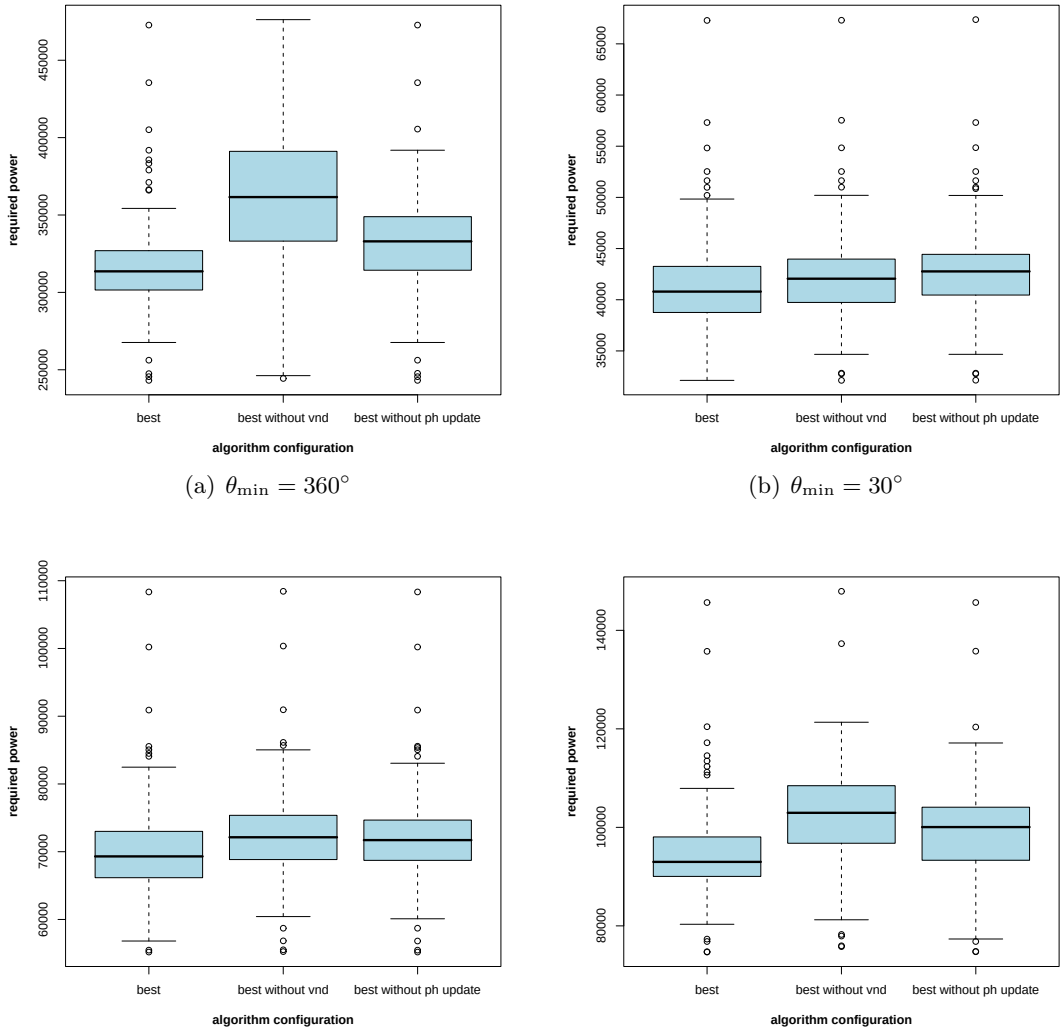

(a) $\theta_{\min} = 360°$ (b) $\theta_{\min} = 30°$

(c) $\theta_{\min} = 60°$ (d) $\theta_{\min} = 90°$

Figure 4.21: Comparison of full MACO/D-MACO with algorithms without VND and with VND but without pheromone update.

Chapter 5

Conclusions and further work

In this work, first the state of the art for the Minimum Energy Multicast/Broadcast problem (MEM/MEB problem) has been reviewed. Next, an Ant Colony Optimization algorithm for these problems when directional or omnidirectional antennas are considered has been described. An exhaustive evaluation of the performance of this algorithm on a large set of problem instances has been done, which has shown that it outperforms popular algorithms from the literature for these problems (in best solutions, average solutions and required time). Note that we also added larger benchmark instances to the ones available in the literature (100 and 200 nodes instances). These results have been used for the elaboration of three different publications, one accepted as full-length paper and chosen for oral presentation at an interantional conference, another one submitted to another international conference (still waiting for acceptance) and a more extensive one to be submitted to an international journal.

The current approach to energy saving in ad-hoc wireless networks has some limitations. The main problem is that information about the nodes is considered centralized and, hence, algorithms must be executed offline, considering the structure of the network at a particular time. This fact makes it impossibile to consider possible changes in network structure during its lifetime, what in some cases disables further energy saving.

In addition, in real applications, nodes in a wireless adhoc network, like PDAs or laptop computers, are often equipped with batteries to be able to work while being unplugged. Furthermore, if these networks have a minimum size, hundreds of multicast/broadcast requests will appear every minute and in any moment batteries can deploy, modifying network topolgy and downgrading its performance, capabilities and functionalites. This idea suggests a slightly different problem consisting in, given a network topology and a list of multicast/broadcast requests (which include the sender and the multicast set), discovering the adecuate communication schemas for each request in order to maximize network lifetime. These problems are known as the *Maximum Lifetime Broadcast* (MLB) and the *Maximum Lifetime Multicast* (MLM) problems.

Notice that if each multicast/broadcast request in a network session is considered as a different MEM/MEB instance, i.e., if the power consumed by each packet routing is minimized, then it is not necessarily true that network lifetime is maximized. For example, if all packets are broadcast and are sent from a reduced set of nodes, their best found broadcast trees will

always be used and the batteries of nodes in these trees will deploy very soon while there may be some unused nodes. Thus, these nodes could and should be used in an appropiate way to extend network lifetime.

In the future, we want to study this problem (MEM/MEB) which is similar to those studied in this work (MLM/MLB). Some versions of this problem have already been studied (for example, in [52, 54, 29, 23, 20]). An extensive review of this problem can be found in [26].

Further work will also be focused on distributed algorithms for energy saving in wireless ad-hoc networks. Distributeness may help in the creation of algorithms more sensible to network topology changes that could, possibly, enable further energy savings.

Bibliography

[1] S. Al-Shihabi, P. Merz, and S. Wolf. Nested partitioning for the minimum energy broadcast. In *Proceedings of LION 2007 – Learning and Intelligent Optimization*. Springer Verlag, Berlin, 2007.

[2] C. Blum and M. Dorigo. The hyper-cube framework for ant colony optimization. *IEEE Transactions on Systems, Man anc Cybernetics – Part B*, 34(2):1161–1172, 2004.

[3] C. Blum and A. Roli. Metaheuristics in combinatorial optimization: Overview and conceptual comparison. *ACM Computing Surveys*, 35(3):268–308, September 2003.

[4] B. Bullnheimer, R. F. Hartl, and C. Strauss. A new rank-based version of the ant system: a computational study. *Central European Journal for Operations Research and Economics*, 7(1):25–38, 1999.

[5] M. Cagalj, J. P. Hubaux, and C. Enz. Minimum-energy broadcast in all-wireless networks: NP-completeness and distribution issues. In *Proccedings of ACM MobiCom*, pages 172–182. ACM press, 2002.

[6] M. Campos, E. Bonabeau, G. Theraulaz, and J. L. Deneubourg. Dynamic Scheduling and Division of Labor in Social Insects. *Adaptive Behavior*, 8(2):83, 2000.

[7] J. Cartigny, D. Simplot, and I. Stojmenovic. Localized minimum-energy broadcasting in ad-hoc networks. *INFOCOM 2003. Twenty-Second Annual Joint Conference of the IEEE Computer and Communications Societies. IEEE*, 3, 2003.

[8] J. Cartigny, D. Simplot, and I. Stojmenovic. An adaptive localized scheme for energy-efficient broadcasting in ad hoc networks with directional antennas. In *Proceedings of PWC 2004 – 9th IFIP International Conference on Personal Wireless Communications*, volume 3260 of *Lecture Notes in Computer Science*, pages 399–413. Springer Verlag, Berlin, 2004.

[9] V. Černỳ. Thermodynamical approach to the traveling salesman problem: An efficient simulation algorithm. *Journal of Optimization Theory and Applications*, 45(1):41–51, 1985.

[10] A. K. Das, R. J. Marks, M. El-Sharkawi, P. Arabshahi, and A. Gray. The minimum power broadcast problem in wireless networks: an ant colony system approach. In *Proceedings of the IEEE CAS Workshop on Wireless Communications and Networking*. IEEE, 2002.

[11] A. K. Das, R. J. Marks, M. El-Sharkawi, P. Arabshahi, and A. Gray. *r*-shrink: A heuristic for improving minimum power broadcast trees in wireless networks. In *Proceedings of GLOBECOM 2003*, pages 523–527. IEEE press, 2003.

[12] J. L. Deneubourg, S. Aron, S. Goss, and J. M. Pasteels. The self-organizing exploratory pattern of the argentine ant. *Journal of Insect Behavior*, 3(2):159–168, 1990.

[13] M. Dorigo. *Optimization, Learning and Natural Algorithms*. PhD thesis, Dipartimento di Elettronica, Politecnico di Milano, Italy, 1992.

[14] M. Dorigo and L. M. Gambardella. Ant colony system: a cooperative learning approach to the travelingsalesman problem. *IEEE Transactions on Evolutionary Computation*, 1(1):53–66, 1997.

[15] M. Dorigo, V. Maniezzo, and A. Colorni. Positive feedback as a search strategy. Technical report, Dipartimento di Elettronica, Politecnico di Milano, Milan, Italy, Tech. Rep, 1991.

[16] M. Dorigo, V. Maniezzo, and A. Colorni. Ant system: optimization by a colony of cooperating agents. *IEEE Transactions on Systems, Man and Cybernetics, Part B*, 26(1):29–41, 1996.

[17] M. Dorigo and T. Stützle. *Ant Colony Optimization*. MIT Press, Cambridge, MA, 2004.

[18] P. P. Grassé. La reconstruction du nid et les coordinations interindividuelles chezBellicositermes natalensis et Cubitermes sp. la théorie de la stigmergie: Essai d'interprétation du comportement des termites constructeurs. *Insectes Sociaux*, 6(1):41–80, 1959.

[19] S. Guo, V. Leung, and O. Yang. A Distributed Minimum Energy Multicast Algorithm in MANETs. In *Proceedings of the 2006 International Symposium on on World of Wireless, Mobile and Multimedia Networks*, pages 134–142. IEEE Computer Society Washington, DC, USA, 2006.

[20] S. Guo, V. Leung, and O. Yang. Distributed multicast algorithms for lifetime maximization in wireless ad hoc networks with omni-directional and directional antennas. In *Proceedings of IEEE Global Telecommunications Conference (GLOBECOM'06)*. IEEE, 2006.

[21] S. Guo and O. Yang. A dynamic multicast tree reconstruction algorithm for minimum-energy multicasting in wireless ad hoc networks. In *IEEE International Conference on Performance, Computing, and Communications, 2004. IPCCC 2004*, pages 637–642. IEEE Computer Society, 2004.

[22] S. Guo and O. Yang. A dynamic multicast tree reconstruction algorithm for minimum-energy multicasting in wireless ad hoc networks. In *Proceedings of IEEE IPCCC*, pages 637–642. IEEE press, 2004.

[23] S. Guo and O. Yang. Multicast lifetime maximization for energy-constrained wireless ad-hoc networks with directional antennas. In *Global Telecommunications Conference, 2004. IEEE GLOBECOM'04*, volume 6. IEEE, 2004.

[24] S. Guo and O. Yang. Improving energy efficiency for multicasting in ad-hoc networks with directional antennas. In *Proceedings of IEEE WiMob 2005 – Wireless and Mobile Computing, Networking and Communications*, pages 344–351. IEEE press, 2005.

[25] S. Guo and O. Yang. Minimum-energy multicast in wireless ad hoc networks with adaptive antennas: MILP formulations and heuristic algorithms. *IEEE Transactions on Mobile Computing*, 5(4):333–346, 2006.

[26] S. Guo and O. W. W. Yang. Energy-aware multicasting in wireless ad hoc networks: A survey and discussion. *Computer Communications*, 30:2129–2148, 2007.

[27] J. Handl, J. Knowles, and M. Dorigo. Ant-Based Clustering and Topographic Mapping. *Artificial Life*, 12(1):35–62, 2006.

[28] P. Hansen and N. Mladenović. Variable neighborhood search: Principles and applications. *European Journal of Operational Research*, 130:449–467, 2001.

[29] Y. T. Hou, Y. Shi, H. D. Sherali, and J. E. Wieselthier. Online lifetime-centric multicast routing for ad hoc networks with directional antennas. In *Proceedings of the 24th Annual Joint Conference of the IEEE Computer and Communications Societies. IEEE INFOCOM 2005*. IEEE, 2005.

[30] F. Ingelrest and D. Simplot-Ryl. Localized broadcast incremental power protocol for wireless ad hoc networks. *Wireless Networks*, 14(3):309–319, June 2008.

[31] I. Kang and R. Poovendran. A novel power-efficient broadcast routing algorithm exploiting broadcast efficiency. *Vehicular Technology Conference, 2003. VTC 2003-Fall. 2003 IEEE 58th*, 5, 2003.

[32] I. Kang and R. Poovendran. Broadcast with heterogeneous node capability. *Global Telecommunications Conference, 2004. IEEE GLOBECOM '04*, 6:4114–4119, November 2004.

[33] I. Kang and R. Poovendran. Iterated local optimization for minimum energy broadcast. In *Proceedings of WiOpt 2005 – Third International Symposium on Modeling and Optimization in Mobile, Ad Hoc, and Wireless Networks*, pages 332–341. IEEE press, 2005.

[34] J. Kennedy and R. Eberhart. Particle swarm optimization. In *Proceedings of IEEE International Conference on Neural Networks, 1995*, volume 4. IEEE, 1995.

[35] S. Kirkpatrick, CD Gelatt, and MP Vecchi. Optimization by Simulated Annealing. *Science*, 220(4598):671–680, 1983.

[36] F. Li and I. Nikolaidis. On minimum-energy broadcasting in all-wireless networks. In *Proceedings of the 26th Annual IEEE Conference on Local Computer Networks (LCN 2001)*, pages 193–202. IEEE, 2001.

[37] F. Li and I. Nikolaidis. On minimum-energy broadcasting in all-wireless networks. In *Proceedings of the IEEE Conference on Local Computer Networks*, pages 14–16. IEEE press, 2001.

[38] N. Li and J. C. Hou. BLMST: A Scalable, Power-Efficient Broadcast Algorithm for Wireless Networks. In *Proceedings First International Conference on Quality of Service in Heterogeneous Wired/Wireless Networks. QSHINE'04*, pages 44–51. publisher = IEEE Computer Society, 2004.

[39] N. Li, J.C. Hou, and L. Sha. Design and analysis of an MST-based topology control algorithm. *INFOCOM 2003. Twenty-Second Annual Joint Conference of the IEEE Computer and Communications Societies. IEEE*, 3, 2003.

[40] X. Y. Li. Approximate MST for UDG locally. In *Proceedings of 9th Annual International Conference on Computing and combinatorics, COCOON*, pages 364–373. Big Sky, 2003.

[41] X. Y. Li, W. Z. Song, and W. Wang. A unified energy-efficient topology for unicast and broadcast. In *Proceedings of the 11th annual international conference on Mobile computing and networking*, pages 1–15. ACM Press New York, NY, USA, 2005.

[42] X. Y. Li, Y. Wang, W. Z. Song, P. J. Wan, and O. Frieder. Localized minimum spanning tree and its applications in wireless ad hoc networks. In *Proceedings of the 23th Annual Joint Conference of the IEEE Computer and Communications Societies. IEEE INFOCOM 2004*. IEEE, 2004.

[43] W. Liang. Constructing minimum-energy broadcast trees in wireless ad hoc networks. In *Proceedings of the 3rd ACM international symposium on Mobile ad hoc networking & computing*, pages 112–122. ACM Press New York, NY, USA, 2002.

[44] W. Liang. Constructing minimum-energy broadcast trees in wireless ad hoc networks. In *Proceedings of ACM MobiHoc 2002*, pages 112–122. ACM, 2002.

[45] E. D. Lumer and B. Faieta. Diversity and adaptation in populations of clustering ants. In *Proceedings of the third international conference on Simulation of adaptive behavior: from animals to animats 3: from animals to animats 3 table of contents*, pages 501–508. MIT Press Cambridge, MA, USA, 1994.

[46] T. Rapport. *Wireless Communications: Principles and Practices*. Prentice Hall, 1996.

[47] T. Stützle and H. H. Hoos. MAX-MIN Ant system. *Future Generation Computer Systems*, 16(9):889–914, 2000.

[48] P. J. Wan, G. Calinescu, X. Li, and O. Frieder. Minimum-energy multicast in routing in static ad hoc wireless networks. *IEEE/ACM Transactions on Networking*, 12(3):507–514, 2004.

[49] P. J. Wan, G. Calinescu, X. Y. Li, and O. Frieder. Minimum-Energy Broadcasting in Static Ad Hoc Wireless Networks. *Wireless Networks*, 8(6):607–617, 2002.

[50] B. Wang and S. K. S Gupta. S-REMiT: a distributed algorithm for source-based energy efficient multicasting in wireless ad hoc networks. In *Global Telecommunications Conference, 2003. IEEE GLOBECOM'03*, volume 6. IEEE, 2003.

[51] J. E. Wieselthier, G. D. Nguyen, and A. Ephremides. On the construction of energy-efficient broadcast and multicast trees in wireless networks. *Proceedings of INFOCOM*

2000 – Nineteenth Annual Joint Conference of the IEEE Computer and Communications Societies, 2:585–594, 2000.

[52] J. E. Wieselthier, G. D. Nguyen, and A. Ephremides. Energy-aware wireless networking with directional antennas: the case of session-based broadcasting and multicasting. *IEEE Transactions on Mobile Computing*, 1(3):176–191, 2002.

[53] J. E. Wieselthier, G. D. Nguyen, and A. Ephremides. Energy-Efficient Broadcast and Multicast Trees in Wireless Networks. *Mobile Networks and Applications*, 7(6):481–492, 2002.

[54] J. E. Wieselthier, G. D. Nguyen, and A. Ephremides. Energy-limited wireless networking with directional antennas: the case of session-based multicasting. In *Proceedings of the Twenty-First Annual Joint Conference of the IEEE Computer and Communications Societies. IEEE INFOCOM 2002*. IEEE, 2002.

[55] S. Wolf and P. Merz. Evolutionary local search for the minimum energy broadcast problem. In C. Cotta and J. van Hemert, editors, *Proceedings of voCOP 2008 – Eigth European Conference on Evolutionary Computation in Combinatorial Optimisation*, volume 4972 of *Lecture Notes in Computer Science*, pages 61–72. Springer Verlag, Berlin, 2008.

[56] J.L. Wong, G. Veltri, and M. Potkonjak. Energy-efficient data multicast in multi-hop wireless networks. In *Proceedings IEEE Workshop on Integrated Management of Power Aware Communications, Computing and Networking*. Not published in paper, 2002.

Appendix A

Tuning of the ACO/D-ACO algorithm

A.1 ACO tuning (omnidirectional)

Table A.1: Comparison of best values among different mode and candidate list size for instances with 20 nodes (omnidirectional antennas).

Instance	ACO (best values)											
	m=1			m=2			m=3			m=4		
	c=4	c=8	c=all	c=4	c=8	c=all	c=4	c=8	c=all	c=4	c=8	c=all
p20.00	407250.81	407250.81	407250.81	407250.81	407250.81	407250.81	407250.81	407250.81	407250.81	407250.81	407250.81	407250.81
p20.01	446905.52	446905.52	446905.52	446905.52	446905.52	446905.52	446905.52	446905.52	446905.52	446905.52	446905.52	446905.52
p20.02	335102.42	335102.42	335102.42	335102.42	335102.42	335102.42	335102.42	335102.42	335102.42	335102.42	335102.42	335102.42
p20.03	488344.90	488344.90	488344.90	488344.90	488344.90	488344.90	488344.90	488344.90	488344.90	488344.90	488344.90	488344.90
p20.04	516117.75	516117.75	516117.75	516117.75	516117.75	516117.75	516117.75	516117.75	516117.75	516117.75	516117.75	516117.75
p20.05	300869.14	300869.14	300869.14	300869.14	300869.14	300869.14	300869.14	300869.14	300869.14	300869.14	300869.14	300869.14
p20.06	250553.15	250553.15	250553.15	250553.15	250553.15	250553.15	250553.15	250553.15	250553.15	250553.15	250553.15	250553.15
p20.07	347454.08	347454.08	347454.08	347454.08	347454.08	347454.08	347454.08	347454.08	347454.08	347454.08	347454.08	347454.08
p20.08	390795.34	390795.34	390795.34	390795.34	390795.34	390795.34	390795.34	390795.34	390795.34	390795.34	390795.34	390795.34
p20.09	447659.11	447659.11	447659.11	447659.11	447659.11	447659.11	447659.11	447659.11	447659.11	447659.11	447659.11	447659.11
p20.10	316734.39	316734.39	316734.39	316734.39	316734.39	316734.39	316734.39	316734.39	316734.39	316734.39	316734.39	316734.39
p20.11	289200.92	289200.92	289200.92	289200.92	289200.92	289200.92	289200.92	289200.92	289200.92	289200.92	289200.92	289200.92
p20.12	314511.98	314511.98	314511.98	314511.98	314511.98	314511.98	314511.98	314511.98	314511.98	314511.98	314511.98	314511.98
p20.13	346234.51	346234.51	346234.51	346234.51	346234.51	346234.51	346234.51	346234.51	346234.51	346234.51	346234.51	346234.51
p20.14	301426.68	301426.68	301426.68	301426.68	301426.68	301426.68	301426.68	301426.68	301426.68	301426.68	301426.68	301426.68
p20.15	457467.93	457467.93	457467.93	457467.93	457467.93	457467.93	457467.93	457467.93	457467.93	457467.93	457467.93	457467.93
p20.16	484437.68	484437.68	484437.68	484437.68	484437.68	484437.68	484437.68	484437.68	484437.68	484437.68	484437.68	484437.68
p20.17	380175.41	380175.41	380175.41	380175.41	380175.41	380175.41	380175.41	380175.41	380175.41	380175.41	380175.41	380175.41
p20.18	320300.23	320300.23	320300.23	320300.23	320300.23	320300.23	320300.23	320300.23	320300.23	320300.23	320300.23	320300.23
p20.19	461267.52	461267.52	461267.52	461267.52	461267.52	461267.52	461267.52	461267.52	461267.52	461267.52	461267.52	461267.52
p20.20	403582.74	403582.74	403582.74	403582.74	403582.74	403582.74	403582.74	403582.74	403582.74	403582.74	403582.74	403582.74
p20.21	271958.28	271958.28	271958.28	271958.28	271958.28	271958.28	271958.28	271958.28	271958.28	271958.28	271958.28	271958.28
p20.22	328659.78	328659.78	328659.78	328659.78	328659.78	328659.78	328659.78	328659.78	328659.78	328659.78	328659.78	328659.78
p20.23	326654.08	326654.08	326654.08	326654.08	326654.08	326654.08	326654.08	326654.08	326654.08	326654.08	326654.08	326654.08
p20.24	395859.67	395859.67	395859.67	395859.67	395859.67	395859.67	395859.67	395859.67	395859.67	395859.67	395859.67	395859.67
p20.25	453517.28	453517.28	453517.28	453517.28	453517.28	453517.28	453517.28	453517.28	453517.28	453517.28	453517.28	453517.28
p20.26	461547.18	461547.18	461547.18	461547.18	461547.18	461547.18	461547.18	461547.18	461547.18	461547.18	461547.18	461547.18
p20.27	389057.00	389057.00	389057.00	389057.00	389057.00	389057.00	389057.00	389057.00	389057.00	389057.00	389057.00	389057.00
p20.28	279251.95	279251.95	279251.95	279251.95	279251.95	279251.95	279251.95	279251.95	279251.95	279251.95	279251.95	279251.95
p20.29	299586.76	299586.76	299586.76	299586.76	299586.76	299586.76	299586.76	299586.76	299586.76	299586.76	299586.76	299586.76
	30/30	30/30	30/30	30/30	30/30	30/30	30/30	30/30	30/30	30/30	30/30	30/30

Table A.2: Comparison of average values among different mode and candidate list size for instances with 20 nodes (omnidirectional antennas).

Instance	ACO (average values)											
	m=1			m=2			m=3			m=4		
	c=4	c=8	c=all	c=4	c=8	c=all	c=4	c=8	c=all	c=4	c=8	c=all
p20.00	**407250.81**	**407250.81**	**407250.81**	**407250.81**	**407250.81**	**407250.81**	**407250.81**	**407250.81**	**407250.81**	**407250.81**	**407250.81**	**407250.81**
p20.01	**446905.52**	**446905.52**	**446905.52**	**446905.52**	**446905.52**	**446905.52**	**446905.52**	**446905.52**	**446905.52**	**446905.52**	**446905.52**	**446905.52**
p20.02	**335102.42**	**335102.42**	**335102.42**	**335102.42**	**335102.42**	**335102.42**	**335102.42**	**335102.42**	**335102.42**	**335102.42**	**335102.42**	**335102.42**
p20.03	**488344.90**	**488344.90**	**488344.90**	**488344.90**	**488344.90**	**488344.90**	**488344.90**	**488344.90**	**488344.90**	**488344.90**	**488344.90**	**488344.90**
p20.04	**516117.75**	**516117.75**	**516117.75**	**516117.75**	**516117.75**	**516117.75**	**516117.75**	**516117.75**	**516117.75**	**516117.75**	**516117.75**	**516117.75**
p20.05	**300869.14**	**300869.14**	**300869.14**	**300869.14**	**300869.14**	**300869.14**	**300869.14**	**300869.14**	**300869.14**	**300869.14**	**300869.14**	**300869.14**
p20.06	**250553.15**	**250553.15**	**250553.15**	**250553.15**	**250553.15**	**250553.15**	**250553.15**	**250553.15**	**250553.15**	**250553.15**	**250553.15**	**250553.15**
p20.07	**347454.08**	**347454.08**	**347454.08**	**347454.08**	**347454.08**	**347454.08**	**347454.08**	**347454.08**	**347454.08**	**347454.08**	**347454.08**	**347454.08**
p20.08	**390795.34**	**390795.34**	**390795.34**	**390795.34**	**390795.34**	**390795.34**	**390795.34**	**390795.34**	**390795.34**	**390795.34**	**390795.34**	**390795.34**
p20.09	**447659.11**	**447659.11**	**447659.11**	**447659.11**	**447659.11**	**447659.11**	**447659.11**	**447659.11**	**447659.11**	**447659.11**	**447659.11**	**447659.11**
p20.10	**316734.39**	**316734.39**	**316734.39**	**316734.39**	**316734.39**	**316734.39**	**316734.39**	**316734.39**	**316734.39**	**316734.39**	**316734.39**	**316734.39**
p20.11	**289200.92**	**289200.92**	**289200.92**	**289200.92**	**289200.92**	**289200.92**	**289200.92**	**289200.92**	**289200.92**	**289200.92**	**289200.92**	**289200.92**
p20.12	**314511.98**	**314511.98**	**314511.98**	**314511.98**	**314511.98**	**314511.98**	**314511.98**	**314511.98**	**314511.98**	**314511.98**	**314511.98**	**314511.98**
p20.13	347104.64	347104.64	**346234.51**	**346234.51**	**346234.51**	**346234.51**	**346234.51**	**346234.51**	**346234.51**	**346234.51**	**346234.51**	**346234.51**
p20.14	**301426.68**	**301426.68**	**301426.68**	**301426.68**	**301426.68**	**301426.68**	**301426.68**	**301426.68**	**301426.68**	**301426.68**	**301426.68**	**301426.68**
p20.15	**457467.93**	**457467.93**	**457467.93**	**457467.93**	**457467.93**	**457467.93**	**457467.93**	**457467.93**	**457467.93**	**457467.93**	**457467.93**	**457467.93**
p20.16	**484437.68**	**484437.68**	**484437.68**	**484437.68**	**484437.68**	**484437.68**	**484437.68**	**484437.68**	**484437.68**	**484437.68**	**484437.68**	**484437.68**
p20.17	**380175.41**	**380175.41**	**380175.41**	**380175.41**	**380175.41**	**380175.41**	**380175.41**	**380175.41**	**380175.41**	**380175.41**	**380175.41**	**380175.41**
p20.18	**320300.23**	**320300.23**	**320300.23**	**320300.23**	320860.91	**320300.23**	**320300.23**	**320300.23**	**320300.23**	**320300.23**	**320300.23**	**320300.23**
p20.19	**461267.52**	**461267.52**	**461267.52**	**461267.52**	**461267.52**	**461267.52**	**461267.52**	**461267.52**	**461267.52**	**461267.52**	**461267.52**	**461267.52**
p20.20	**403582.74**	**403582.74**	**403582.74**	**403582.74**	**403582.74**	**403582.74**	**403582.74**	**403582.74**	**403582.74**	**403582.74**	**403582.74**	**403582.74**
p20.21	**271958.28**	**271958.28**	**271958.28**	**271958.28**	**271958.28**	**271958.28**	**271958.28**	**271958.28**	**271958.28**	**271958.28**	**271958.28**	**271958.28**
p20.22	342339.86	342339.86	**328659.78**	**328659.78**	**328659.78**	**328659.78**	**328659.78**	**328659.78**	**328659.78**	**328659.78**	**328659.78**	**328659.78**
p20.23	**326654.08**	**326654.08**	**326654.08**	**326654.08**	**326654.08**	**326654.08**	**326654.08**	**326654.08**	**326654.08**	**326654.08**	**326654.08**	**326654.08**
p20.24	**395859.67**	**395859.67**	**395859.67**	**395859.67**	**395859.67**	395959.70	**395859.67**	**395859.67**	**395859.67**	**395859.67**	**395859.67**	**395859.67**
p20.25	**453517.28**	**453517.28**	**453517.28**	**453517.28**	466183.93	**453517.28**	**453517.28**	**453517.28**	**453517.28**	**453517.28**	**453517.28**	**453517.28**
p20.26	**461547.18**	**461547.18**	**461547.18**	**461547.18**	**461547.18**	**461547.18**	**461547.18**	**461547.18**	**461547.18**	**461547.18**	**461547.18**	**461547.18**
p20.27	**389057.00**	**389057.00**	**389057.00**	**389057.00**	**389057.00**	**389057.00**	**389057.00**	**389057.00**	**389057.00**	**389057.00**	**389057.00**	**389057.00**
p20.28	**279251.95**	**279251.95**	**279251.95**	**279251.95**	**279251.95**	**279251.95**	**279251.95**	**279251.95**	**279251.95**	**279251.95**	**279251.95**	**279251.95**
p20.29	**299586.76**	**299586.76**	**299586.76**	**299586.76**	**299586.76**	**299586.76**	**299586.76**	**299586.76**	**299586.76**	**299586.76**	**299586.76**	**299586.76**
	374234.48	374234.48	**373749.47**	**373749.47**	374190.38	373752.81	**373749.47**	**373749.47**	**373749.47**	**373749.47**	**373749.47**	**373749.47**

Table A.3: Comparison of average time values among different mode and candidate list size for instances with 20 nodes (omnidirectional antennas).

Instance	ACO (average time values)											
	m=1			m=2			m=3			m=4		
	c=4	c=8	c=all	c=4	c=8	c=all	c=4	c=8	c=all	c=4	c=8	c=all
p20.00	0.34	0.34	0.02	0.02	0.08	0.03	**0.01**	**0.01**	**0.01**	0.04	**0.01**	**0.01**
p20.01	**0.00**	**0.00**	0.01	0.01	**0.00**	**0.00**	**0.00**	**0.00**	**0.00**	**0.00**	**0.00**	**0.00**
p20.02	**0.00**	**0.00**	0.01	0.01	**0.00**	**0.00**	**0.00**	**0.00**	**0.00**	**0.00**	**0.00**	**0.00**
p20.03	**0.00**	**0.00**	0.02	0.02	**0.00**	0.01	**0.00**	**0.00**	0.01	**0.00**	**0.00**	0.01
p20.04	0.04	0.04	0.03	0.03	0.01	0.01	0.01	0.01	0.01	0.01	**0.00**	0.01
p20.05	**0.01**	**0.01**	0.02	0.02	**0.01**	0.02	**0.01**	**0.01**	**0.01**	0.03	**0.01**	**0.01**
p20.06	**0.00**	**0.00**	0.01	0.01	**0.00**	**0.00**	**0.00**	**0.00**	**0.00**	**0.00**	**0.00**	**0.00**
p20.07	0.08	0.08	0.01	0.01	0.01	**0.00**	0.01	**0.00**	**0.00**	0.01	0.01	**0.00**
p20.08	**0.00**	**0.00**	0.01	0.01	**0.00**	**0.00**	**0.00**	**0.00**	**0.00**	**0.00**	**0.00**	**0.00**
p20.09	**0.00**	**0.00**	0.03	0.03	**0.00**	**0.00**	0.01	0.01	0.01	0.01	0.01	0.01
p20.10	**0.00**	**0.00**	0.01	0.01	**0.00**	**0.00**	**0.00**	**0.00**	**0.00**	**0.00**	**0.00**	**0.00**
p20.11	0.01	0.01	0.06	0.06	**0.00**	**0.00**	0.01	0.01	0.02	0.01	0.01	0.01
p20.12	**0.00**	**0.00**	0.01	0.01	0.01	**0.00**	**0.00**	**0.00**	**0.00**	**0.00**	**0.00**	**0.00**
p20.13	0.61	0.61	0.04	0.04	0.42	0.37	**0.02**	**0.02**	0.03	0.03	0.04	0.04
p20.14	**0.00**	**0.00**	0.01	0.01	**0.00**	**0.00**	**0.00**	**0.00**	**0.00**	**0.00**	**0.00**	**0.00**
p20.15	0.01	0.01	0.01	0.01	**0.00**	**0.00**	0.01	**0.00**	**0.00**	0.01	**0.00**	**0.00**
p20.16	0.01	0.01	0.01	0.01	0.01	**0.00**	0.01	**0.00**	**0.00**	**0.00**	0.01	**0.00**
p20.17	**0.00**	**0.00**	0.01	0.01	**0.00**	**0.00**	**0.00**	**0.00**	**0.00**	**0.00**	**0.00**	**0.00**
p20.18	0.43	0.43	0.02	0.02	0.03	0.01	**0.00**	0.01	0.01	0.01	0.01	0.01
p20.19	**0.01**	**0.01**	0.03	0.03	0.02	0.03	**0.01**	**0.01**	**0.01**	**0.01**	**0.01**	**0.01**
p20.20	0.03	0.03	0.02	0.02	**0.00**	**0.00**	0.01	**0.00**	0.01	**0.00**	**0.00**	0.01
p20.21	**0.00**	**0.00**	0.01	0.01	**0.00**	**0.00**	**0.00**	**0.00**	**0.00**	**0.00**	**0.00**	**0.00**
p20.22	1.28	1.28	0.01	0.01	0.01	**0.00**	**0.00**	**0.00**	**0.00**	0.02	**0.00**	**0.00**
p20.23	0.18	0.18	0.01	0.01	0.01	**0.00**	**0.00**	**0.00**	**0.00**	0.03	**0.00**	0.01
p20.24	0.03	0.03	0.43	0.43	0.05	0.54	**0.01**	**0.01**	0.02	0.02	0.02	0.03
p20.25	0.26	0.26	0.01	0.01	0.76	0.02	0.01	0.01	**0.00**	0.03	0.01	0.01
p20.26	**0.00**	**0.00**	0.01	0.01	**0.00**	**0.00**	**0.00**	**0.00**	**0.00**	**0.00**	**0.00**	**0.00**
p20.27	**0.00**	**0.00**	0.02	0.02	**0.00**	**0.00**	0.01	**0.00**	0.01	**0.00**	0.01	0.01
p20.28	**0.00**	**0.00**	0.01	0.01	**0.00**	**0.00**	**0.00**	**0.00**	**0.00**	**0.00**	**0.00**	**0.00**
p20.29	**0.00**	**0.00**	0.01	0.01	**0.00**	**0.00**	**0.00**	**0.00**	**0.00**	**0.00**	**0.00**	**0.00**
	0.11	0.11	0.03	0.03	0.05	0.03	0.01	**0.00**	0.01	0.01	0.01	0.01

Table A.4: Comparison of best values among different mode and candidate list size for instances with 50 nodes (omnidirectional antennas).

Instance	ACO (best values)											
	m=1			m=2			m=3			m=4		
	c=4	c=8	c=all	c=4	c=8	c=all	c=4	c=8	c=all	c=4	c=8	c=all
p50.00	**399074.64**	**399074.64**	**399074.64**	**399074.64**	**399074.64**	**399074.64**	**399074.64**	**399074.64**	**399074.64**	**399074.64**	**399074.64**	**399074.64**
p50.01	**373565.15**	**373565.15**	**373565.15**	**373565.15**	**373565.15**	**373565.15**	**373565.15**	**373565.15**	**373565.15**	**373565.15**	**373565.15**	**373565.15**
p50.02	**393641.09**	**393641.09**	**393641.09**	**393641.09**	394366.52	**393641.09**	**393641.09**	**393641.09**	**393641.09**	**393641.09**	**393641.09**	**393641.09**
p50.03	**316801.09**	**316801.09**	**316801.09**	**316801.09**	**316801.09**	**316801.09**	**316801.09**	**316801.09**	**316801.09**	**316801.09**	**316801.09**	**316801.09**
p50.04	327699.97	327699.97	**325774.22**	**325774.22**	327699.97	**325774.22**	**325774.22**	**325774.22**	**325774.22**	**325774.22**	**325774.22**	**325774.22**
p50.05	389063.19	389063.19	**382235.90**	**382235.90**	**382235.90**	**382235.90**	**382235.90**	**382235.90**	**382235.90**	**382235.90**	**382235.90**	**382235.90**
p50.06	387923.10	387923.10	**384438.46**	**384438.46**	387923.10	**384438.46**	**384438.46**	**384438.46**	**384438.46**	**384438.46**	**384438.46**	**384438.46**
p50.07	**401836.85**	**401836.85**	**401836.85**	**401836.85**	**401836.85**	**401836.85**	**401836.85**	**401836.85**	**401836.85**	**401836.85**	**401836.85**	**401836.85**
p50.08	341705.28	341705.28	**334418.45**	**334418.45**	341705.28	**334418.45**	**334418.45**	**334418.45**	**334418.45**	**334418.45**	**334418.45**	**334418.45**
p50.09	**346732.05**	**346732.05**	**346732.05**	**346732.05**	**346732.05**	**346732.05**	**346732.05**	**346732.05**	**346732.05**	**346732.05**	**346732.05**	**346732.05**
p50.10	**416783.45**	**416783.45**	**416783.45**	**416783.45**	**416783.45**	**416783.45**	**416783.45**	**416783.45**	**416783.45**	**416783.45**	**416783.45**	**416783.45**
p50.11	373375.14	373375.14	**369869.41**	**369869.41**	**369869.41**	**369869.41**	**369869.41**	**369869.41**	**369869.41**	**369869.41**	**369869.41**	**369869.41**
p50.12	**392326.01**	**392326.01**	**392326.01**	**392326.01**	**392326.01**	**392326.01**	**392326.01**	**392326.01**	**392326.01**	**392326.01**	**392326.01**	**392326.01**
p50.13	**400563.83**	**400563.83**	**400563.83**	**400563.83**	**400563.83**	**400563.83**	**400563.83**	**400563.83**	**400563.83**	**400563.83**	**400563.83**	**400563.83**
p50.14	415928.49	415928.49	**388714.91**	**388714.91**	415928.49	**388714.91**	**388714.91**	**388714.91**	**388714.91**	**388714.91**	**388714.91**	**388714.91**
p50.15	**371694.65**	**371694.65**	**371694.65**	**371694.65**	372601.97	**371694.65**	**371694.65**	**371694.65**	**371694.65**	**371694.65**	**371694.65**	**371694.65**
p50.16	**414587.42**	**414587.42**	**414587.42**	**414587.42**	**414587.42**	**414587.42**	**414587.42**	**414587.42**	**414587.42**	**414587.42**	**414587.42**	**414587.42**
p50.17	363539.45	363539.45	**355937.07**	**355937.07**	**355937.07**	**355937.07**	**355937.07**	**355937.07**	**355937.07**	**355937.07**	**355937.07**	**355937.07**
p50.18	**376617.33**	**376617.33**	**376617.33**	**376617.33**	**376617.33**	**376617.33**	**376617.33**	**376617.33**	**376617.33**	**376617.33**	**376617.33**	**376617.33**
p50.19	**335059.72**	**335059.72**	**335059.72**	**335059.72**	**335059.72**	**335059.72**	**335059.72**	**335059.72**	**335059.72**	**335059.72**	**335059.72**	**335059.72**
p50.20	**414768.96**	**414768.96**	**414768.96**	**414768.96**	**414768.96**	415380.30	**414768.96**	**414768.96**	415380.30	**414768.96**	**414768.96**	**414768.96**
p50.21	380292.93	380292.93	**361354.27**	**361354.27**	**361354.27**	**361354.27**	**361354.27**	**361354.27**	**361354.27**	**361354.27**	**361354.27**	**361354.27**
p50.22	366633.73	366633.73	**329043.51**	**329043.51**	**329043.51**	**329043.51**	**329043.51**	**329043.51**	**329043.51**	**329043.51**	**329043.51**	**329043.51**
p50.23	**383321.04**	**383321.04**	**383321.04**	**383321.04**	**383321.04**	**383321.04**	**383321.04**	**383321.04**	**383321.04**	**383321.04**	**383321.04**	**383321.04**
p50.24	**404855.92**	**404855.92**	**404855.92**	**404855.92**	**404855.92**	**404855.92**	**404855.92**	**404855.92**	**404855.92**	**404855.92**	**404855.92**	**404855.92**
p50.25	421071.91	421071.91	**363200.32**	**363200.32**	393216.57	**363200.32**	**363200.32**	**363200.32**	**363200.32**	**363200.32**	**363200.32**	**363200.32**
p50.26	**406631.51**	**406631.51**	**406631.51**	**406631.51**	**406631.51**	**406631.51**	**406631.51**	**406631.51**	**406631.51**	**406631.51**	**406631.51**	**406631.51**
p50.27	453571.24	453571.24	**451059.62**	**451059.62**	**451059.62**	**451059.62**	**451059.62**	**451059.62**	**451059.62**	**451059.62**	**451059.62**	**451059.62**
p50.28	**415832.44**	**415832.44**	**415832.44**	**415832.44**	**415832.44**	**415832.44**	**415832.44**	**415832.44**	**415832.44**	**415832.44**	**415832.44**	**415832.44**
p50.29	399794.39	399794.39	**380492.77**	**380492.77**	395486.18	**380492.77**	**380492.77**	**380492.77**	**380492.77**	**380492.77**	**380492.77**	**380492.77**
	18/30	18/30	**30/30**	**30/30**	22/30	29/30	**30/30**	**30/30**	29/30	**30/30**	**30/30**	**30/30**

Table A.5: Comparison of average values among different mode and candidate list size for instances with 50 nodes (omnidirectional antennas).

Instance	ACO (average values)											
	m=1			m=2			m=3			m=4		
	c=4	c=8	c=all	c=4	c=8	c=all	c=4	c=8	c=all	c=4	c=8	c=all
p50.00	**399074.64**	**399074.64**	403364.36	403364.36	**399074.64**	400260.34	**399074.64**	**399074.64**	**399074.64**	**399074.64**	**399074.64**	**399074.64**
p50.01	**373565.15**	**373565.15**	373753.93	373753.93	**373565.15**	**373565.15**	**373565.15**	**373565.15**	**373565.15**	**373565.15**	**373565.15**	**373565.15**
p50.02	394389.68	394389.68	393810.36	393810.36	394366.52	**393641.09**	394027.99	**393641.09**	**393641.09**	394221.43	**393641.09**	**393641.09**
p50.03	319438.09	319438.09	318179.84	318179.84	**316801.09**	**316801.09**	**316801.09**	**316801.09**	**316801.09**	**316801.09**	**316801.09**	**316801.09**
p50.04	328525.08	328525.08	326878.60	326878.60	327699.97	**325774.22**	328092.97	**325774.22**	325829.91	326353.51	**325774.22**	**325774.22**
p50.05	396082.10	396082.10	**382235.90**	**382235.90**	**382235.90**	**382235.90**	386104.70	**382235.90**	**382235.90**	387697.73	382463.48	**382235.90**
p50.06	392334.94	392334.94	385019.23	385019.23	391480.57	384935.97	384903.08	**384438.46**	**384438.46**	385367.70	**384438.46**	**384438.46**
p50.07	**401836.85**	**401836.85**	407784.10	407784.10	**401836.85**	**401836.85**	**401836.85**	**401836.85**	**401836.85**	**401836.85**	**401836.85**	**401836.85**
p50.08	343625.75	343625.75	**334418.45**	**334418.45**	341705.28	**334418.45**	335875.82	**334418.45**	**334418.45**	338790.55	**334418.45**	**334418.45**
p50.09	**346732.05**	**346732.05**	350824.07	350824.07	**346732.05**	**346732.05**	**346732.05**	**346732.05**	**346732.05**	**346732.05**	**346732.05**	**346732.05**
p50.10	420442.97	420442.97	418599.19	418599.19	421820.91	**416783.45**	**416783.45**	**416783.45**	**416783.45**	**416783.45**	**416783.45**	**416783.45**
p50.11	373738.26	373738.26	379294.69	379294.69	372907.71	371941.67	370336.84	**369869.41**	372707.89	371872.27	371081.18	370985.83
p50.12	**392326.01**	**392326.01**	393828.98	393828.98	**392326.01**	**392326.01**	**392326.01**	**392326.01**	**392326.01**	**392326.01**	**392326.01**	**392326.01**
p50.13	400755.17	400755.17	404675.35	404675.35	402472.51	**400563.83**	**400563.83**	**400563.83**	400722.12	**400563.83**	**400563.83**	400886.12
p50.14	415928.49	415928.49	**388714.91**	**388714.91**	416000.67	388859.58	389968.75	388763.13	**388714.91**	390733.53	388907.81	**388714.91**
p50.15	374015.07	374015.07	**371694.65**	**371694.65**	374856.48	371724.89	372018.61	**371694.65**	**371694.65**	371802.64	371863.12	**371694.65**
p50.16	**414587.42**	**414587.42**	417405.16	417405.16	414622.46	**414587.42**	**414587.42**	**414587.42**	**414587.42**	**414587.42**	**414587.42**	**414587.42**
p50.17	366703.68	366703.68	356252.34	356252.34	356803.14	**355937.07**	**355937.07**	**355937.07**	**355937.07**	**355937.07**	**355937.07**	**355937.07**
p50.18	379949.81	379949.81	**376617.33**	**376617.33**	376619.01	**376617.33**	**376617.33**	**376617.33**	**376617.33**	**376617.33**	**376617.33**	**376617.33**
p50.19	335138.15	335138.15	**335059.72**	**335059.72**	**335059.72**	**335059.72**	**335059.72**	**335059.72**	**335059.72**	**335059.72**	**335059.72**	**335059.72**
p50.20	417182.82	417182.82	415359.92	415359.92	418125.11	415380.30	414952.36	414952.36	415380.30	**414935.53**	415095.01	415339.54
p50.21	383115.81	383115.81	**361354.27**	**361354.27**	381988.07	**361354.27**	**361354.27**	**361354.27**	**361354.27**	**361354.27**	**361354.27**	**361354.27**
p50.22	366633.73	366633.73	**329043.51**	**329043.51**	330880.93	**329043.51**	330162.01	**329043.51**	**329043.51**	332505.46	329549.54	**329043.51**
p50.23	386893.57	386893.57	390865.72	390865.72	386610.44	**383321.04**	**383321.04**	**383321.04**	**383321.04**	**383321.04**	**383321.04**	**383321.04**
p50.24	408391.36	408391.36	405395.20	405395.20	**404855.92**	**404855.92**	**404855.92**	**404855.92**	**404855.92**	**404855.92**	**404855.92**	**404855.92**
p50.25	421592.89	421592.89	**363200.32**	**363200.32**	408279.52	**363200.32**	**363200.32**	**363200.32**	**363200.32**	363361.62	**363200.32**	**363200.32**
p50.26	**406631.51**	**406631.51**	422693.41	422693.41	408764.05	409432.90	**406631.51**	**406631.51**	407147.93	407272.43	407147.93	407272.43
p50.27	453571.24	453571.24	453412.07	453412.07	451896.83	**451059.62**	451325.05	**451059.62**	451143.34	451227.06	**451059.62**	**451059.62**
p50.28	415936.71	415936.71	419406.08	419406.08	**415832.44**	**415832.44**	**415832.44**	**415832.44**	**415832.44**	**415832.44**	**415832.44**	**415832.44**
p50.29	401368.46	401368.46	**380492.77**	**380492.77**	399650.78	**380492.77**	380770.78	**380492.77**	**380492.77**	381602.44	**380492.77**	**380492.77**
	387683.58	387683.58	381987.81	381987.81	384862.36	379952.51	380120.64	**379715.46**	379849.87	380433.07	379812.71	379796.08

Table A.6: Comparison of average time values among different mode and candidate list size for instances with 50 nodes (omnidirectional antennas).

Instance	ACO (average time values)											
	m=1			m=2			m=3			m=4		
	c=4	c=8	c=all	c=4	c=8	c=all	c=4	c=8	c=all	c=4	c=8	c=all
p50.00	0.45	0.45	11.06	11.06	3.03	7.57	0.58	0.52	1.58	**0.39**	0.75	2.95
p50.01	**0.96**	**0.96**	7.54	7.54	1.79	1.13	1.16	1.97	2.05	1.38	1.56	1.86
p50.02	6.17	6.17	8.82	8.82	**0.46**	1.05	4.76	2.84	2.27	3.07	5.26	1.12
p50.03	8.66	8.66	10.92	10.92	6.47	2.07	0.80	**0.36**	1.12	1.14	1.32	1.34
p50.04	5.19	5.19	11.53	11.53	**1.46**	2.13	4.19	1.89	6.11	7.04	2.75	1.57
p50.05	6.19	6.19	3.13	3.13	2.61	1.94	3.84	3.42	**0.72**	5.67	2.27	0.77
p50.06	10.09	10.09	7.05	7.05	5.68	6.55	6.40	3.54	**1.05**	6.64	5.66	2.77
p50.07	1.34	1.34	11.81	11.81	1.78	0.80	0.57	**0.54**	1.48	0.90	1.07	1.53
p50.08	6.57	6.57	0.47	0.47	4.15	**0.06**	5.86	0.73	0.11	4.96	1.90	**0.06**
p50.09	4.14	4.14	12.25	12.25	**1.51**	2.23	2.20	1.88	3.39	1.64	1.65	2.73
p50.10	8.48	8.48	9.16	9.16	7.18	3.71	1.11	**0.85**	4.00	2.21	1.37	3.22
p50.11	**3.77**	**3.77**	8.64	8.64	5.16	7.44	7.35	4.47	7.43	3.99	5.33	6.97
p50.12	0.41	0.41	13.78	13.78	**0.28**	2.15	0.50	0.42	1.37	0.43	0.63	2.04
p50.13	5.75	5.75	10.29	10.29	8.68	5.65	**1.19**	1.38	8.07	3.16	2.38	5.90
p50.14	3.96	3.96	3.84	3.84	5.53	8.49	3.53	2.65	**0.71**	4.04	3.71	1.24
p50.15	4.75	4.75	2.51	2.51	1.67	1.65	4.89	1.12	**0.44**	5.39	2.75	0.50
p50.16	4.92	4.92	13.33	13.33	4.91	5.30	0.65	**0.48**	1.31	1.65	1.31	2.13
p50.17	2.08	2.08	9.66	9.66	11.01	2.69	1.05	**0.38**	0.94	2.53	0.78	1.19
p50.18	2.29	2.29	9.38	9.38	5.25	1.00	1.14	**0.55**	0.84	3.37	1.23	0.70
p50.19	5.81	5.81	7.05	7.05	3.02	**0.28**	0.42	0.39	0.94	0.84	0.42	0.54
p50.20	6.20	6.20	1.90	1.90	5.05	0.50	4.97	5.85	**0.37**	5.68	5.09	1.01
p50.21	7.65	7.65	3.42	3.42	7.26	**0.25**	0.76	0.29	0.32	2.22	0.43	0.30
p50.22	1.80	1.80	0.47	0.47	4.18	0.45	4.45	0.74	**0.10**	5.64	1.45	**0.10**
p50.23	2.12	2.12	16.22	16.22	2.58	5.48	2.61	**1.06**	1.53	3.02	2.30	1.73
p50.24	7.15	7.15	8.69	8.69	0.86	1.27	**0.37**	0.53	1.35	0.44	0.53	1.11
p50.25	6.44	6.44	0.29	0.29	9.40	**0.06**	1.47	0.45	0.09	3.20	0.88	0.07
p50.26	4.49	4.49	14.73	14.73	7.76	6.45	2.67	**2.16**	4.33	6.97	5.72	5.73
p50.27	**1.39**	**1.39**	11.55	11.55	5.55	4.64	2.76	1.50	4.32	7.91	4.06	3.58
p50.28	2.87	2.87	14.33	14.33	**0.26**	0.57	0.31	0.38	2.53	0.30	0.34	1.02
p50.29	6.84	6.84	0.67	0.67	0.77	0.41	5.41	1.92	**0.11**	7.20	3.82	0.22
	4.63	4.63	8.15	8.15	4.18	2.80	2.60	**1.51**	2.03	3.43	2.29	1.87

Table A.7: Comparison of best values among different mode and candidate list size for instances with 100 nodes (omnidirectional antennas).

Instance	ACO (best values)											
	m=1			m=2			m=3			m=4		
	c=4	c=8	c=all	c=4	c=8	c=all	c=4	c=8	c=all	c=4	c=8	c=all
p100.00	358134.65	358134.65	341273.31	341273.31	358134.65	**340869.27**	**340869.27**	**340869.27**	**340869.27**	**340869.27**	**340869.27**	**340869.27**
p100.01	365522.03	365522.03	365676.46	365676.46	365522.03	**355284.77**	**355284.77**	**355284.77**	357285.74	355795.98	**355284.77**	**355284.77**
p100.02	**377145.59**	**377145.59**	388931.61	388931.61	**377145.59**	**377145.59**	**377145.59**	**377145.59**	381744.04	**377145.59**	**377145.59**	379924.99
p100.03	**356942.53**	**356942.53**	373290.00	373290.00	357067.04	357357.35	**356942.53**	**356942.53**	**356942.53**	**356942.53**	**356942.53**	357357.35
p100.04	392279.82	392279.82	402448.86	402448.86	**384446.36**	**384446.36**	384864.91	**384446.36**	**384446.36**	**384446.36**	**384446.36**	**384446.36**
p100.05	428445.53	428445.53	437108.09	437108.09	427265.49	**416758.58**	**416758.58**	**416758.58**	**416758.58**	**416758.58**	**416758.58**	**416758.58**
p100.06	387967.49	387967.49	393441.97	393441.97	380136.53	380136.53	**376408.49**	**376408.49**	**376408.49**	**376408.49**	**376408.49**	**376408.49**
p100.07	360541.47	360541.47	358642.39	358642.39	363661.25	**343798.46**	**343798.46**	**343798.46**	**343798.46**	**343798.46**	**343798.46**	**343798.46**
p100.08	392439.07	392439.07	391345.74	391345.74	**372254.06**	372465.28	374215.94	**372254.06**	**372254.06**	374215.94	374215.94	**372254.06**
p100.09	370076.36	370076.36	380713.54	380713.54	**366993.89**	**366993.89**	**366993.89**	**366993.89**	**366993.89**	**366993.89**	**366993.89**	**366993.89**
p100.10	**334579.00**	**334579.00**	347158.94	347158.94	**334579.00**	**334579.00**	**334579.00**	**334579.00**	**334579.00**	**334579.00**	**334579.00**	**334579.00**
p100.11	361994.06	361994.06	371371.01	371371.01	358989.38	**356219.14**	**356219.14**	**356219.14**	**356219.14**	**356219.14**	**356219.14**	**356219.14**
p100.12	402860.79	402860.79	410898.89	410898.89	393939.18	**393854.17**	**393854.17**	**393854.17**	**393854.17**	**393854.17**	**393854.17**	**393854.17**
p100.13	337195.22	337195.22	342553.05	342553.05	**331270.37**	**331270.37**	**331270.37**	**331270.37**	**331270.37**	**331270.37**	**331270.37**	**331270.37**
p100.14	346292.73	346292.73	365560.36	365560.36	346292.73	344229.79	**344175.57**	**344175.57**	**344175.57**	**344175.57**	**344175.57**	**344175.57**
p100.15	355782.87	355782.87	365183.74	365183.74	355039.90	**352884.55**	352984.00	**352884.55**	**352884.55**	352984.00	**352884.55**	**352884.55**
p100.16	342063.48	342063.48	342022.80	342022.80	342063.48	**338713.69**	**338713.69**	**338713.69**	**338713.69**	**338713.69**	**338713.69**	**338713.69**
p100.17	383072.77	383072.77	383510.13	383510.13	383072.77	**374059.25**	376931.43	**374059.25**	**374059.25**	376931.43	**374059.25**	**374059.25**
p100.18	339470.46	339470.46	344984.20	344984.20	339470.46	**331926.13**	**331926.13**	**331926.13**	**331926.13**	**331926.13**	**331926.13**	**331926.13**
p100.19	382156.12	382156.12	372261.37	372261.37	387078.74	**365078.37**	**365078.37**	**365078.37**	**365078.37**	**365078.37**	**365078.37**	**365078.37**
p100.20	359803.66	359803.66	363069.45	363069.45	366177.37	**355078.27**	**355078.27**	**355078.27**	**355078.27**	**355078.27**	**355078.27**	**355078.27**
p100.21	369807.21	369807.21	369771.26	369771.26	365499.29	362913.04	**362204.29**	**362204.29**	362913.04	**362204.29**	**362204.29**	**362204.29**
p100.22	366180.73	366180.73	389839.51	389839.51	366180.73	**366125.96**	**366125.96**	**366125.96**	**366125.96**	**366125.96**	**366125.96**	**366125.96**
p100.23	**409062.55**	**409062.55**	433187.59	433187.59	**409062.55**	412164.84	**409062.55**	**409062.55**	409815.81	**409062.55**	**409062.55**	412164.84
p100.24	359225.69	359225.69	364486.27	364486.27	358821.98	**357772.11**	**357772.11**	**357772.11**	**357772.11**	**357772.11**	**357772.11**	**357772.11**
p100.25	358697.57	358697.57	369429.04	369429.04	358697.57	**357191.63**	**357191.63**	**357191.63**	358400.12	**357191.63**	**357191.63**	**357191.63**
p100.26	358599.68	358599.68	357436.72	357436.72	358599.68	**352148.02**	**352148.02**	**352148.02**	**352148.02**	**352148.02**	**352148.02**	**352148.02**
p100.27	374395.66	374395.66	378479.27	378479.27	371658.15	**370033.07**	**370033.07**	**370033.07**	370187.41	**370033.07**	370187.41	**370033.07**
p100.28	351229.81	351229.81	357911.29	357911.29	**348889.36**	**348889.36**	**348889.36**	**348889.36**	**348889.36**	**348889.36**	**348889.36**	**348889.36**
p100.29	364204.35	364204.35	366976.96	366976.96	**357595.04**	**357595.04**	**357595.04**	**357595.04**	**357595.04**	**357595.04**	**357595.04**	**357595.04**
	4/30	4/30	0/30	0/30	9/30	24/30	26/30	**30/30**	24/30	26/30	28/30	27/30